UNIVERSIDADE D
COIMBRA

Inês Martins Andrade

On the Performance of Seizure Prediction Methods Across Different Databases

Thesis submitted to the Faculty of Sciences and Technology of the University of Coimbra for the degree of Master in Biomedical Engineering with specialization in Clinical Informatics and Bioinformatics, supervised by Prof. Dr. César Teixeira and Prof. Dr. Mauro Pinto.

September 2023

FACULDADE DE CIÊNCIAS E TECNOLOGIA
UNIVERSIDADE D COIMBRA

On the Performance of Seizure Prediction Methods Across Different Databases

Inês Martins Andrade

Thesis submitted to the Faculty of Sciences and Technology of the University of Coimbra for the degree of Master in Biomedical Engineering with specialization in Clinical Informatics and Bioinformatics.

Supervisors:
Prof. Doutor César Alexandre Domingues Teixeira (CISUC)
Prof. Doutor Mauro Filipe da Silva Pinto (CISUC)

Coimbra, 2023

This work was developed in collaboration with:

Center for Informatics and Systems of the University of Coimbra

This work is funded by FCT- Foundation for Science and Technology, I.P., within the scope of the projects: CISUC - UID/CEC/00326/2020 with funds from the European Social Fund, through the Regional Operational Program Centro 2020; and project RECoD - PTDC/EEI-EEE/5788/2020 financed with national funds (PIDDAC) via the Portuguese State Budget.

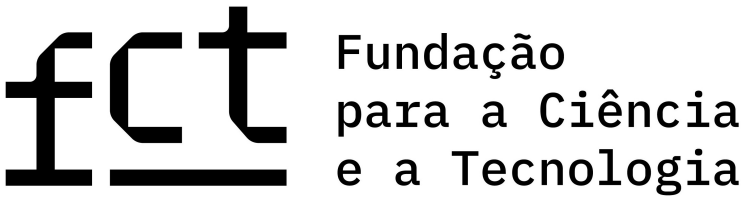

Agradecimentos

Este projeto de Mestrado foi uma longa viagem, marcada por vários desafios, alegrias, incertezas, tristezas e alguns percalços pelo caminho. Apesar do processo solitário que é escrever uma tese, os contributos de várias pessoas foram indispensáveis para encontrar o melhor rumo nesta caminhada. Assim, dedico especialmente este projeto a todos aqueles que me deram apoio, energia e motivação.

Em primeiro lugar, quero agradecer aos dois orientadores que me acompanharam no decorrer de todo o projeto. Ao Professor Doutor César Teixeira, o meu profundo agradecimento pelos conhecimentos que me transmitiu, indispensáveis para a realização deste projeto, frutos da sua longa experiência académica e científica. Ao Professor Doutor Mauro Pinto, o meu mais sincero obrigado. A sua paixão pelo tema foi talvez dos pontos mais inspiradores e motivadores com que me deparei ao longo destes meses. Agradeço especialmente a disponibilidade, o discurso positivo mas realista e tudo o que me ensinou, tanto a nível científico como pessoal.

Quero também agradecer a todos os colegas de laboratório por toda a ajuda, partilha de materiais e conhecimentos. Ao Costini, o meu agradecimento especial, por todos os momentos de companheirismo, brainstorming, entreajuda e diversão vividos tanto ao longo deste projeto como durante os 2 anos de Mestrado.

Agradeço a todos os colegas e amigos que fizeram parte da minha vida ao longo destes últimos 5 anos. Em especial, um grande obrigado ao grupo de amigos que tive a sorte de me cruzar e que serão para sempre os "Cruzados". Foram muitos os momentos vividos em conjunto, fossem eles mais ou menos bons. Tenho profunda gratidão pelas pessoas que me fizeram viver a tradição de Coimbra da forma mais bonita. Um agradecimento especial à minha madrinha Xará, padrinhos Amado e Vasco, afilhada Carol e afilhado João Nuno. Sem esquecer três boas amigas, Milene, Filipa e Lúcia, que foram um grande apoio ao longo de todo o percurso.

Ao Filipe, só consigo dizer que não há palavras que cheguem para lhe agradecer tudo o que fez por mim. Foi sempre o meu pilar, o meu companheiro e, acima de tudo, a pessoa que nunca duvidou do meu potencial. Obrigada por todo o apoio, amor, ajuda e positivismo.

Aos meus pais e irmão, agradeço por sempre me apoiarem. O que alcancei não seria possível sem o vosso esforço. Obrigada pela confiança que depositaram em mim, pela pessoa que me moldaram a ser e por serem sempre "casa".

Por fim, obrigado a Coimbra, a cidade que me acolheu e me fez apaixonar desde o primeiro dia. Será sempre a minha segunda casa e aquela que me deu a conhecer o verdadeiro significado da palavra saudade.

"It is your reaction to adversity, not the adversity itself, that determines how your life's story will develop."
Dieter F. Uchtdorf

Resumo

A epilepsia é uma das condições neurológicas mais prevalentes, afetando cerca de 1% da população mundial. Embora os medicamentos antiepiléticos tenham mostrado eficácia no controlo de crises em grande parte dos casos, cerca de 1/3 dos doentes continuam a enfrentar episódios recorrentes. Nesse sentido, a busca por abordagens alternativas torna-se imperativa para melhorar a qualidade de vida desses doentes. Uma das estratégias promissoras é a previsão de crises, que pode ser implementada em sistemas de intervenção ou alerta, com o intuito de evitar ou minimizar os efeitos adversos das crises epiléticas.

Um dos desafios cruciais nesse campo de pesquisa é identificar o período pré-ictal, caracterizado por ser o intervalo que marca a transição da atividade cerebral regular para uma crise. Vários estudos têm explorado métodos recorrendo ao uso de dados de eletroencefalograma (EEG) para essa finalidade. No entanto, foram poucos os que se mostraram viáveis para aplicação clínica.

Um aspeto que se revela determinante nos resultados obtidos é o conjunto de dados usado. Pelos vários estudos presentes na literatura é possível concluir que a performance é bastante influenciada pela base de dados utilizada. São várias as caraterísticas que diferem entre as bases de dados disponíveis: o tipo de sinal EEG, as condições a que os doentes foram sujeitos durante a recolha dos dados, o tipo de epilepsia, informações temporais de cada crise, entre outros.

O presente trabalho teve como objetivo avaliar a performance de um algoritmo de previsão quando aplicado a diferentes bases de dados. O desenvolvimento desse algoritmo foi realizado para a base de dados European Epilepsy Database (EPILEPSIAE) [1], que serviu como base de comparação com as restantes (Children's Hospital Boston from the Massachusetts Institute of Technology (CHB-MIT) [2], American Epilepsy Society (AES) [3] e Epilepsy Ecosystem [4]). Apenas as mudanças necessárias foram aplicadas ao algoritmo base, de forma a garantir a uniformização do processo para uma comparação justa e direta.

O modelo desenvolvido utilizou um classificador de Regressão Logística e foi aplicado a dados de 40 doentes da base de dados EPILEPSIAE, 6 da CHB-MIT, 7 da AES e 3 da Epilepsy Ecosystem.

Os resultados de treino obtidos mostraram que para os dados que não possuíam informações temporais das crises (AES e Epilepsy Ecosystem) a performance foi bastante superior. É possível concluir que lidar com o problema de forma menos rigorosa, sem considerar a natureza real dos dados, leva a melhores resultados. No entanto, estes bons resultados não são representativos da realidade.

Além disso, os valores de performance obtidos na fase de teste revelaram-se mais baixos

que os reportados por outros estudos utilizando estas bases de dados. São as assumpções para simular situações de alarme realistas que levam a esses maus resultados. Assim, verifica-se que os resultados excelentes obtidos por muitos autores se devem à falta de rigor na abordagem prática do problema.

Por último, a análise comparativa das duas abordagens distintas (alarmes e amostra) permitiu verificar que os resultados obtidos são menos satisfatórios na abordagem de alarmes. Este aspeto permite concluir que lidar com o problema de uma forma mais realista leva a piores resultados.

Em suma, este estudo, embora tenha enfrentado algumas dificuldades no processo de padronização devido à heterogeneidade dos dados, encontrou algumas caraterísticas dos bancos de dados que influenciam a performance de um modelo de previsão de crises epiléticas. É, portanto, o ponto de partida para explorar mais detalhadamente a influência da base de dados usada, bem como a definição de período pré-ictal no contexto de previsão de crises.

Abstract

Epilepsy is one of the most prevalent neurological conditions, affecting approximately 1% of the global population. While Antiepileptic Drugs (AEDs) have demonstrated effectiveness in controlling seizures in many cases, approximately one-third of patients continue to experience recurrent episodes. In this context, pursuing alternative approaches becomes imperative to enhance the quality of life for these patients. One promising strategy is the prediction of seizures, which can be implemented in intervention or alert systems to prevent or minimize the adverse effects of epileptic seizures.

One of the crucial challenges in this research field is identifying the preictal period, characterized as the interval marking the transition from regular brain activity to a seizure. Numerous studies have explored methods using Electroencephalogram (EEG) data for this purpose. However, few have proven viable for clinical application.

A critical determinant of the results achieved is the dataset in use. The dataset used significantly influences performance, as evident from various studies in the literature. Various characteristics vary across the available databases, encompassing differences in the type of recorded EEG signal, the conditions patients faced during data collection, the type of epilepsy, and temporal information for each seizure, among others.

This study aimed to evaluate the performance of a prediction algorithm when applied to different datasets. The algorithm's development primarily centered on the European Epilepsy Database (EPILEPSIAE) [1], which was then used as a reference point for comparisons across other datasets, namely Children's Hospital Boston from the Massachusetts Institute of Technology (CHB-MIT) [2], American Epilepsy Society (AES) [3], and Epilepsy Ecosystem [4]. Only necessary modifications were made to the base algorithm to ensure a fair and direct comparison. The developed model utilized a Logistic Regression classifier and was applied to data from 40 patients from the EPILEPSIAE database, six from CHB-MIT, seven from AES, and three from the Epilepsy Ecosystem.

The training results obtained showed that for datasets lacking temporal seizure information (AES and Epilepsy Ecosystem), performance was significantly higher. Handling the problem less rigorously, without considering the real nature of the data, leads to better results. However, these favorable results do not accurately represent reality.

Furthermore, the performance values obtained in the testing phase were lower than those reported by other studies using these databases. Assumptions made to simulate realistic alarm situations account for these poor results. Thus, it is evident that the excellent results achieved by many authors stem from a lack of practical rigor in approaching the problem.

Finally, the comparative analysis of the two approaches (alarm and sample) has revealed that the outcomes achieved are less favorable in the alarm approach. This finding suggests that employing realistic metrics in problem-solving leads to comparatively poorer results.

In summary, while encountering some difficulties in standardization due to data heterogeneity, this study identified specific dataset characteristics that influence the performance of an epileptic seizure prediction model. It serves as a starting point for a more detailed exploration of the influence of the dataset used and the definition of the preictal period in the context of seizure prediction.

Contents

List of Figures

List of Tables

List of Acronyms

AASM American Academy of Sleep Medicine.
ACC Accelerometry.
AED Antiepileptic Drug.
AES American Epilepsy Society.
ANFIS Adaptive Neuro-Fuzzy Inference Systems.
ANT-DBS Anterior Nucleus of Thalamus Deep Brain Stimulation.
ARS Acute Repetitive Seizures.
ATN Anterior Thalamic Nucleus.
AUC Area Under the ROC Curve.

BSS Brier Skill Score.
BVP Blood Volume Pulse.
BZD Benzodiazepine.

CD Concept Drift.
CHB-MIT Children's Hospital Boston from the Massachusetts Institute of Technology.
CNN Convolutional Neural Network.

DBS Deep Brain Stimulation.
DL Deep Learning.
DRE Drug Resistant Epilepsy.
DRSN Deep Residual Shrinkage Network.
DSI Dynamic Similarity Index.

ECG Electrocardiogram.
EDA Electrodermal Activity.
EEG Electroencephalogram.
Ei2 Epilepsy Innovation Institute.
EMG Electromyography.
EPILEPSIAE European Epilepsy Database.

FFT Fast Fourier Transform.
FP Firing Power.
FPR/h False Prediction Rate per hour.

GA Genetic Algorithms.

GAN Generative Adversarial Network.
GRU Gated Recurrent Unit.

HR Heart Rate.

IBE International Bureau for Epilepsy.
ICA Independent Component Analysis.
IEA Interictal Epileptiform Activity.
iEEG Intracranial Electroencephalogram.
ILAE International League Against Epilepsy.
IT Intervention time.

KF Kalman Filter.
kNN k-Nearest Neighbor.

LOOCV Leave-One-Out Cross-Validation.
LSTM Long-term Memory Network.

mDAD maximum Difference Amplitude Distribution.
ML Machine Learning.
MPC Mean Phase Coherence.
mRMR minimum Redundancy Maximum Relevance.
MTLE Mesial Temporal Lobe Epilepsy.

NREM Non-Rapid Eye Movement.

PCA Principal Component Analysis.
PPG Photoplethysmography.
PSD Power Spectral Density.

RBF Radial Basis Function.
REM Rapid Eye Movement.
RMS Root Mean Square.
RNN Recurrent Neural Network.
RNS Responsive Neurostimulation.

SEF Spectral Edge Frequency.
SEP Spectral Edge Power.
SOP Seizure Occurrence Period.
SPH Seizure Prediction Horizon.
sqEEG Subcutaneous Electroencephalography.
SUDEP Sudden Unexpected Death in Epilepsy.
SVM Support Vector Machine.

TiW Time in Warning.
TLE Temporal Lobe Epilepsy.

USA United States of America.

vEEG Video Electroencephalography.
VNS Vagus Nerve Stimulation.

WT Wavelet Transform.

1

Introduction

This chapter begins by addressing the motivation that led to the development of this project in Section 1.1. Subsequently, Section 1.2 delineates the project's objectives and anticipated contributions. Section 1.3 addresses the main limitations associated with predicting epileptic seizures. Finally, Section 1.4 offers a succinct overview of the document's structural organization, chapter by chapter.

1.1 Motivation

Epilepsy is one of the prevalent neurological disorders, affecting about 1% of the world's population. It results from abnormal brain activity culminating in seizures, notable for their unpredictable nature, which presents a considerable challenge for patients and healthcare professionals. Alongside the immediate seizure-related symptoms, epilepsy also triggers a series of neurological, cognitive, psychological, and social effects, making it a complex and multifaceted condition [5].

The first line of treatment for epilepsy involves the use of Antiepileptic Drugs (AEDs), offering significant relief to a considerable number of patients. Nevertheless, a third of epilepsy patients face a condition known as Drug Resistant Epilepsy (DRE), wherein AEDs are not enough to provide a seizure-free life [6, 7, 8]. The inability to effectively manage seizures places these patients at risk of numerous complications. Beyond physical complications like accidental injuries and brain damage, DRE leads to severe psychological issues, including psychosis, neuropsychological deficits, depression, and anxiety [9, 10, 11].

Although epilepsy surgery is an effective option for select DRE patients, stringent selection criteria restrict the number of individuals eligible for this intervention [12]. Considering this challenging scenario, exploring alternative approaches to improve epilepsy management, particularly for individuals with DRE, becomes paramount. A promising approach in this context is the development of warning devices capable of predicting the occurrence of seizures. These devices can play a crucial role in patient's lives by providing advanced information about impending seizures, allowing them to take appropriate preventive measures [13].

The motivation for developing this work stems from enhancing the quality of life for individuals with epilepsy, particularly those grappling with DRE. Through exploring and enhancing seizure prediction capabilities utilizing warning devices, this study aims to provide a noteworthy contribution to the field of clinical neurology. The overarching objective is to furnish patients with practical tools for navigating the unpredictability of seizures while concurrently mitigating the physical and psychological risks associated with DRE. In doing so, this work will positively

impact patients' quality of life and emotional well-being, giving them greater control over their medical condition.

1.2 Goals and Contributions

The central objective of this research is to elevate the realm of epileptic seizure prediction through the comparative assessment of performance across multiple databases. The primary mission is to develop an algorithm for seizure prediction and alarm activation before their onset, suitable for application across diverse datasets. At the core of this entire domain of seizure prediction lies the foundational concept of the preictal period – a transitional phase that precedes the onset of an epileptic seizure. The conceptual basis for this approach hinges on the existence of this preictal phase. The ability of Electroencephalogram (EEG) signals to record the preictal period has been crucial to advances in this field, opening doors to the creation of more effective warning and intervention systems.

For this reason, the development of a system capable of continuous real-time data monitoring and, importantly, the timely notification of the patient regarding an impending epileptic seizure is the ultimate objective. This alert must occur within a clearly defined time interval (Seizure Occurrence Period (SOP)) with a pre-established time horizon (Seizure Prediction Horizon (SPH)). This advanced notice period must offer adequate time for the implementation of preventive measures. An accurate prediction system has the potential to open up new therapeutic possibilities, including alert devices to help patients avoid risky situations or even intervention devices capable of managing seizures through anticonvulsant medication administration or electrical stimulation.

Considering the profound impact of the selected database on the resultant outcomes, there emerges an imperative need to formulate an algorithm with universal applicability, thereby facilitating a direct cross-database comparison of results. In this context, utilizing EEG data sourced from the European Epilepsy Database (EPILEPSIAE), Children's Hospital Boston from the Massachusetts Institute of Technology (CHB-MIT), American Epilepsy Society (AES), and Epilepsy Ecosystem databases, this research can be partitioned into 3 fundamental contributions:

- Development of a patient-specific seizure prediction algorithm using a subset of EPILEPSIAE data;
- Adaptation of the seizure prediction algorithm originally devised for the remaining databases (CHB-MIT, AES, and Epilepsy Ecosystem);
- Comprehensive evaluation and comparative analysis of the model's performance when applied across these four distinct databases.

1.3 Seizure Prediction Limitations

Predicting epileptic seizures presents substantial challenges primarily due to the complex nature of epilepsy. A significant proportion of EEG recordings available for use are collected during pre-surgical monitoring, which does not accurately represent the daily seizure activity of patients. This discrepancy arises because patients undergoing pre-surgical monitoring typically undergo

medication withdrawal and experience sleep deprivation, factors that do not reflect their usual conditions. Although databases containing long-term data exist, they are often only partially accessible, providing limited data and information. Additionally, these databases often lack critical information essential for seizure prediction, such as epilepsy type, focus location and lateralization, vigilance state, seizure onset and end times, medication details, and more. The available databases also suffer from a lack of data organization and standardized structures, making it challenging to establish meaningful comparisons between them [14].

Among the foremost challenges is the marked diversity in seizure types and epileptic syndromes, which vary significantly among patients. This diversity complicates the creation of a universally effective algorithm. Additionally, the relatively rare occurrence of epileptic seizures results in a notable data imbalance, which can lead to classifier specialization on the interictal class [15, 16].

Despite the valuable role played by the EEG in seizure prediction, due to its complexity it is still not fully understood, complicating the analysis and interpretation of EEG data. The precise determination of the preictal period is crucial for effective seizure prediction, but consensus regarding its ideal duration also remains elusive. Furthermore, evidence suggests that the preictal period can vary between patients and even between seizures in the same patient, amplifying the challenges associated with its identification [15, 17].

Concept Drifts (CDs) are also a key concern. These drifts denote alterations in a patient's susceptibility to seizures, influenced by numerous factors, including circadian rhythms, vigilance levels, sleep patterns, and adjustments in medication. These CDs introduce supplementary complexities and can have implications for the effectiveness of predictive models [14, 18, 19].

These limitations bring attention to the inherent complexity of predicting epileptic seizures and highlight the ongoing need for research and innovative solutions in this critical area of clinical neurology.

1.4 Structure

Beyond the introductory section, this document comprises five additional chapters:

Chapter 2 provides essential information about epilepsy, EEG, an introduction to the seizure prediction field, and the concept of CDs.

Chapter 3 offers an extensive overview of the literature concerning EEG seizure prediction and introduces the databases employed in this study.

Chapter 4 comprehensively describes the entire methodology employed, including necessary adaptations for each of the analyzed databases.

Chapter 5 presents the results achieved for each database, accompanied by interpretative analysis and cross-database comparisons.

Chapter 6 concludes this thesis by summarizing its principal conclusions and discussing future perspectives.

2

Background concepts

This chapter covers the fundamental concepts for a transparent background understanding of this document's topic. It begins with Section 2.1, which delves into concepts and definitions related to epilepsy and seizures, providing a solid foundation. Section 2.2 examines the Electroencephalogram (EEG) signal and its significance in epilepsy. Section 2.3 covers current treatment and therapeutic options, offering a comprehensive view of the clinical context. The fundamental principles underlying seizure prediction are clarified in Section 2.4, while Section 2.5 addresses concept drifts relevant to seizure prediction. Finally, Section 2.6 summarizes the key conceptual elements covered in this chapter.

2.1 Epilepsy and Seizure Concepts

About 1% of people worldwide have epilepsy, one of the most prevalent nervous system disorders [20]. The International League Against Epilepsy (ILAE) and the International Bureau for Epilepsy (IBE) conceptualized epilepsy as "*a disorder of the brain characterized by an enduring predisposition to generate epileptic seizures and by the neurobiological, cognitive, psychological, and social consequences of this condition*" in 2005 [21].

Considering that the previous definition requires at least one occurrence of an epileptic seizure, it is also essential to define it as "*a transitory manifestation of signs and/or symptoms due to abnormal excessive or coordinated neuronal activity in the brain.*"

The ILAE created an operational, clinical definition of epilepsy in 2014 to have a more helpful terminology for clinical use and to be consistent with how epileptologists interpret epilepsy [22]. According to this practical viewpoint, epilepsy is considered a brain disease rather than a problem that can manifest as any of the following symptoms:

1. "*At least two unprovoked (or reflex) seizures occurring >24 h apart.*"
2. "*One unprovoked (or reflex) seizure and a probability of further seizures similar to the general recurrence risk (at least 60%) after two unprovoked seizures, occurring over the next 10 years.*"
3. "*Diagnosis of an epilepsy syndrome.*"

This approach enables early treatment by increasing clinicians' awareness of the possibility of recurrence following a single unprovoked incident. "Unprovoked" refers to the absence of a transient or reversible component that would typically lower the threshold and trigger a seizure at that moment.

2.1.1 Classification of Epilepsy

The ILAE also reviewed the classification of epilepsy diagnoses in 2017. The key was to use more straightforward nomenclature, allowing more flexibility and transparency and adding the lack of seizure types. Figure 2.1 illustrates this new classification, which consists of three ordered states. The seizure type comes first, then the epilepsy type, and the epilepsy syndrome [23].

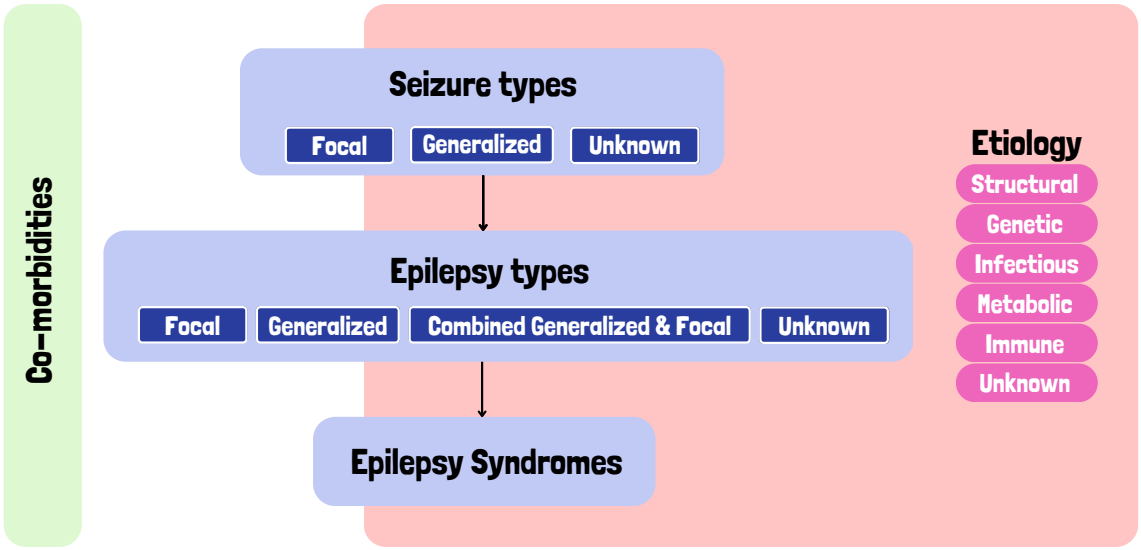

Figure 2.1: ILAE 2017 framework for classification of epilepsies. Adapted from: Scheffer et al. (2017) [23].

The etiology is present throughout each classification level, as it affects the treatment of a patient, whether as a result of genetic variables, networks involved, or clinical trials, among others. However, this document will not discuss this topic.

2.1.1.1 Seizure Types

In order to diagnose epilepsy, the first step for a clinician is to assess whether a particular episode exhibits seizure features and if it derives from an abnormal electrophysiological discharge within the brain. According to the classification shown in the Figure 2.2, it is, therefore, necessary to classify the seizure into one of the recognized categories. Since this classification is not hierarchical, if insufficient or ambiguous information exists, specific rows may be purposefully excluded from this classification [24].

Knowing the seizure's origin is crucial for its classification. If the starting point remains obscured, the seizure is considered an unknown onset seizure. Seizures originating in networks limited to one cerebral hemisphere are known as focal seizures. Bilaterally dispersed networks that span both hemispheres originate and identify the generalized seizures.

The remaining classification levels are entirely optional. The next level is awareness, which refers to self-awareness and environmental awareness, even when it is immobile. It is an essential characteristic in the classification of focal seizures. However, it is not a classifier for generalized onset seizures since most seizures cause compromised or complete loss of consciousness [24, 25].

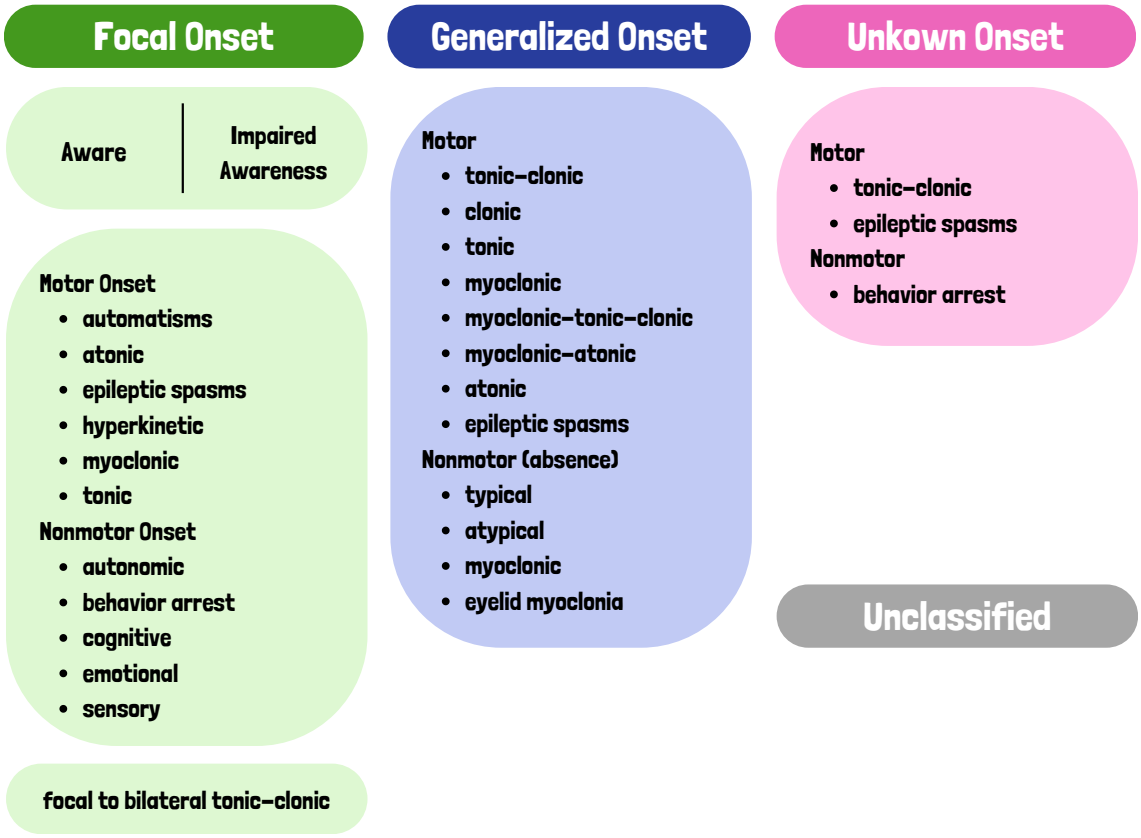

Figure 2.2: ILAE 2017 expanded framework for classification of seizure types. Adapted from: Fisher et al. (2017) [24].

For focal and generalized seizures, the following classification level is optional and can be either motor or non-motor, depending on the seizure's first prominent sign or symptom. Unless non-motor signals are significant, motor signals often prevail when both signals are present. Unknown onset seizures may be referred by unclassified or with additional attributes, such as motor or nonmotor [24]. Seizures with patterns that do not fall within the ILAE classification categories or with insufficient data are called unclassified seizures.

Due to its prevalence and severity, the category "generalized onset tonic-clonic" is the most significant among the several types of seizures. These seizures are described as violent, accompanied by a loss of consciousness and severe autonomic dysfunction. A clonic seizure involves bilaterally rhythmic jerking, and it can happen alone or in conjunction with tonic activity, with a bilateral increase in limb tone [26].

Other factors, which clinicians frequently examine, must be considered in addition to these. For a comprehensive assessment, recording the state of vigilance at the time of the seizure (awake, REM, non-REM stages I-IV), as well as the location of the seizure onset in terms of brain lobes (frontal, temporal, central, occipital, and parietal) and hemispheres (left, right, and bilateral), is a common approach.

2.1.1.2 Epilepsy Types

The next step in classification is to determine the type of epilepsy for which the patient must meet the criteria for epilepsy as established in 2014. As it considers information about the overall clinical picture, image, genetics, examinations, and others, and the possibility of having different types of seizures, the classification of the type of epilepsy is broader than the classification of seizures [23, 27].

Epilepsies share the exact characterization as seizures, exhibiting three main types: focal, generalized, or unknown. In addition, the system identifies a new category: combined focal and generalized epilepsy [28]. It is referred to as unknown epilepsy when the clinician knows the patient has epilepsy but cannot specify which type due to a lack of information, an EEG recording, a video or an imaging study.

The patient with focal epilepsy may suffer various seizures, such as focal aware seizures, focal impaired awareness seizures, focal motor seizures, focal non-motor seizures, and focal to bilateral tonic-clonic seizures. The interictal EEG in these circumstances typically reveals focused epileptiform discharges. This category of epilepsy comprises seizures involving only one cerebral hemisphere and unifocal and multifocal disorders.

Absence, myoclonic, atonic, tonic, and tonic-clonic seizures, as well as other types of seizures, may occur in people with generalized epilepsies. Typically, the patient's EEG shows generalized peak-wave activity. Patients who experience both generalized and focal seizures fall under the combined focal and generalized epilepsy category. The interictal EEG reveals visible epileptiform activity and generalized spike-wave discharges, although the existence of epileptiform activity is not necessary for diagnosis [23].

2.1.1.3 Epilepsy Syndrome

Epilepsy type is distinct from epilepsy syndrome. A diagnosis of epilepsy syndrome refers to clusters of features that occur together, allowing the acquisition of more detailed information than a diagnosis of a specific type of epilepsy. Although there is no official ILAE categorization, most syndromes have well-known names [27].

These features include seizure types, EEG, and imaging resources. It usually contains age-dependent features such as age at onset and remission, seizure triggers, diurnal variation, and prognosis [23]. Proper diagnosis of epilepsy syndrome is critical since studies have demonstrated that specific Antiepileptic Drugs (AEDs) can exacerbate seizures in various epilepsy syndromes [29].

TLE

The most prevalent epilepsy syndrome is Temporal Lobe Epilepsy (TLE), exclusively represented among patients within the EPILEPSIAE data subset employed for this project. TLE is a broad term for epilepsy conditions marked by focal seizures brought on by lesions in the temporal lobe or otherwise mediated by temporal lobe structures. However, the ILAE's classification scheme does not include TLE as a distinct syndrome.

Most clinicians distinguish Mesial Temporal Lobe Epilepsy (MTLE) from neocortical or lateral temporal lobe epilepsy. MTLE is known to exhibit high drug resistance and is the epileptic syndrome where most surgeries are performed. This distinction becomes crucial when considering these patients' mechanisms and ongoing therapy.

2.1.2 Seizure Clusters

Seizure clusters, commonly referred to as Acute Repetitive Seizures (ARS), describe the occurrence of consecutive seizures grouped, often with shorter interictal periods than what is considered typical (ranging from several hours to minutes). These clusters predominantly manifest in patients with Drug Resistant Epilepsy (DRE) and harm their quality of life, linked to several complications. Inadequate management of these clusters may lead to progressing into status epilepticus, a more severe and potentially life-threatening condition. The lack of a standardized clinical definition for clusters leads to variations in the criteria used to classify them across different studies. Some studies define clusters as at least three seizures within 24 hours [30, 31, 32], while others consider it to be 2-4 seizures within 48 hours [33].

2.2 EEG

Due to its relatively low cost and ability to show the physiological signs and manifestations of abnormal cortical excitability that underlie epilepsy, EEG is crucial in diagnosing and treating patients with seizure disorders. Neurons are responsible for enabling communication within the brain through electrical impulses. In its most basic description, an epileptic seizure resembles a short circuit characterized by irregular electrical activity in the brain. Consequently, what the EEG captures corresponds to the cumulative effect of electric fields generated by millions of these cells [34, 35].

Therefore, electrophysiological brain signals captured on EEG are a complex variety of patterns reflecting the activation of numerous neural networks. Some patterns are transient, consisting of sharp brain waves that last only one or two cycles, while others are long-term oscillations (see Figure 2.3) [36].

Oscillatory activity, which has stationary features during a brief EEG segment, is regarded as "normal" or spontaneous. Bands divide their frequencies, with delta activity being the most prevalent in the lowest frequency range (2-4 Hz). Theta rhythms are present in the 4-8 Hz range, while alpha activity depicts the calm waking state from 8 to 13 Hz. Beta activity is predominant at frequencies between 13 and 30 Hz, and gamma activity is present above 30 Hz [37]. The various frequency ranges produced by the neurological system's various operations are influenced by various parameters, including age and state of alertness, among others [35].

The transient or "abnormal" waveform adopts specific waveforms and exhibits short-term non-stationary characteristics. There are two types of transients: normal and abnormal. Examples of transients identified as abnormal epileptic phenomena are spikes, polyspikes, spike and wave complexes, sharp waves, and sharp and slow wave discharges. Within the category of abnormal transients, non-epileptiform transients are also identified, such as periodic complexes

and triphasic waves. Numerous sleep potentials, including vertex waves, K complexes, positive occipital sharp sleep transients, and benign epileptiform sleep transients, are examples of normal transients [37, 38].

Artifacts are recorded electrical potentials that do not originate in the brain and frequently imitate actual EEG activity, which makes it challenging to distinguish between the transients mentioned above when they are present. One way to classify them is by dividing them into groups based on source, persistence, and amplitude. They can come from the patient (e.g., muscle activity, eye blinking, chewing, and cardiac impulses) [39, 38], external interference (ambient electromagnetic interference, which occurs at frequencies of 50 or 60 Hz), or electrodes and leads [37, 40].

Oscillation and transient can coexist or, in some circumstances, can be directly connected through phase-resetting processes. Investigating these patterns requires the ability to characterize their spatiotemporal properties, which is not simple accurately. A significant difficulty lies in the frequency bands of transient and oscillatory activities that can overlap [36].

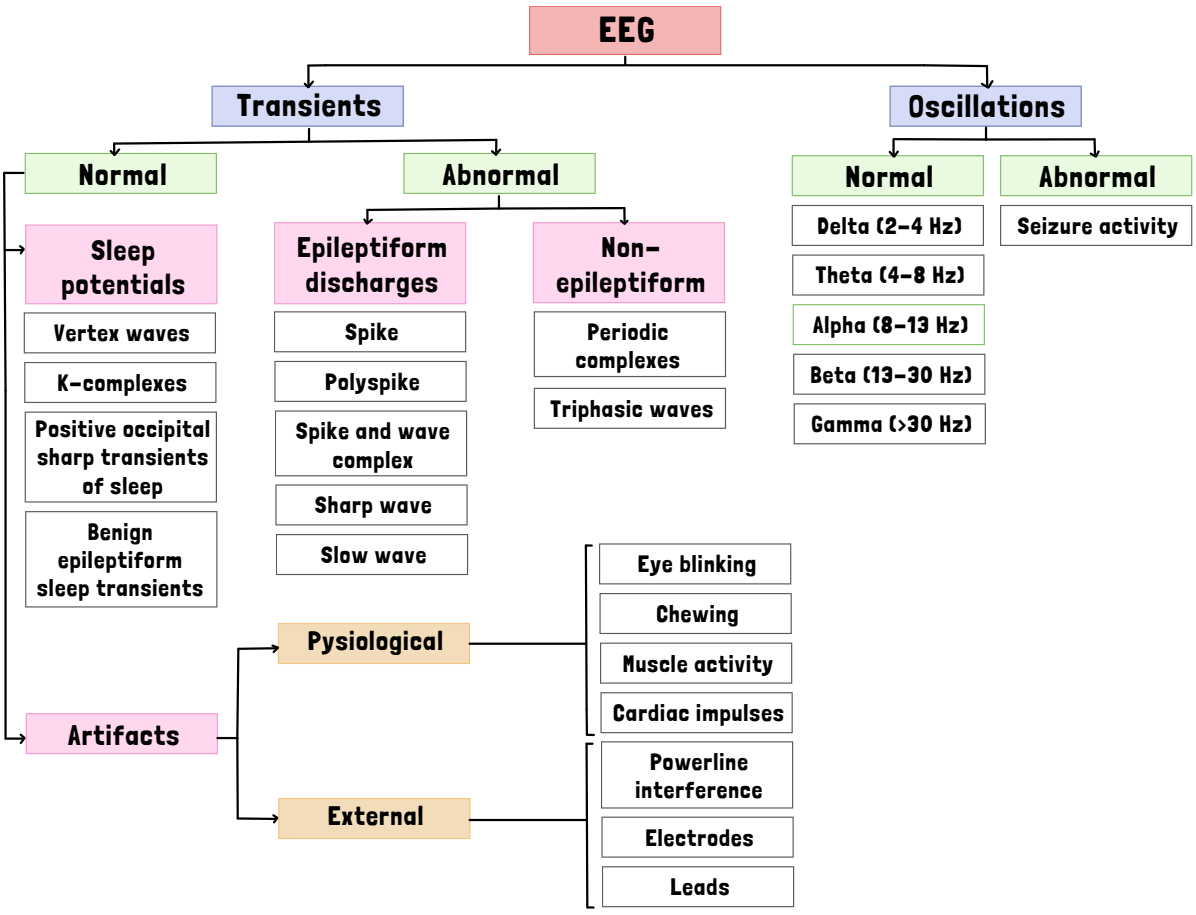

Figure 2.3: EEG activity categorization. Adapted from: Sanei and Chambers (2013) [41].

2.2.1 Signal Acquisition

The EEG is critical for obtaining most of the information required to diagnose epilepsy, as it can define rapid changes in current flows due to its high temporal resolution. However, it lacks spatial resolution since the number of electrodes, positioning, and head features constrain measurements. Measurements on different spatial scales involve performing macroscopic non-invasive recordings obtained through the scalp or employing surgical procedures that enable intracranial registration [42].

2.2.1.1 Scalp EEG

It is a simple, low-cost method typically used as a diagnostic tool. At times, such measurements can provide sufficient information, while in other instances, they merely serve as an initial step toward conducting more in-depth intracranial recordings [42]. EEG scalp detection involves "synchronous" brain activity. As a result, most epileptiform discharges recorded directly on the cortical surface are either invisible on the surface EEG or do not sufficiently reveal their epileptic origin [38].

The signal is influenced in various ways by passing through several layers of non-neural tissue (cerebrospinal fluid, skull, and scalp) [42]. This acquisition approach cannot effectively record lower amplitude faster frequencies in the beta and gamma bands due to the prevalence of extracranial artifacts, primarily muscular [38].

A standard electrode positioning system called the international 10-20 system (see Figure 2.4) enables data comparison between patients and the patient himself [42]. The relative distances between cranial landmarks on the head surface are used in this system to describe head surface locations. Electrodes on the left receive odd numbers, while those on the right receive even numbers. The suffix "Z" is allocated to those in the midline. The prefix "F" indicates electrode placement in the frontal regions, whereas "C", "T", "P", and "O" indicate electrode placement in the central, temporal, parietal, and occipital regions, respectively [38, 43].

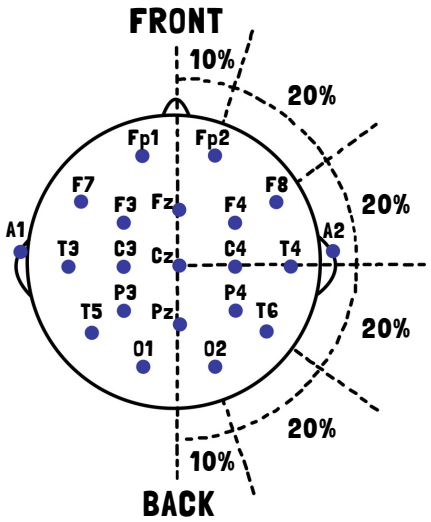

Figure 2.4: International 10-20 system used for electrode placement. Adapted from: Varsavsky et al. (2011) [42].

Different electrode combinations are employed in "channels", with each channel including two electrode inputs, the second being the next electrode in the line or a reference, placed in bipolar or referential montages (see Figure 2.5), respectively.

In the organization of bipolar montages, chains of electrodes are frequently arranged in a straight line. The second input of the first channel becomes the second channel's first input, allowing the localization of maximums and minimums of electric fields by the so-called "phase reversal". This type of montage is generally preferred because it produces "cleaner" traces due to the proximity of the electrode pairs, which leads to more efficient noise cancellation. The anteroposterior longitudinal bipolar or "double banana" montage (see Figure 2.5a) is the most commonly used in clinical practice [44].

Referential or monopolar montages are bipolar arrangements except that the reference electrode, which serves as the second input to each channel, is located farthest from the first electrode position. The electrodes are typically placed on the scalp, although they can also be positioned on the mastoids or earlobes and, less commonly, across the cervical spine or nose [38].

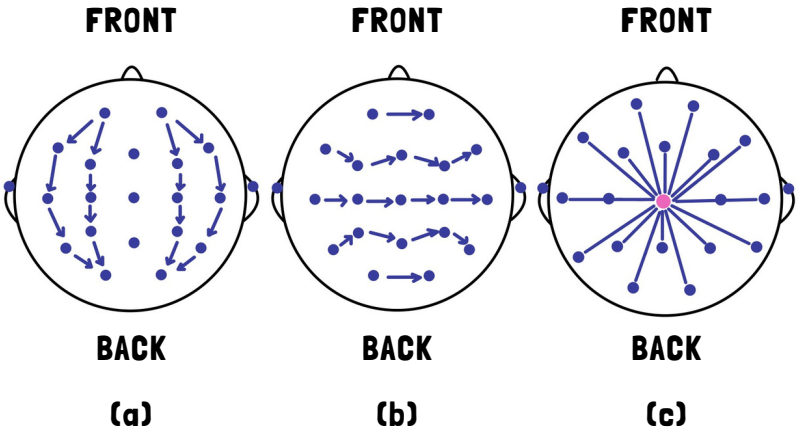

Figure 2.5: EEG montages in which scalp electrodes are used as reference. (a) Longitudinal bipolar montage. (b) Transversal bipolar montage. (c) Referential montage (to Cz). Adapted from: Varsavsky et al. (2011) and Beniczky et al. (2020) [42, 45].

Long-term recording of brain electrical activity is necessary, as it increases the likelihood of capturing seizures. The traditional method of collecting EEGs requires a time-consuming setup process that includes skin preparation, electrode attachment, gel application, mounting, and connection selection. In addition, it takes the patient out of their typical environment, which restricts the patient's natural behavior while signal acquisition occurs. As a result, in the past 20 years, innovative non-invasive mobile electroencephalography solutions have been created to overcome the drawbacks of traditional clinical EEG and enhance the monitoring of patients with long-term conditions. Despite the availability of mobile technologies, their adoption remains quite limited [46, 47].

2.2.1.2 iEEG

Intracranial recordings are typically performed during pre-surgical analysis to identify the specific brain areas needing resecting [42]. This diagnostic procedure is crucial in mapping the seizure onset zone, essential for targeting the epileptogenic zone. The epileptogenic zone refers to the specific region in the brain that is indispensable for initiating seizures. By surgically removing the epileptogenic zone, it is possible to achieve seizure freedom for the patient. The epileptogenic zone is the smallest cortical area necessary to remove the patient from seizures. Specifying the safety boundaries for removing this area during surgery becomes necessary [48].

In this scenario, the placement of electrodes lacks standardization, with placement decisions tailored to each patient's needs and circumstances [42]. Electrodes of different types, including subdural electrodes (grid or strip electrodes) placed on the brain's surface or depth electrodes that undergo stereotactic implantation within the brain, enable the acquisition of recordings. Each has advantages and downsides and is thus utilized based on the clinical context [49].

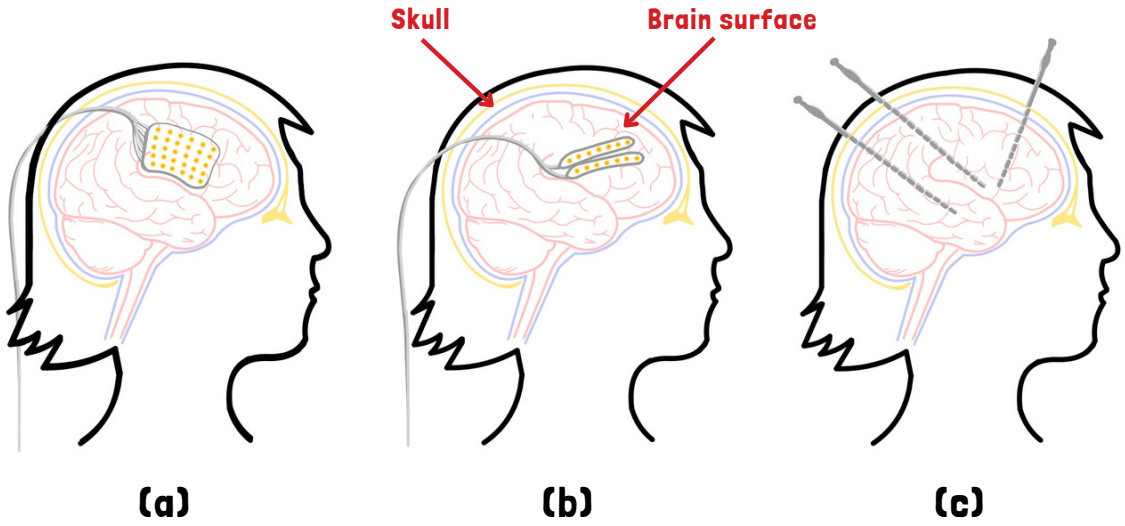

Figure 2.6: Placement electrodes for intracranial recordings: grid (a) and strip (b) electrodes positioned on the brain surface, while depth electrodes (c) inserted into deeper brain regions. Adapted from: [50].

The benefits of the intracranial EEG signal include (generally) much less contamination with artifacts, closer proximity to seizure-generating sites, allowing for high spatial resolution, and fewer problems with reference electrode - provided an extracranial reference is used [38]. Another significant advantage of Intracranial Electroencephalogram (iEEG) over scalp EEG is the ability to record at a considerably higher frequency range of detectable brain signals [48].

On the other hand, intracranial recordings are more invasive and cannot be used in an outpatient setting to track a patient's seizure status in their familiar environment [17]. Furthermore, because the implanted electrodes can only detect activity in a small area around them, they cannot detect any previous or concurrent activity in nearby or distant areas [51].

2.3 Treatment and Therapeutics

The principal objectives inherent in any treatment or therapeutic methodology for epilepsy encompass suppressing seizures while mitigating adverse effects on the patient within the shortest conceivable span. The pursuit of these targets collectively poses significant difficulties [52].

2.3.1 Antiepileptic Drugs

The decision to initiate treatment requires a meticulous evaluation of the risk-to-benefit ratio and the patient's preferences, given the enduring nature of the treatment for a minimum duration of two years and, in some circumstances, for the entirety of the patient's life [53].

The first line of treatment is the intake of AEDs. The primary goal of administering AEDs is to counterbalance the disturbed excitation and inhibition equilibrium resulting from the hyper excitatory or hypersynchronous neuronal activity observed in the condition. To accomplish this objective, AEDs can modulate voltage-gated ion channels, enhance inhibitory mechanisms, or attenuate excitatory mechanisms, depending on their specific mechanism of action [54].

Approximately two-thirds of epilepsy patients achieve seizure freedom through AEDs [53]. Nonetheless, despite the fraction of positive cases observed and the existence of accessible AEDs, approximately one-third of individuals who have epilepsy endure DRE, a condition characterized by persistent seizure episodes throughout their lifetime. This condition is associated with an increased likelihood of injuries, lower socioeconomic status, compromised quality of life, cognitive impairments, and mood fluctuations. Moreover, behavioral disorders, including depression and anxiety, manifest more frequently among these patients and their families than among the broader populace [55].

The emergence of novel AED in the past few decades has proven beneficial because they have introduced distinct adverse effects profiles. However, the proportion of patients with DRE remained virtually unchanged, indicating that the new drugs only impact the treatment of patients already treated with the existing drugs [52].

2.3.2 Surgery

After the failure of two well-tolerated antiepileptic drug treatment regimens, the consideration of surgery becomes imperative [56]. This surgical procedure involves resecting the specific brain region responsible for generating seizures, called the epileptic zone. The medical community widely acknowledges it as the most effective treatment modality for patients who have DRE [53].

Determining the suitability for effective epilepsy surgery relies on a thorough pre-surgical assessment, allowing for the precise delineation of the epileptogenic zone and crucial brain areas. This assessment enables the development of a personalized resection plan for each patient. The epileptogenic zone is the minimal cortical area that, when removed, leads to seizure freedom while considering the potential for postoperative morbidity [53].

Within this evaluation, it is crucial to acquire a sufficient number of seizure records. The utilization of provocation methods, such as sleep deprivation and gradual withdrawal of AEDs,

aims to reduce hospitalization duration and associated expenses while enhancing the performance of the recordings. However, it is essential to exercise caution and gradually conduct the drug withdrawal process, as it may trigger tonic-clonic seizures, thereby elevating the risk of Sudden Unexpected Death in Epilepsy (SUDEP), seizure clusters, or even life-threatening status epilepticus [57].

Surgical treatment offers notable benefits, considering the limited number of patients who achieve seizure freedom after failing to respond to two appropriate AEDs. Despite the substantial growth in the number of established epilepsy surgery centers, the volume of therapeutic, surgical procedures performed for epilepsy has not experienced a corresponding increase [58].

2.3.3 Neurostimulation

Neurostimulation refers to the utilization of electrical stimulation on a specific structure within the nervous system, employing various techniques to interfere with and potentially prevent or terminate ictal events, aiming to decrease the occurrence of seizures [59]. Neurostimulation is a palliative treatment, and only a subset of individuals may achieve seizure freedom for more than 12 months. The consideration of this therapeutic option is often appropriate for patients with refractory epilepsy who are unwilling or ineligible for surgical intervention [60].

Among the invasive neurostimulation procedures, three commonly utilized methods consistently demonstrate both safety and efficacy: Vagus Nerve Stimulation (VNS), Deep Brain Stimulation (DBS), and Responsive Neurostimulation (RNS) [61, 62]. VNS stimulates the vagus nerve, RNS focuses on the cortex, and Anterior Nucleus of Thalamus Deep Brain Stimulation (ANT-DBS) specifically targets the anterior nucleus of the thalamus. Regarding device placement, VNS exclusively resides within the chest, featuring an electrode encircling the left vagus nerve and a subcutaneously implanted pulse generator in the upper left chest region. In contrast, the RNS involves a device implanted in the cortex, while ANT-DBS requires sensor placement in the Anterior Thalamic Nucleus (ATN) and a chest-implanted pulse generator. All these specificities, along with additional details, are visually presented in the accompanying Figure 2.7.

The neurostimulation techniques can be further categorized based on the mechanism employed, distinguishing between open-loop and closed-loop systems. DBS and older-generation VNS are examples of open-loop systems, whereas RNS and newer-generation VNS operate as closed-loop systems [62].

When deciding between these three therapies, several factors influence the choice, including the patient's age, type of epilepsy, and location. All three therapies are suitable for adults with focal epilepsies. VNS may be an option for four-year-old and older children with focal or generalized epilepsy. VNS and RNS can be offered to individuals with 2-drug-resistant epilepsy, while the ANT-DBS requires 3-drug resistance. Regarding geographic approval, many global regions have approved VNS, whereas RNS exclusively holds approval in the United States of America (USA), and ANT-DBS has gained approval in North America, Europe, and other countries [60].

Comparisons directly assessing these three techniques in controlled studies have yet to be

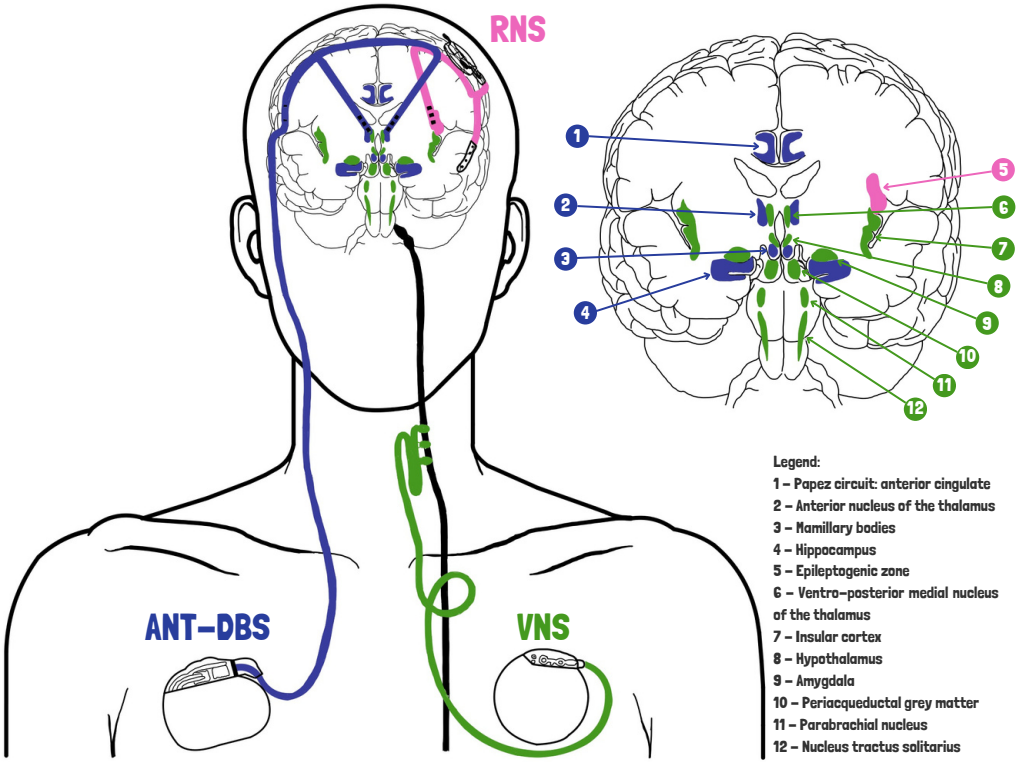

Figure 2.7: Approved neurostimulation therapies in epilepsy and brain targets for each neurostimulation approach according to sites of stimulation and known primary anatomical pathways. Adapted from: Ryvlin et al. (2021) [60].

conducted, primarily due to the absence of standardized or equivalent stimulation parameters across the devices. Nonetheless, all three approaches have shown that many patients achieve at least six months without seizures and are generally well tolerated. Additionally, they have been associated with statistically significant improvements in quality of life, although the clinical significance of these changes remains unclear [59]. Despite this, when considering data from the blind period of the main controlled trials, DBS and RNS have demonstrated better performance compared to VNS. However, VNS has certain advantages, such as easier implantation, not requiring advanced equipment, shorter surgical procedures, potentially shorter hospital stays, and no risk of intracranial complications [62].

Device-based neurostimulation offers advantages in terms of tolerability compared to AEDs. However, it is crucial to consider the specific risks of adverse events and some disadvantages associated with neurostimulation. A comparison between the three neurostimulation solutions is available in the provided Table 2.1.

Drawbacks of neurostimulation techniques include the requirement for surgery, battery replacement, and frequent visits for stimulation parameter adjustments. Due to these limitations and the lack of robust evidence guiding the selection of neurostimulation over AEDs, choosing the most appropriate treatment remains an individual decision based on risk-benefit analysis and personal preference for each case [60]. Moreover, it is imperative to regard current stimulation techniques as a variant of palliative intervention and recognize that they do not substitute more definitive resective or ablative therapies if it is safe to administer them [63].

	VNS	RNS	ANT-DBS
Category of treatment	Palliative		
Ideal epileptogenic zones	Not localised, multifocal, or not resectable	Bitemporal or eloquent focus	Bitemporal, multifocal, or not localised
Level of accessibility	Moderate	Low	
Level of invasiveness	Moderate	High	
Risk of therapy-induced brain lesion	None	Low	
Chance of long-term seizure freedom	Low		
Average gain in quality of life	Moderate		
Level of adherence	High		

Table 2.1: Key characteristics of the presently approved neurostimulation therapies. Adapted from: Ryvlin et al. 2021 [60].

2.3.4 Rescue Medication

Urgent measures are required in acute seizure emergencies, such as prolonged seizures, acute seizures, status epilepticus, cluster seizures, and out-of-hospital seizures, to avert neuronal injury and mitigate associated morbidities [64]. In such cases, established guidelines recommend the prompt administration of a rescue medication, typically a Benzodiazepine (BZD), within 5 to 10 minutes after the seizure initiates [65].

Patients diagnosed with epilepsy may require access to at-home rescue medication, particularly those with an increased vulnerability to prolonged seizures. However, studies have indicated low utilization of these rescue drugs in home environments, which presents a problem as most seizures initiate in a pre-hospital context. In the absence of available rescue medication, treatment can only start when emergency medical services arrive or when the patient reaches the hospital, which is typically beyond the 10-minute timeframe preceding the onset of the seizure [65].

Multiple factors, including the infrequent prescription of these drugs, insufficient training, or a lack of involvement from educational institutions, contribute to the low percentage of rescue drug utilization in at-home settings. One possible explanation for the reluctance to prescribe rescue medication for the general epilepsy population may be the apprehension of adverse effects, particularly respiratory depression [64]. Nonetheless, studies have shown that significant adverse effects usually occur and intensify only after administering more than two BZDs, suggesting that most patients can safely receive at least one dose [65].

2.3.5 Warning Devices

Researchers have undertaken extensive research to investigate intervention devices and their potential for improving the quality of life for patients. A crucial aspect of these devices is their ability to issue timely alarms when a seizure is impending, achieved by continuously monitoring changes in the biosignal. This functionality allows patients or their caregivers to take measures to mitigate the consequences of the seizure or facilitate the administration of rescue medication. These devices incorporate algorithms that analyze long-term signals to accomplish this objective, triggering alarms while disregarding data segments contaminated by artifacts. Notable EEG acquisition technologies include UNEEG SubQ, EpiMinder Subscalp, and Byteflies Sensor Dots [66].

The first human clinical trial of an implantable alerting device, the NeuroVista Seizure Advisory System, holds significant relevance in this domain, marking the first successful implementation utilizing ambulatory EEG data. In this trial, a continuous recording device was surgically implanted in 15 patients with refractory epilepsy, ranging from 6 months to 3 years in duration. The system involved the connection of intracranially implanted electrodes to a subdermal telemetry unit implanted in the thorax through subdermal wires. This telemetry unit wirelessly transmitted EEG data to a portable unit, as illustrated in the accompanying Figure 2.8. The device continuously monitors brain activity by recording the EEG using intracranial electrodes, giving patients a probability assessment of experiencing a seizure [14, 67, 68].

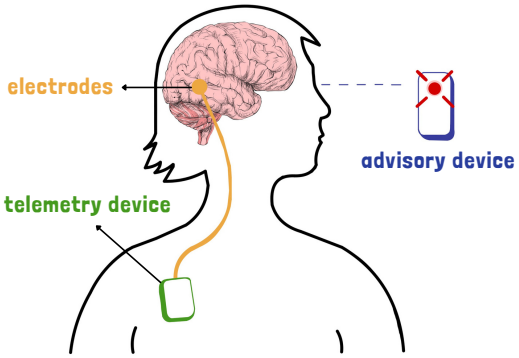

Figure 2.8: Ambulatory seizure warning system. Adapted from: Kuhlmann et al. (2021) [14].

The recent rapid progress in wearable devices provides non-invasive alternatives. Despite the swift improvement in technology and the availability of new devices, the utilization of wearable devices for the daily clinical management of epilepsy remains rare, lacking sufficient evidence to support their potential benefits adequately. The launch of the My Seizure Gauge challenge aimed to develop a personalized seizure advisory system device and incorporated Empatica E4, Byteflies Sensor Dots, and Epilog data. These devices enable the analysis of signals beyond EEG, including Accelerometry (ACC), Blood Volume Pulse (BVP), Electrodermal Activity (EDA), Photoplethysmography (PPG), Electromyography (EMG), Heart Rate (HR), and temperature [69]. Currently, alongside the devices previously discussed, there exists a wide variety of commercially accessible wearable devices, and an increasing number of these devices are receiving regulatory approval for the control of specific types of seizures [70].

2.4 Seizure Prediction

The unpredictability of epilepsy is a perpetual worry for patients. Developing new therapeutic strategies that can anticipate seizures would help overcome some of the challenges presented by this characteristic. The primary aim of seizure prediction is to develop tools to promptly notify patients of an upcoming seizure based on online physiological data by activating alarms [15].

Four distinct stages divide a seizure event, including the preictal stage before the seizure onset, the ictal stage throughout the seizure, the postictal stage following the seizure offset, and the interictal stage between seizures. These stages are visually represented in the accompanying Figure 2.9 [71].

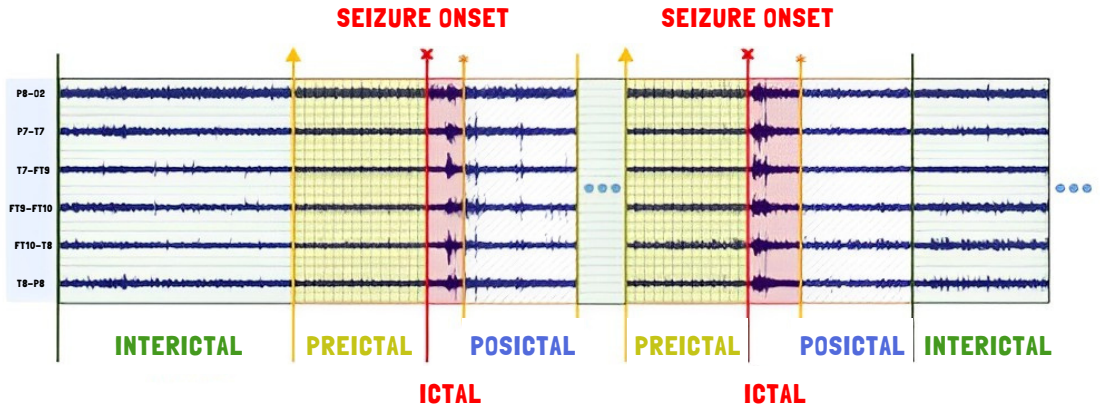

Figure 2.9: Periods of a seizure episode represented on an EEG signal. Adapted from: Cui et al. (2018) [71].

Accurate seizure prediction relies on distinguishing the preictal from the interictal period, which depends on identifying seizure biomarkers that can capture the transition from a seizure-free state to a seizure. The preictal stage poses the most significant challenge in correct annotation because it lacks a recurring pattern, presenting the primary obstacle in seizure prediction [14]. Customized algorithms for patients have demonstrated greater efficacy than general models in light of the heterogeneity of seizures and epilepsies [17].

2.4.1 Seizure Onset

A key aspect in the prediction of seizures is the identification of the onset time. The onset time can be either electrographic or clinical. Detecting the first clinical symptoms determines the clinical onset, while the first visible changes in the EEG recordings establish the electrographic onset. Since the EEG signal forms the basis of these models, prediction algorithms typically consider the electrographic onset [17]. Researchers have noted that initiating an electrographic event may precede the onset of clinical symptoms in seconds or minutes [42]. An optimal intervention system could interrupt the progression of a seizure prior to the clinical onset [17].

2.4.2 Lead Seizure

It is common for seizures to occur in clusters, and predicting the initial seizure in a cluster, known as the lead seizure, is significantly more challenging. The selection of a minimum seizure-free interval by authors is a common practice to demonstrate that subsequent seizures are independent events while maintaining a balance between the necessity of a sufficient quantity of seizures and the requirement for independence. Studies have defined lead seizures as consecutive seizures separated by a minimum of 1 hour [72], 1.5 hours [73], 2 hours [74, 75], 4 hours [67, 76, 77, 78, 79], 4.5 hours [80, 81], 5 hours [18], or 8 hours [68].

2.4.3 Seizure Detection vs Prediction

Seizure detection pertains to the act of ascertaining whether seizures are currently occurring or not [82]. Early detection of epileptic seizures targets the short period between the start of observable changes in brain activity that signal the onset of an ictal episode and the emergence of clinical symptoms that affect the patient. This detection occurs just a few seconds before the first clinical symptoms, which is different from prediction techniques that look for a preictal state sufficiently long before the EEG onset. Nevertheless, the limited time available for detection offers little opportunity for intervention, if any [17, 83].

In the case of early seizure-detection algorithms, the main concern is to determine whether, following the onset of electrographic seizure activity, it is possible to prevent the seizure through stimulation or if the brain has already reached a point beyond which stimulation is ineffective and will inevitably proceed towards a clinical manifestation of seizure. If the brain has not passed the "point of no return", early detection algorithms can be employed to support responsive intervention within closed-loop stimulation systems [17, 84].

2.4.4 Forecasting vs Prediction

The concept of forecasting deviates from predicting whether a seizure will occur. Instead, it highlights identifying the brain state with a high probability of a seizure. The evaluation of the risk of seizure occurrence is possible because of the presence of cycles of Interictal Epileptiform Activity (IEA) on diverse time scales, such as circadian (over hours), multidien (over days), and circannual cycles (over years) [85, 86, 87].

The variations in IEA on circadian, multidien, or circannual temporal scales may be associated with environmental fluctuations, metabolic processes, or intrinsic brain factors like sleep homeostasis or arousal levels [88]. The critical phases of these cycles help determine distinct intervals with elevated seizure risk, commonly referred to as proictal states, thus opening the possibility of forecasting seizures over extended periods [85, 87].

The ambiguity surrounding the risk of a seizure (forecasting) and its realization in an actual seizure (prediction) has repercussions for the preictal and proictal states' concepts. The preictal phase is the period preceding a seizure, where a point of no return is assumed, typically lasting seconds to minutes. This perspective considers epilepsy a deterministic process, where increased cortical excitability will inevitably progress to seizures unless individuals take stabi-

lization measures. In contrast, the proictal state reflects a probabilistic perspective, representing antecedents that strongly constrain the probability of seizures. Consequently, seizures may or may not occur during a given proictal period, despite the high momentary risk. Figure 2.10 enables a straightforward visualization of these differences.

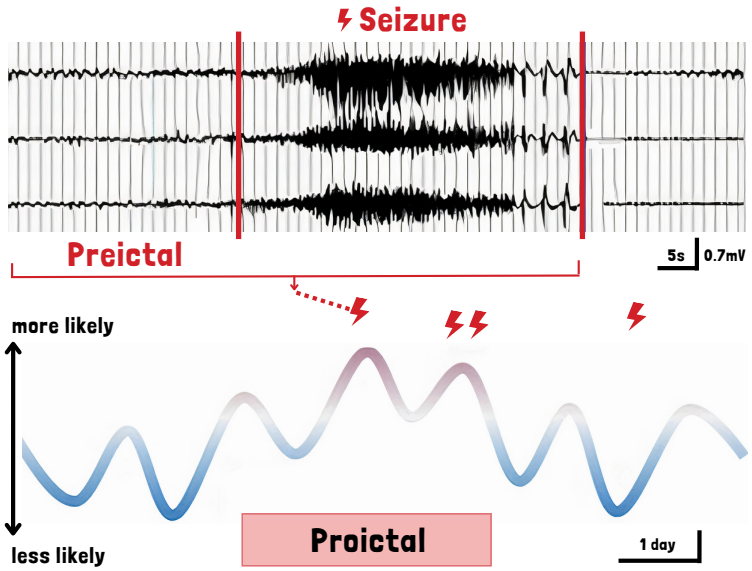

Figure 2.10: Visual representation illustrating the temporal dynamics of preictal and proictal states. Shown in this figure is an example of a daily cycle overlaid by an about-weekly cycle of seizure likelihood. Adapted from: Stirling et al. (2021) [72].

Therefore, one can compare the contrast between forecasting and predicting seizures to the disparity between gauging the likelihood of a thunderstorm and identifying the precise timing of lightning bolts, respectively [85, 87, 88].

2.4.5 Seizure Prediction Characterization

Since the 1970s, researchers have been exploring the seizure prediction domain, and by the 2000s, numerous algorithms were already using EEG signals to predict seizures. However, evaluating the suitability of an algorithm's performance for clinical implementation took much work due to the need for recognized standards. In brief, a prediction method examines successive EEG time windows and triggers timely alarms that enable intervention [17].

Winterhalder et al. [89] proposed the "seizure prediction characteristic" in 2003 to address this issue, a framework for evaluating seizure prediction techniques based on clinical, behavioural, and statistical factors. The evaluation involved two metrics adjusted to an alarm system: seizure sensitivity and the False Prediction Rate per hour (FPR/h).

Additionally, since predictive models cannot determine the exact timing of a seizure, they suggest two concepts to handle this uncertainty: the Seizure Occurrence Period (SOP) and the Seizure Prediction Horizon (SPH). The SPH represents the time frame within which a prediction tool alerts the patient to an impending seizure. It spans from the activation of the alarm to the beginning of SOP. SPH is also known as Intervention time (IT). SOP refers to the expected period of a seizure occurrence. The Figure 2.11 offers a visual representation that can assist in

comprehending the periods pertaining to the SOP and SPH.

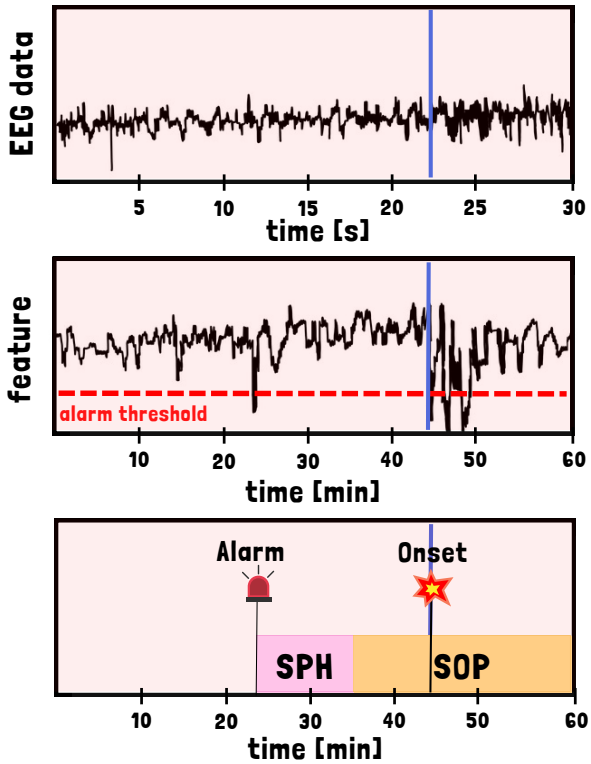

Figure 2.11: Visual representation of SOP and SPH using an EEG recording and an example of a feature extracted by a seizure prediction algorithm. Adapted from Schelter et al. (2006) [90].

If a seizure occurs during the raised alarm's SOP period, the alarm correctly predicted the seizure. Conversely, if an alarm is triggered, but no seizure occurs within the specified SOP, the alarm is considered a false one. Figure 2.12 exhibits a visual representation that elucidates the classification of alarms.

Therapeutic devices must maintain a minimum window of time corresponding to the SPH to minimize the impact of seizures effectively. A specific period, dependent on the type of intervention, is necessary for intervention systems to take effect and prevent dangerous circumstances. As a result, determining the minimum prediction horizon is critical for successful clinical application [89].

Similarly, determining a maximum time frame for SOP is necessary. According to existing literature, this period can last from several minutes to several hours, potentially affecting the performance of algorithms in the patient's daily life. To ensure the efficacy of interventions such as electrical stimulation and anticonvulsant drug administration during the SOP, they must persist for the entire period, as the exact time of seizure onset is unknown. However, prolonged interventions can lead to increased side effects, and longer SOPs can cause more significant psychological stress to patients. Hence, defining an upper limit for SOP is crucial for these reasons [89]. Ensuring patient confidence and minimizing the need for complex interventions requires using reasonable values for SPHs and SOPs, despite the challenge of achieving optimal parameter adjustment.

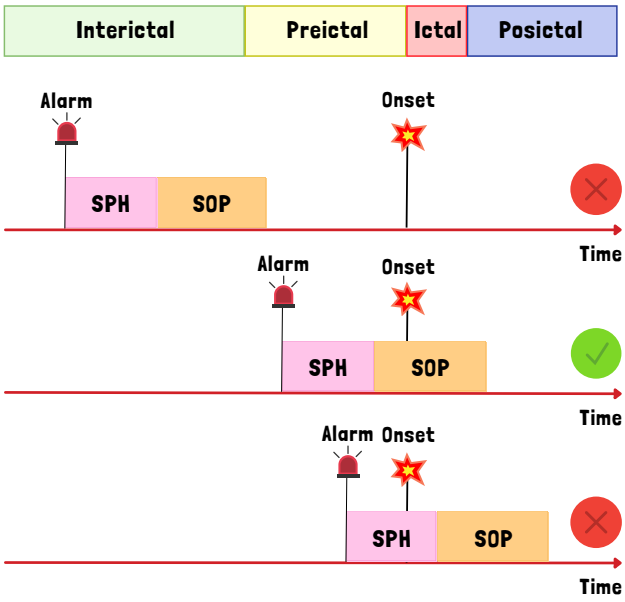

Figure 2.12: Visual representation of the true and false alarm concept in seizure prediction. Adapted from: Winterhalder et al. (2003) [89].

2.4.5.1 Performance Assessment

When evaluating the performance of a system with particular emphasis on the temporal aspects of a prediction, sensitivity and FPR/h are critical metrics. Distinguishing whether the alarm was triggered correctly or not is imperative to compute these metrics [91]. The visual representation of this distinction in alarm categories can be observed in Figure 2.12.

Sensitivity (Equation 2.1) defines the ratio between the number of accurate predictions and the total number of actual seizures. For prediction systems, FPR/h is a reliable measure of specificity. FPR/h quantifies the number of false predictions generated per hour (Equation 2.2) by dividing the number of false alarms by the interictal period's duration, during which the model may generate false alarms. An activated alarm relates to a specific SPH and SOP, and this time frame (refractory period) does not allow for triggering any additional alarms. The refractory period should be excluded from the FPR/h calculation, although some authors may not consider this.

$$SS = \frac{N_{true\ alarms}}{N_{seizures}}. \tag{2.1}$$

$$FPR/h = \frac{N_{false\ alarms}}{\triangle_{interictal} - N_{false\ alarms} * (\triangle_{SPH} + \triangle_{SOP})}. \tag{2.2}$$

The primary goal of a prediction technique is to accurately predict as many seizures as possible, with the ideal scenario resulting in a sensitivity score of 1. However, an interdependent relationship exists between sensitivity and FPR/h, whereby an increase in sensitivity generally increases FPR/h, and achieving a sensitivity score of 1 may come at the cost of numerous false alarms.

The patient experiences more adverse implications as the value of FPR/h increases. The

higher number of false alarms may make the patient complacent and ignore the alerts, leading to inadequate preparation for actual seizures. On the other hand, if the patient takes all the alarms seriously, he may experience significant unnecessary psychological stress, expecting seizures that never occur. FPR/h also influences the possibility of causing unintended outcomes in specific treatments. In cases where AEDs or neurostimulation are administered based on false predictions, there is a risk of overmedication or excessive brain electrical stimulation, leading to side effects.

Therefore, it is imperative to identify a maximum rate of acceptable false predictions from a clinical perspective. Winterhalder et al. (2003) [89] reported that the pre-surgical context generally exhibits an average of 0.15 seizures per hour, equivalent to 3.6 per day. In contrast, in everyday circumstances, the average is 0.0042 seizures per hour, corresponding to 3 seizures per month. Setting the FPR/h_{max} to 0.15 would result in approximately 50% of the alarms being false for patients under monitoring, which is deemed acceptable. However, this value becomes unthinkable in normal conditions, where it increases to 97%. Thus, the appropriate maximum value for this metric should be context-dependent and based on the average incidence of seizures [89].

The occurrence of false alarms throughout the day is also a crucial consideration for implementing a seizure prediction approach. False alarms during a patient's sleep state may be less detrimental than during wakefulness, as patients are less susceptible to harm or injury while asleep [91].

The evaluation of a seizure prediction system is distinct from traditional machine learning problems, as it involves triggering alarms. The evaluation of the binary classification of interictal and preictal samples, using sensitivity (Equation 2.3) and specificity (Equation 2.4), would be the approach for a typical Machine Learning (ML) problem, as shown in the Figure 2.13.

$$SS_{sample} = \frac{TP}{TP + TN}. \qquad (2.3)$$

$$SP_{sample} = \frac{TN}{TN + FP}. \qquad (2.4)$$

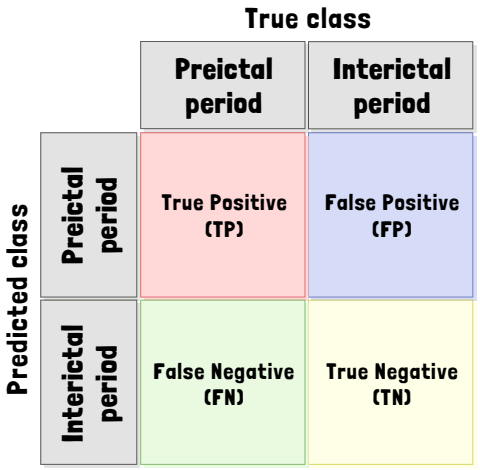

Figure 2.13: Confusion matrix for assessing sample seizure prediction.

2.4.5.2 Statistical Validation

Determining whether a prediction system is adequate for clinical use requires testing whether its performance is better than chance [15, 17]. Statistical validation techniques, such as nonspecific predictors [89, 90, 92] and surrogate analysis [92, 93, 94], are commonly employed to conduct such evaluations.

Unspecific predictors

Winterhalder et al. (2003) [89] introduced the term "random prediction" to describe a non-specific approach to seizure prediction, where alarms are activated randomly without any input from EEG. Typically, seizure prediction methods are optimized to maximize sensitivity until the false prediction rate reaches its FPR_{max}. Thus, during a brief interictal period (I), the probability that an alarm trigger is (Equation 2.5):

$$p = FPR/h \times I \tag{2.5}$$

When considering a longer time interval (W), the formula allows for computing the probability P of at least one alarm (Equation 2.6):

$$P = 1 - (1 - FPR/h \times I)^{W/I} \approx 1 - e^{-FPR/hW} for\ I \ll W \tag{2.6}$$

When $W = SOP$, this accurately reflects the sensitivity of a random prediction method since it represents the probability that at least one alarm triggers during the seizure occurrence period.

Schelter et al. (2008) [92] introduced a new approach to random prediction using a Poisson process for false predictions. The probability of triggering an alarm at any point in a time series with FP (number of false predictions) and N samples is given by Equation 2.7:

$$P_{Poiss} = \frac{FP}{N} \tag{2.7}$$

When the time interval is SOP, and it is possible to confirm that the patient is not persistently under warning, i.e., when the product of FPR_{max} and SOP is significantly lower than 1, the Equation **??** gives the likelihood of triggering at least one alarm during that interval.

$$P \approx 1 - e^{-FPR/hW} \approx FPR/h \times SOP \tag{2.8}$$

The probability mentioned above corresponds to the sensitivity of the random predictor. It acts as the basis for testing the significance level to determine if the prediction method's sensitivity can surpass it.

Nonetheless, at this level of significance, it is necessary to take other factors into account, such as the number of analyzed seizures and the dimension of the extracted feature vector (d), as an increase in the number of channels and/or measures raises the probability of chance predictions of seizures. However, machine learning models can produce a one-dimensional output (d=1) even when utilizing multi-dimensional inputs. Therefore, $d > 1$ is employed when execut-

ing multiple predictions simultaneously. Hence, the binomial distribution, as defined in Equation 2.9, allows for calculating the probability of predicting at least k out of K seizures.

$$P_{binom}(k,K,P) = 1 - \left[\sum_{1}^{j \leq k} \binom{K}{j} P^j (1-P)^{K-j}\right]^d \tag{2.9}$$

Obtaining the critical value using the following formula (Equation 2.10) allows for testing statistical significance.

$$\sigma = \frac{argmax_k\{P_{binom}(k,K,P) > \alpha\}}{K} \times 100\% \tag{2.10}$$

In summary, the random predictor has the advantage of being computationally lightweight since it does not require EEG input in its analytical expression. Nonetheless, following a Poisson homogeneous distribution, which assumes a uniform distribution of false alarms over time, may not be suitable for managing non-random seizure occurrences brought on by Concept Drifts (CDs) or drug withdrawal. Moreover, overcoming the random predictor for a small number of seizures tested can be challenging, given that seizures are rare events and models often need to be customized to individual patients.

Surrogate Analysis

Surrogate seizure predictors are generated based on Monte Carlo simulations that involve constrained randomizations of the original seizure times. Although stochastic, they share specific properties of the original data. This approach requires large computational resources; however, it provides greater flexibility than analytical random predictors, allowing multiple null hypotheses to be evaluated based on specific assumptions and constraints. As a result, if the original seizure predictor outperforms the surrogate predictors with statistical significance, it is possible to reject the null hypothesis, indicating that the developed algorithm is more effective than mere chance [15, 92].

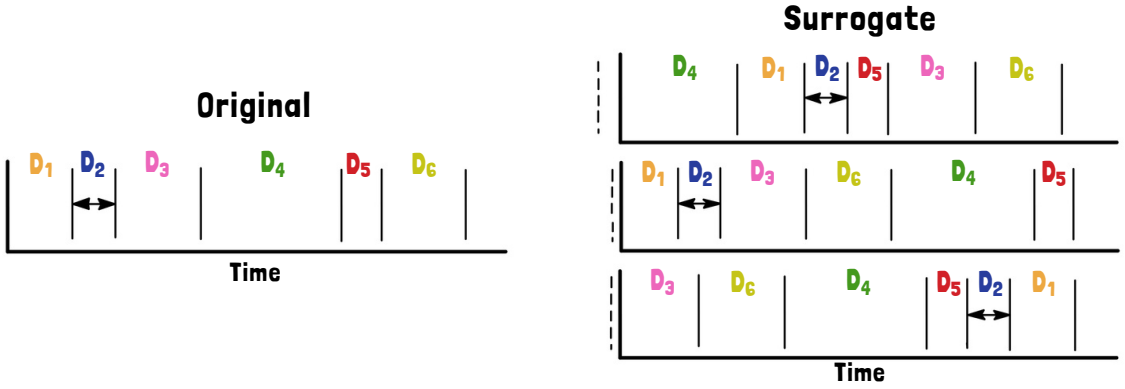

Figure 2.14: Representation of the original seizure and surrogate times bootstrapped from the inter-seizure intervals. The arbitrary onset times for the surrogates are originated through a uniform distribution and represented by the dashed vertical lines. Adapted from: Schelter et al. (2008) [92].

The seizure-times surrogate method proposed by Andrzejak et al. (2003) [94] involves substituting the original seizure times with randomly generated times. The random onset times are generated from the original interictal periods and maintain the original measurement profiles and the distribution of the interval between seizures and the total number of seizures, as illustrated in the Figure 2.14. Therefore, implementing the algorithm utilizes the same EEG data and the new seizure onset times, enabling a comparison of the performance attained here with that achieved using the original seizure onset times.

Both algorithmic and statistical analyses can be validated using this technique, thereby providing high reliability. As such, this technique found application in the statistical validation presented in this document. Nonetheless, it is essential to emphasize that the application of this method can pose challenges due to the small number of seizures captured in the EEG recordings.

2.4.5.3 Postprocessing

Typically, a post-classification process minimizes the number of false alarms, which involves regulating the classifier output using methods like Firing Power (FP) or Kalman Filter (KF).

Applying the FP method involves rounding the prediction rates to a set of binary values first, then averaging them over a sliding window of duration τ, equal to the SOP's length. Whenever the computed average value is more significant than an arbitrary threshold value, the classifier generates a prediction for the subsequent crisis. The Equation 2.11 provides the mathematical formulation for this moving average filter, utilizing $fp[n]$ and $O[k]$ as key variables. Here, $fp[n]$ represents the trigger power at time n, varying between 0 and 1, while $O[k]$ denotes the binary output generated by the classifier.

$$fp\,[n] = \frac{\sum_{k=n-\tau}^{n} O\,[k]}{\tau}. \tag{2.11}$$

The triggering of an alarm occurs when the value of $fp[n]$ exceeds this threshold. The threshold value determines the level of conservatism exhibited by the alarm generator. Following the triggering of an alarm, a refractory period is typically considered.

KF represents another potential approach to consider, given its recursive filter structure intended for the estimation of a linear dynamical system's state (Equation 2.12):

$$\begin{cases} s_{k+1} = \begin{bmatrix} 1 & T_p \\ 0 & 1 \end{bmatrix} s_k + w_k \\ y_k = \begin{bmatrix} 1 & 0 \end{bmatrix} s_k + z_k \end{cases}. \tag{2.12}$$

where s_k denotes the system state at time k, y_k corresponds to the measured variable, and w_k and z_k represent white noise vectors with zero mean. An alarm activates when the KF output classifies it as a preictal sample. Multiple studies [95, 96, 97] have employed the FP technique repeatedly, yet the search for an optimal threshold value remains ongoing. While KF demonstrated enhanced sensitivity, FP yielded better outcomes in reducing the number of false positives. Additionally, it is worth noting that, according to Teixeira et al. (2012) [98], the trigger power method triggers alarms more conservatively [15, 98, 99].

2.5 Concept Drifts

CD denotes the unpredictable changes occurring in the fundamental distribution of streaming data over time, leading to a decline in the performance of trained prediction models (see Figure 2.15). Several factors, such as seizure events, alterations in the type or dosage of AEDs, and biological rhythms (e.g., circadian rhythms), can induce these alterations in the distribution of EEG data [100].

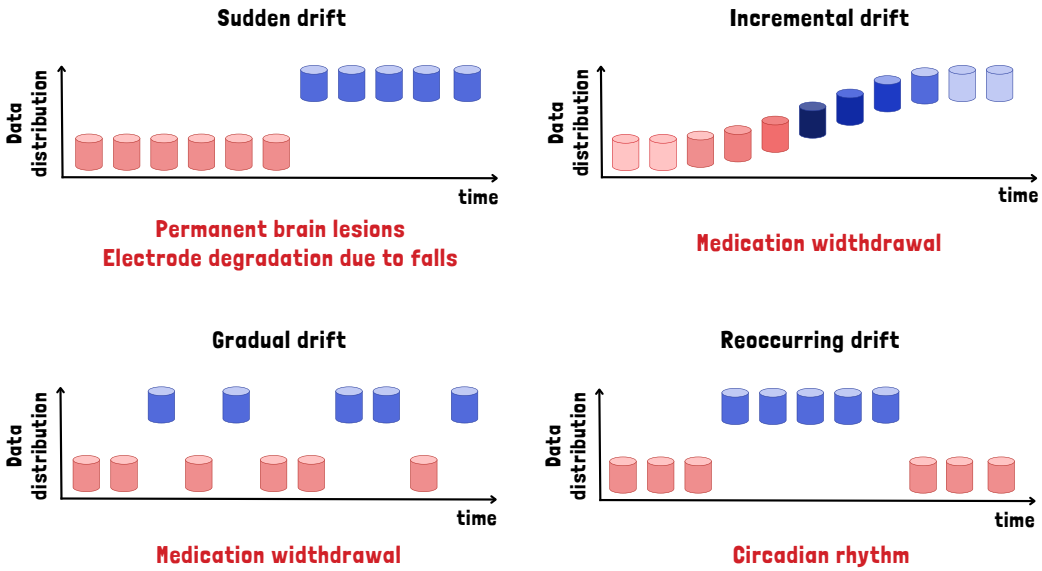

Figure 2.15: Graphical representation of the concept drifts change types and their possible translation for the specific case of epilepsy seizure prediction in pre-surgical monitoring conditions. Adapted from: Lu et al. (2018) [100] and Gama et al. (2014) [101].

The predominant data collection in the pre-surgical context is responsible for the higher prevalence of CDs. This trend is associated with patients undergoing AEDs withdrawal and experiencing sleep deprivation. Patients' exposure to these conditions impacts their circadian rhythm and sleep-wake cycles, ultimately causing an "artificial" increase in seizure frequency, an unusual occurrence [102].

For a considerable time, the presence of daily to monthly patterns in seizure occurrence, indicating the regulation of brain activity over long time scales, has been a matter of discussion. However, the accomplishment of the precise definition of these patterns has occurred only recently. As stated by Khan et al. (2018) [103], the rhythms can be categorized as follows:

- Circadian: "*A biological rhythm is considered to be a circadian rhythm if it meets three criteria: the rhythm should have an endogenous free-running (approximately) 24 h period, should be entrainable (i.e., be capable of phase reset by environmental cues and synchronisation to the 24 h day), and should exhibit temperature compensation.*";
- Multidien: "*Refers to rhythms with a time period covering several days.*";
- Ultradian: "*Refers to rhythms with periods of less than 24 h; ultradian rhythm cycles can occur with a frequency of more than once per day. A prominent ultradian rhythm is the non-REM–REM cycle, which in humans has a period of approximately 90 min.*"

2.5.1 Sleep-wake Cycle

The sleep-wake cycle holds immense significance in this context, as it instigates significant alterations in behavioral and physiological states. Sleep, a reversible physiological process for roughly one-third of human life, involves decreased mobility, consciousness, and responsiveness. It plays a vital role in safeguarding both physical and mental well-being.

Sleep comprises two distinct stages: Non-Rapid Eye Movement (NREM) and Rapid Eye Movement (REM). Typically, these stages follow a cyclic pattern, with each cycle spanning an average of 90 to 110 minutes. During a typical sleep period in adults, 4 to 6 cycles occur, as illustrated in the accompanying Figure 2.16.

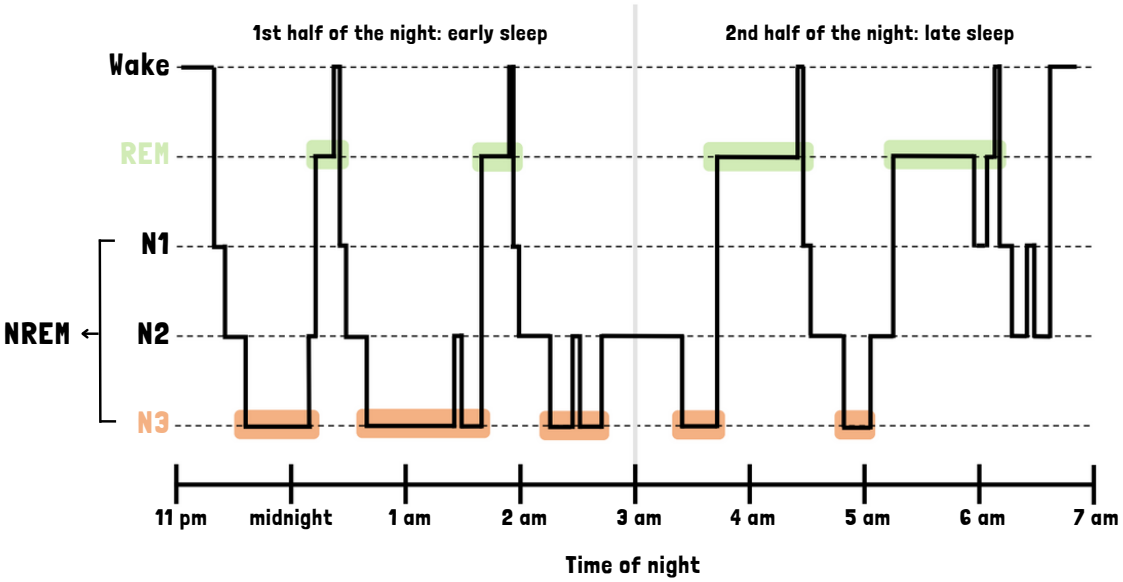

Figure 2.16: Hypnogram representing the sleep stages during a whole night of sleep in a healthy human adult. Adapted from: Blume et al. (2015) [104].

The NREM stage constitutes approximately 75 to 80% of the total sleep duration in adults. The American Academy of Sleep Medicine (AASM) categorizes it into three sleep stages (N1-N3) based on EEG criteria. These stages occur repetitively throughout the entire sleep episode. The NREM stage exhibits synchronized low-frequency, high-amplitude EEG oscillations, including sleep spindles and K-complexes (particularly in the N2 substage). Stage N3 of NREM sleep, often called slow-wave sleep, corresponds to deep sleep [103].

The REM stage of sleep does not undergo subdivision into distinct substages; however, low-amplitude mixed-frequency EEG oscillations, rapid eye movements, and reduced muscle tone are distinctive characteristics of this stage of sleep [103].

To summarize, in the regular sleep pattern of adults, a systematic transition occurs from wakefulness to sleep initiation, subsequently progressing to NREM sleep and ultimately reaching REM sleep. The Figure 2.16 shows a clear tendency for the duration of REM sleep to increase while the duration of NREM sleep progressively shortens throughout the successive sleep cycles [105, 106].

2.6 Summary

Epilepsy, a neurological condition, displays notable clinical diversity concerning the nature of seizures, types of epilepsy, and epileptic syndromes. Seizures can be categorized based on initial signs/symptoms, level of consciousness, and the location of the epileptic focus. The most common epileptic syndrome is TLE, characterized by seizures primarily originating from the temporal lobe. Seizure clusters refer to consecutive seizures with short interictal periods, requiring critical management to prevent progression to status epilepticus, a life-threatening condition. In such cases, the usual approach is to administer rescue medications.

Seizure prediction focuses on patients suffering from DRE (approximately one-third of cases) who face unpredictable seizures' physical and social consequences. These patients often undergo extensive pre-surgical monitoring over weeks or months to evaluate their condition before considering surgical interventions. Consequently, most datasets in this field consist of data collected during this monitoring period. Resective surgery represents a highly effective option for alleviating crises. Although it is an invasive technique, it is considered relatively safe. Neurostimulation may be considered an alternative for patients who are not suitable candidates for surgery.

EEG constitutes the principal medical tool for monitoring the brain's electrical activity, although numerous aspects of its morphology still need to be understood. There are two ways to conduct EEG acquisition: scalp EEG, a non-invasive technique that records brain activity from the brain's surface, and iEEG, which involves the application of subdural or depth electrodes. Despite the invasive nature of iEEG and its associated risks, it exhibits reduced susceptibility to noise and yields a more precise representation of high-frequency activity. Not all detected epileptic activity can reliably predict seizures, necessitating the comprehensive analysis of diverse EEG patterns to enhance predictive accuracy.

In seizure prediction, the EEG signal consists of interictal, preictal, ictal, and postictal periods. The goal is to identify the preictal period and issue alerts promptly to anticipate seizures. In this context, a connection exists between each alert and a specific period of occurrence (SOP) and intervention time (SPH). However, identifying this interval poses challenges due to the inherent variability of the preictal period across patients and seizure episodes.

The evaluation of a seizure prediction system should encompass sensitivity and false positive rate per hour (FPR/h). A practical methodology should incorporate suitable periods of occurrence and intervention times, enabling practical interventions in real-life situations. Furthermore, statistical validation is imperative to ensure the system surpasses chance-level performance. Moreover, the proposed methodologies must effectively handle challenges associated with data imbalance and CDs, including the circadian cycle, sleep-wake cycle, and medication tapering during pre-surgical monitoring.

3

State of the Art

This chapter outlines the current state of the art in seizure prediction and the most relevant databases pivotal to several studies and for the development of this document. Section 3.1 presents the common framework, exploring historically utilized techniques and resources. Section 3.2 furnishes a detailed exposition of selected databases, elucidating their relevance in recent research pursuits. Finally, Section 3.3 offers a summative overview of the core concepts discussed throughout this chapter and closing remarks.

3.1 Seizure Prediction

Numerous research studies actively sought to manage the difficulty of predicting seizures, aiming to improve the quality of life for individuals with epilepsy. After years of endeavour and investigation, contemporary prediction algorithms follow a conventional framework, as illustrated in the Figure 3.1.

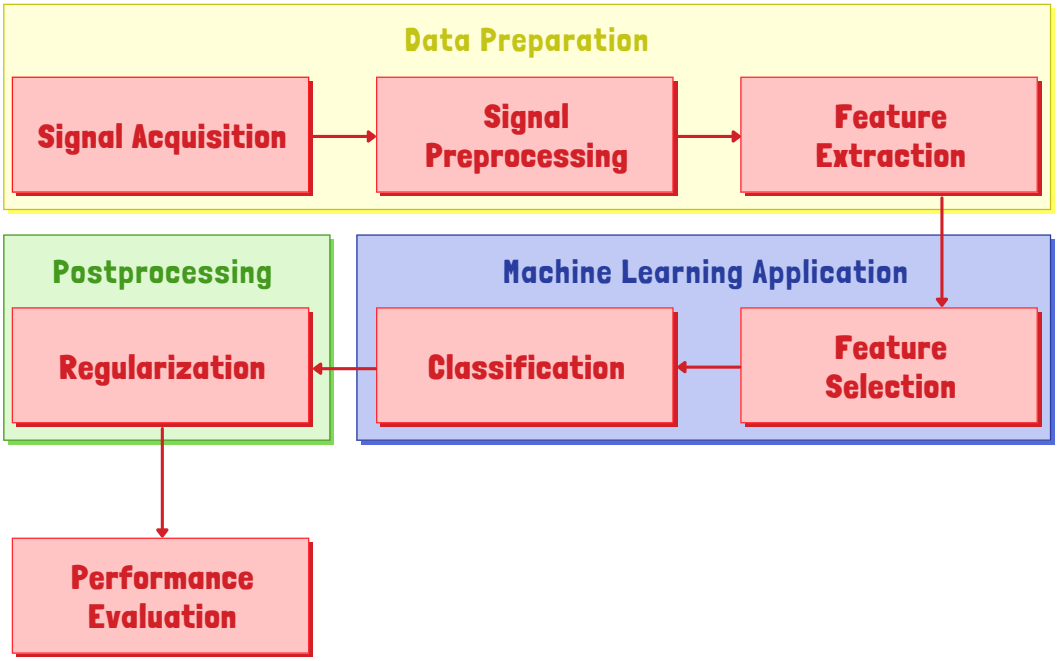

Figure 3.1: Flowchart of the typical seizure prediction framework. Adapted from: Assi et al. (2017) [15].

The components of this framework can be summarized as follows:

- Signal acquisition refers to the collection of Electroencephalogram (EEG) data, which serves as the primary research tool;
- The signal undergoes preprocessing to enhance EEG quality and enable transmission of signal information via time window analysis;
- Extracting and selecting features involves calculating and selecting the most relevant characteristics that are capable of differentiating between distinct EEG phases (interictal/preictal);
- Classification entails training Machine Learning (ML) models that use the previously selected characteristics to identify periods as interictal or preictal;
- Regularization aims to improve the classifier's output by smoothing it while disregarding isolated classifications and assigning them temporal meaning;
- The performance assessment and the findings' significance are accomplished by utilizing the established metrics.

Although frequently employed, this structure exhibits variability in existing approaches, which results from the absence of a gold standard algorithm and the resulting range of possibilities. Deep Learning (DL) can effectively merge several phases into an integrated workflow, demonstrating its prowess in optimizing data analysis.

Differences in Deep Learning approaches

Extracting the most discriminative features of the proposed methods with the mentioned structure poses a significant challenge, as it relies on the complexity of the process. DL models offer a viable solution to address this complexity, given their inherent ability to perform feature extraction and learn features intricately associated with the problem. More sophisticated ML models, specifically DL algorithms, were explored to address this challenge due to the exponential growth in available data and computational power.

These algorithms can automate preprocessing, feature extraction, and classification when handling raw data, improving performance. As such, the structure described above is subject to several changes, as the three approaches in the Figure 3.2 depict [107].

According to the Figure 3.2, the most straightforward approach, represented by letter A, involves the model undertaking preprocessing (e.g., artifact removal, noise reduction, and filtering), feature engineering, and classification. This option involves providing raw input, which may not have undergone significant processing, and extracting classification output via sequence analysis [108, 109, 110, 111, 112].

Some authors who adopt another alternative in the Figure 3.2, represented by the path of B, extract features in advance instead of using raw data as input [113]. Then the models are provided with the resulting measures. This approach emphasizes feature selection, dimensionality reduction, and classification.

In the last option (C), the acquired coefficients are extracted and provided to another classifier, as the authors [72, 107] use these models as feature engineering. Despite the advantages of these approaches, they demand more extensive databases to prevent overfitting issues and to

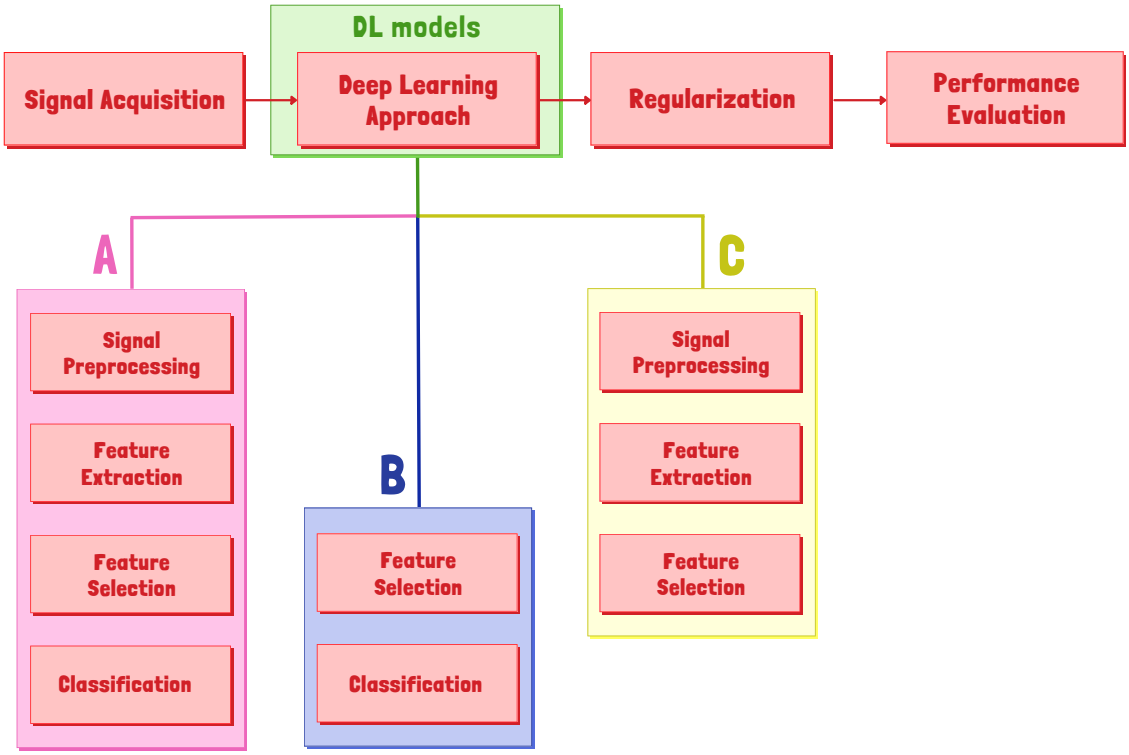

Figure 3.2: Current DL pipelines for predicting seizures. The colors represent the use of DL models. Adapted from: Assi et al. (2017) [15].

yield better outcomes than other methods. Additionally, their increased complexity results in difficulties interpreting the results, making their clinical applicability challenging [16, 113].

3.1.1 Signal Acquisition

Signal acquisition and data selection represent the starting point of a seizure prediction investigation, wherein the selection of signal type and dataset profoundly influence the outcomes and conclusions drawn across various studies.

The Table 3.1 presents an overview of the data employed in seizure prediction research over the past decade, highlighting the EEG signal as the primary focus of the analysis, albeit including other signals like Blood Volume Pulse (BVP), Accelerometry (ACC), Electrodermal Activity (EDA), temperature, and sleep.

The most commonly used databases (Children's Hospital Boston from the Massachusetts Institute of Technology (CHB-MIT), EPILEPSIAE, Freiburg, American Epilepsy Society (AES), and NeuroVista) include traditional scalp EEG or Intracranial Electroencephalogram (iEEG) data.

Despite efforts, patient discomfort remained unresolved, underscoring the importance of conducting studies that enable real-time data acquisition using more comfortable and portable devices like wristbands and smartwatches. Anticipated success in these studies stems from using a larger volume of data and exploring variations in research hypotheses. The addition of other signal types to the Table 3.1, aside from the EEG, is attributable to these investigations, as

Table 3.1: Overview of the signal acquisition from seizure prediction over the past 11 years.

Study	Database	Patients	No. of Seizures (analyzed time)	Signal	Electrodes
Assali et al. (2023) [116]	CHB-MIT	17	61 (-)	Scalp EEG	-
Hu et al. (2023) [117]	CHB-MIT	22	198 (26.8 days)	Scalp EEG	-
Li et al. (2023) [118]	Kaggle (AES) CHB-MIT	4 dogs+18	41+90 (-)	iEEG Scalp EEG	-
Lopes et al. (2023) [102]	EPILEPSIAE	41	227 (233.3 days)	Scalp EEG	-
Pinto et al. (2023) [119]	EPILEPSIAE	40	224 (135.6 days)	Scalp EEG	-
Xu et al. (2023) [120]	CHB-MIT	4	27 (-)	Scalp EEG	-
Liang et al. (2022) [121]	CHB-MIT Kaggle (AES)	13+5 dogs+2	64+- (-+55.57 days)	Scalp EEG iEEG	-
Pal Attia et al. (2022) [108]	ZUH KCL's clinical trial	6	- (409 days)	Subcutaneous EEG	-
Peng et al. (2022) [122]	CHB-MIT Freiburg	16+20	74+82 (-)	Scalp EEG iEEG	- 3 in focal region and 3 far from local region
Pinto et al. (2022) [123]	EPILEPSIAE	93	238t (153.6t days)	Scalp EEG	-
Singh et al. (2022) [124]	CHB-MIT	24	173 (38.17 days)	Scalp EEG	-
Viana et al. (2022) [114]	ZUH KCL's clinical trial	6	82 (594 days)	Subcutaneous EEG	-
Zhang et al. (2022) [125]	SeizeIT1 SeizeIT2	42+39	182+67 (168.1+133.3 days)	Scalp EEG BTE EEG	-
Nasseri et al. (2021) [76]	NeuroPace	6	278 (4 years)	ACC BVP, EDA TEMP	Wristband
Pinto et al. (2021) [126]	EPILEPSIAE	19	49t (29.6t days)	Scalp EEG	-
Proix et al. (2021) [86]	NeuroPace	18	- (> 6 months p.p.)	iEEG	-
Stirling et al. (2021a) [115]	Personal	1	134 (6 months)	Subcutaneous EEG	-
Stirling et al. (2021b) [72]	Personal	11	1493 (13.5 years)	BVP Sleep stages	Smartwatch
Tamanna et al. (2021) [127]	CHB-MIT	6	40 (-)	Scalp EEG	-
Usman et al. (2021) [128]	CHB-MIT	22	198 (26.8 days)	Scalp EEG	-
Vandecasteele et al. (2021) [129]	SeizeIT1 EPILEPSIAE	42+93	221+675 (-)	Scalp EEG BTE EEG ECG	-
Gabara et al. (2020) [130]	CHB-MIT	6	34 (8.4 days)	Scalp EEG	-
Meisel et al. (2020) [74]	Personal	69	-	ACC BVP, EDA TEMP	Wristband
Stojanović et al. (2020) [131]	EPILEPSIAE Epilepsy Ecosystem	5+3	50+692 (1.32+33.17 days)	iEEG	31-122, 16
Xu et al. (2020) [109]	Kaggle (AES) CHB-MIT	5 dogs+22	44+45 (1.85+1.18 days)	iEEG Scalp EEG	-
Daoud and Bayoumi (2019) [107]	CHB-MIT	8	43 (-)	Scalp EEG	-
Nejedly et al. (2019) [78]	NeuroVista Canines	4 dogs	75 (1608 days)	iEEG	16
Truong et al. (2019) [132]	Freiburg CHB-MIT EPILEPSIAE	13+13+30	59+64+261 (12.95+8.7+120 days)	Scalp EEG iEEG	6, 22, 19
Zhang et al. (2019) [110]	CHB-MIT	22	182 (-)	Scalp EEG	-
Chamseddine et al. (2018) [99]	Kaggle (AES)	1 dog	- (85 hours)	Scalp EEG	16
Kiral-Kornek et al. (2018) [133]	NeuroVista	15	2817 (16.29 years)	iEEG	16
Kitano et al. (2018) [134]	CHB-MIT	9	59 (30.57 hours)	Scalp EEG	-
Kuhlmann et al. (2018) [67]	NeuroVista	3	211 (442 days)	iEEG	16
Truong et al. (2018) [111]	Freiburg CHB-MIT Kaggle (AES)	13+13+5 dogs+2	59+64+48 (13+8.7+26 days)	Scalp EEG iEEG	6, 22, 19
Tsiouris et al. (2018) [112]	CHB-MIT	12	185 (40 days)	Scalp EEG	-

Table 3.1 continued from previous page

Study	Database	Patients	No. of Seizures (analyzed time)	Signal	Electrodes
Yang et al. (2018) [135]	Freiburg	19	83 (-)	iEEG	-
Aarabi et al. (2017) [136]	Freiburg	10	38 (242 hours)	iEEG	3 in focal region and 3 far from local region
Direito et al. (2017) [97]	EPILEPSIAE	216	1206t (697t days)	Scalp EEG iEEG	F7, FZ, F8, T5, PZ, T6 6 random 6 in focal region
Karoly et al. (2017) [18]	NeuroVista	9	1458 (10.35 years)	iEEG	-
Khan et al. (2017) [137]	MSSM CHB-MIT	12+15	15+18 (21.25+18 hours)	Scalp EEG	-
Assi et al. (2015) [138]	Kaggle (AES)	5 dogs	44 (-)	iEEG	16
Bandarabadi et al. (2015) [96]	EPILEPSIAE	24	183t (150t days)	Scalp EEG iEEG	3 in focal region and 3 far from local region
Rasekhi et al. (2015) [139]	EPILEPSIAE	10	86 (58 days)	Scalp EEG iEEG	3 in focal region and 3 far from local region
Alvarado-Rojas et al. (2014) [73]	EPILEPSIAE	53	558 (531 days)	iEEG	-
Moghim and Corne (2014) [140]	Freiburg	21	- (24 days)	iEEG	3 in focal region and 3 far from local region
Teixeira et al. (2014) [95]	EPILEPSIAE	278	2702 (2031 days)	Scalp EEG iEEG	F7, FZ, F8, T5, PZ, T6 6 random 6 in focal region
Cook et al. (2013) [68]	NeuroVista	15	1392 (≈ 16 years)	iEEG	16
Rabbi et al. (2013) [141]	EPILEPSIAE	1	7 (1.5 days)	iEEG	2
Rasekhi et al. (2013) [142]	EPILEPSIAE	10	46t (31t days)	Scalp EEG iEEG	3 in focal region and 3 far from local region

AES stands for American Epilepsy Society. CHB-MIT for the Children's Hospital Boston from the Massachusetts Institute of Technology, MSSM for Mount Sinai Epilepsy Center at the Mount Sinai Hospital, ZUH for Zealand University Hospital, and KCL for King's College London. BTE for Behind-The-Ear. In analysed time and seizures, "t" stands for testing data. BVP, ACC, EDA, and TEMP stand for blood volume pulse, accelerometry, electrodermal activity, and temperature.

evidenced by Stirling et al. (2021b) [72], Nasseri et al. (2021) [76], and Meisel et al. (2020) [74]. Also, this extends to examining newly introduced EEG acquisition modalities, specifically Subcutaneous Electroencephalography (sqEEG) and Video Electroencephalography (vEEG). The outlook for research suggests a shift toward investigating sqEEG data. This represents a promising direction, with initial studies [108, 114, 115] starting to investigate its utility, although the data is not yet publicly accessible.

Electrode selection

Research endeavors concerning EEG have unveiled several approaches to selecting electrodes for data acquisition, encompassing quantity and location. A subset of studies (including Assali et al. (2023) [116], Hu et al. (2023) [117], Li et al. (2023) [118], Lopes et al. (2023) [102], Pinto et al. (2023) [119], Xu et al. (2023) [120], Liang et al. (2022) [121], Pinto et al. (2022) [123], Usman et al. (2021) [128], Zhang et al. (2019) [110], Daoud and Bayoumi (2019) [107], Tsiouris et al. (2018) [112], and others) elects to use all obtainable electrodes. In contrast, others prefer a restricted number of electrodes situated in specific regions or at random, intending to increase patient comfort and simulate real-life scenarios as closely as possible. Such choices generate different assumptions that call for in-depth analysis.

Opting for a random selection of electrodes is based on the assumption that the processes that generate seizures can be detected anywhere in the brain. Using a specific set of electrodes (such as F7, FZ, F8, T5, PZ, and T6) makes it possible to maximize scalp coverage while mini-

mizing the number of electrodes used. On the other hand, the exclusive selection of electrodes in focal and non-focal regions [95, 97] assumes that the differential on activity is sufficient to capture seizure generation. In more detail, three electrodes close to the focal region and three others farther away were chosen for studies: Peng et al. (2022) [122], Aarabi et al. (2017) [136], Bandarabadi et al. (2015) [96], Rasekhi et al. (2015) [139], Moghim and Corne (2014) [140], and Rasekhi et al. (2013) [142].

Although selecting all electrodes may appear intuitive, given its comprehensive data coverage, this approach can result in significant computational costs and discomfort for patients. Nevertheless, the chaotic nature of the entire brain makes it challenging to identify any assumption that can accurately predict seizures [143].

3.1.2 Preprocessing

Obtaining precise information from raw biomedical signals, especially EEG is complex. Proper preprocessing is necessary to improve signal quality, reduce noise and artifacts, and normalize the data for comparison with other patients' recordings. The central goal is to develop an effective real-time method for receiving and processing data [144].

Figure 3.3 displays a general pipeline for signal preprocessing. First, the data is segmented using window analysis to work with smaller information blocks. Following that, performing actions such as denoising, filtering, artifact removal, and/or decomposition is possible. Taking careful note of defined steps, such as outlining the preictal period, Seizure Occurrence Period (SOP), and Seizure Prediction Horizon (SPH), is essential. These aspects should be established early in the research and tailored to align with the intended intervention, whether alerting the patient, initiating rescue medication, or electrostimulation.

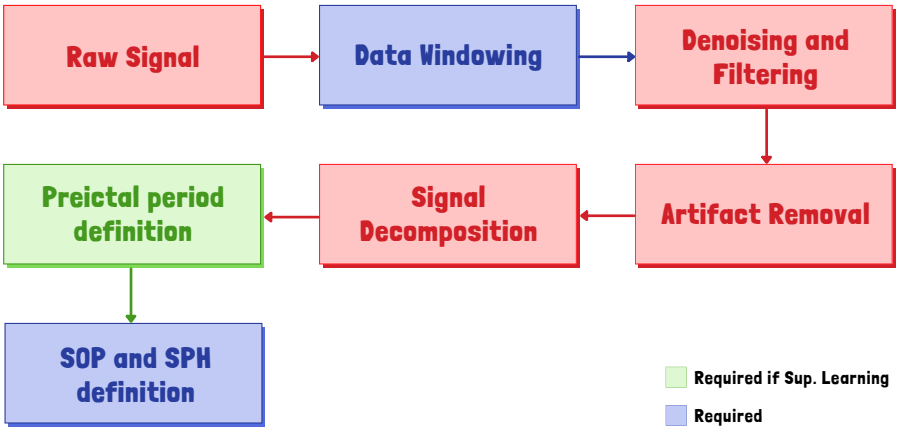

Figure 3.3: Flowchart of the typical signal processing pipeline in seizure prediction. The definition of the preictal period is required when using a supervised learning approach.

Table 3.2 provides an overview of the authors' decisions on signal preprocessing. Most studies tend not to emphasize noise removal, filtering, and artifact removal due to the complexity of the EEG signal. Overusing these methods could result in the loss of relevant brain information.

Data segmentation

A moving window analysis approach is employed in seizure prediction systems to extract chronological features and enable online time series analysis simulations. This involves partitioning the EEG signal into small windows, with potential overlap between consecutive windows.

In accordance with the selected studies provided in the Table 3.2, window duration falls essentially within the range of 2 to 60 seconds, with non-overlapping 5-second windows being the most widely used [68, 73, 95, 96, 97, 99, 110, 112, 117, 122, 123, 138, 139]. The selection of these values primarily depends on computational cost and execution speed, with variables such as the number of electrodes, sampling frequency, and recording duration influencing the decision. Additionally, there is a prevailing belief that windows spanning from 1 second to 1 minute effectively compromise spatial and temporal resolution for examining EEG dynamics while maintaining a level of stationarity. Hence, 5-second windows find widespread use for this reason.

Denoising, Filtering and Artifact Removal

It is unavoidable that noise and artifacts from various sources will corrupt the captured EEG signals. Accordingly, signal filtration becomes an indispensable step, and the specific methodologies to be applied depending on the particular form of noise or artifacts requiring eradication [145].

A notch filter effectively removes powerline interference within the 50 to 60 Hz frequency range. Moreover, the principal strategies include filtering the signals within specified frequency ranges of interest, decomposing wavelet coefficients, and excluding visually recognized defective segments [15].

Using bandpass filters is a widely prevalent practice, with only the chosen cut-off frequencies differing across studies. In most cases, respiratory artifacts manifest as low-frequency components below 0.5 Hz, making it the typical choice for the lower limit of cut-off frequencies. The higher limit value is typically more challenging to delimit since it consists mainly of environmental noise.

The available evidence suggests that the authors did not give extensive attention to this step at this stage, given the potential risk of losing important information and the potential robustness of subsequent steps to handle noise and artifacts. Thus, it is possible to address this aspect during the classification tasks.

Preictal Period Duration, SOP, and SPH

The duration of the preictal period lacks a clear and consistent definition, owing to its heterogeneity across patients and seizures. Consequently, there is no consensual ideal value for its length [146]. A range of values has been employed in research, with some utilizing a fixed preictal period (5 min [140], 10 min [134, 137], 15 min [133], 30 min [18, 102, 109, 110, 118, 121, 124, 127, 132], 60 min [73, 74, 76, 78, 99, 107, 108, 114, 138], or other values [67, 117, 120, 128]) while others exploring multiple values [72, 95, 96, 97, 112, 116, 119, 123, 139, 141, 142]. The fixed periods established in these studies span from 5 to 240 minutes.

Table 3.2: Overview of the signal preprocessing steps, preictal period, and SPH duration over the last 11 years.

Study	Sliding Window	Filtering	Preictal Period	SPH
Assali et al. (2023) [116]	2s No overlap	-	30 min and 60 min	-
Hu et al. (2023) [117]	5s N.A. overlap	5th-order Butterworth band-pass 5-50Hz	25 min	5 min
Li et al. (2023) [118]	30s No overlap	-	30 min	1 min (CHB-MIT) 5 min (Kaggle)
Lopes et al. (2023) [102]	10s No overlap	0.5–100Hz 4th-order band-pass 50Hz 2nd-order notch	30 min	10 min
Pinto et al. (2023) [119]	5s No overlap	-	30, 40, 50, 60 min	10 min
Xu et al. (2023) [120]	30s 50% overlap	Trap 57-63Hz and 117-123Hz	4 hours	5 min
Pal Attia et al. (2022) [108]	60s No overlap	0.5-48Hz band-pass 40dB attenuation	60 min	5 min
Liang et al. (2022) [121]	30s S samples overlap (CHB-MIT) No overlap (AES)	57-63 and 117-123Hz band-pass and DC removal (CHB-MIT)	30 min (CHB-MIT)	-
Peng et al. (2022) [122]	5s No overlap	57-63 and 117-123Hz (CHB-MIT), 47-53 and 97-103Hz (FREI) band-pass	30 min	30 min
Pinto et al. (2022) [123]	5s No overlap	50Hz notch 0.5Hz high-pass	30, 35, 40, 45, 50, 55, 60, 65, 70, 75, 80, 85, 90 min	-
Viana et al. (2022) [114]	60s No overlap	0.5-48Hz band-pass, 25Hz low-pass, 40dB attenuation	60 min	-
Singh et al. (2022) [124]	5, 10, 15, 20, 25, 30s No overlap	2nd-order Butterworth band-pass 0.1-127Hz	30 min	5 min
Zhang et al. (2022) [125]	2s 50% overlap	1-25Hz band-pass	-	-
Nasseri et al. (2021) [76]	1, 4s N.A. overlap	-	60 min	15 min
Pinto et al. (2021) [126]	5s No overlap	50Hz notch 0.5Hz high-pass	30, 35, 40, 45, 50, 55, 60, 65, 70, 75, 80, 85, 90 min	-
Stirling et al. (2021a) [115]	N.A.	0th-order Butterworth band-pass Hilbert transform	-	-
Stirling et al. (2021b) [72]	5, 60s No overlap	Butterworth band-pass Hilbert transform	60 min and 24 hours	-
Tamanna et al. (2021) [127]	10s (-)	-	30 min	-
Usman et al. (2021) [128]	29s No overlap	Empirical Mode Decomposition	32 min	-
Vandecasteele et al. (2021) [129]	2, 60s 50 and 17% overlap	-	-	-
Gabara et al. (2020) [130]	4s N.A. overlap	-	-	-
Meisel et al. (2020) [74]	30s No overlap	-	60 min	-
Stojanović et al. (2020) [131]	20s 50% overlap	50Hz Parks-McClellan optimal equiripple FIR (FSP) 50Hz Butterworth IIR (ECO)	5 min (FSP) 60 min (ECO)	30s (FSP 5 min (ECO)
Xu et al. (2020) [109]	20s No overlap	-	30 min	5 min
Daoud and Bayoumi (2019) [107]	5s No overlap	-	60 min	-
Nejedly et al. (2019) [78]	30s 15s overlap	-	60 min	-
Truong et al. (2019) [132]	28s No overlap	Band-pass as notch 47-53Hz and 97-103Hz	30 min	5 min
Zhang et al. (2019) [110]	5s No overlap	5th-order Butterworth band-pass 5-50Hz	30 min	-
Chamseddine et al. (2018) [99]	5s No overlap	0-190Hz bandpass 60Hz notch	60 min	-
Kiral-Kornek et al. (2018) [133]	5s No overlap	Octave-wide digital and notch 8Hz-128Hz	15 min	-
Kitano et al. (2018) [134]	4s No overlap	-	10 min	-
Truong et al. (2018) [111]	30s No overlap	Notch DC removed	30 min	5 min
Tsiouris et al. (2018) [112]	5s No overlap	-	15, 30, 60, 120 min	-
Kuhlmann et al. (2018) [67]	0s to 600s 0 to 50% overlap	-	55 min	5 min
Yang et al. (2018) [135]	5, 120, 360s No overlap	Notch	-	-
Direito et al. (2017) [97]	5s No overlap	50Hz notch	10, 20, 30, 40 min	10s

Table 3.2 continued from previous page

Study	Sliding Window	Filtering	Preictal Period	SPH
Aarabi et al. (2017) [136]	10s No overlap	50Hz notch 0.5-100Hz 4th-order Butterworth	30, 50 min	10s
Karoly et al. (2017) [18]	60s 50% overlap	50Hz notch 1-140Hz band-pass	30 min	1 min
Khan et al. (2017) [137]	1s No overlap	0-128Hz low-pass	10 min	-
Assi et al. (2015) [138]	5s No overlap	50Hz notch 0.5 - 180Hz band-pass	60 min	5s
Bandarabadi et al. (2015) [96]	5s No overlap	50Hz notch	10, 20, 30, 40 min	-
Rasekhi et al. (2015) [139]	5s No overlap	50Hz notch	10, 20, 30, 40 min	-
Alvarado-Rojas et al. (2014) [73]	5s No overlap	8th-order Butterworth in bands of interest from 0.5Hz to 140Hz Hilbert transform	60 min	1 min
Moghim and Corne (2014) [140]	5s and 9s No overlap	Artifact removal with EEGLAB	5 min	-
Teixeira et al. (2014) [95]	5s No overlap	50Hz notch	10, 20, 30, 40 min	10s
Cook et al. (2013) [68]	5s No overlap	Octave-wide digital and notch 8Hz-128Hz	minutes to hours	-
Rabbi et al. (2013) [141]	10s 50% overlap	60Hz notch 0.5 - 100Hz band-pass	15, 30, 45 min	-
Rasekhi et al. (2013) [142]	5s No overlap	50Hz notch	10, 20, 30, 40 min	-

An accurate definition of the preictal period holds great significance in supervised learning techniques. Nonetheless, unsupervised learning methods can also be used in prediction systems to identify preictal labels [147, 148].

The spectrum of SPH values in Table 3.2, ranging from 5 seconds to 30 minutes, indicates that there is still no definitive answer regarding the ideal duration of SPH. Despite the absence of a defined value, it is crucial to consider that the duration should be sufficient to enable timely alerts or interventions, as required.

In this sense, the prevailing belief is that most studies present an unrealistic scenario of what is necessary for practical applications since they do not specify the SPH value, creating the perception that this period receives no attention. Given that the preictal period comprises both the SOP and SPH, ignoring the SPH duration would result in the SOP period representing the entire preictal period [149].

3.1.3 Feature Extraction

Feature extraction, an intrinsically heterogeneous step, encompasses several methodological approaches. It involves extracting the most discriminative features from the EEG signals. Nevertheless, the search for a combination of ideal features persists. Although it is possible to exclusively employ black-box methodologies, the ongoing search for an optimal combination is advantageous as it ensures a higher level of reliability. This approach allows for understanding the overall EEG dynamics, evaluating potential external influences such as artifacts or noise, and providing more comprehensive explanations regarding signal behavior.

The core objective revolves around capturing three essential dimensions that characterize seizure activity [15, 17, 141]:

- the increase in energy due to cerebral electrical discharges;
- the shift in spectral power from lower to higher frequencies;
- the augmentation of neural synchronization.

The Figure 3.4 reveals the arrangement of these characteristics into four main classes, classifying them based on their linearity and the number of channels used. In terms of linearity, these features assume designations of linear or nonlinear. Regarding channel usage, the classification separates into univariate – for single-channel applications – and bivariate/multivariate, which account for analyses that use two or more channels [15, 150, 151].

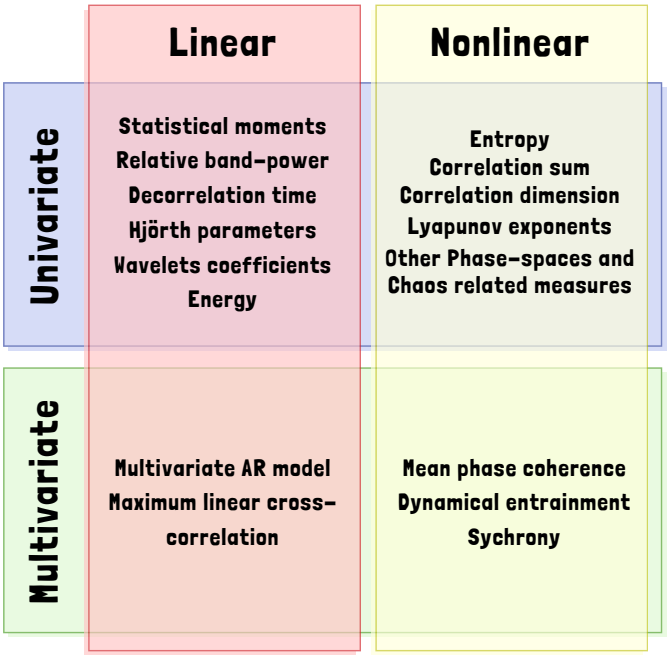

Figure 3.4: Classification of frequently utilized EEG features in seizure prediction studies, organized according to number of channels and linearity.

Table 3.3 delivers a comprehensive panorama of the attributes extracted across several seizure prediction studies in the last 11 years. Rasekhi et al. (2015) [139] revealed that employing multivariate features results in fewer incorrect predictions than univariate ones. However, although multivariate approaches offer a greater wealth of information, univariate measures are computationally more efficient and have a straightforward interpretation. Notably, linear univariate features have found more application than nonlinear options, driven by their simplicity and the clarity of their interpretation. Despite the absence of a definitive, essential feature, Morman et al. in 2005 [152] used a set of multivariate and univariate characteristics, showcasing remarkably satisfactory predictive outcomes. Moreover, their elevated computational demands might constrain the real-time viability of nonlinear features. The comparative performance analysis between different types of features has generated conflicting results in the literature [152, 153, 154], so no conclusion has yet been drawn [15, 155]. Nevertheless, the scientific community has heavily invested in using well-established univariate linear features in long-term data analysis. This investment affirms that progress in this field has primarily revolved around database developments.

With the growth of DL techniques [107, 112, 117, 118, 120, 128, 156], some approaches combine Convolutional Neural Network (CNN) for automatic feature extraction and Long-term Memory Network (LSTM) for classification, particularly when the temporal dimension of the

data holds significance. Nonetheless, even in DL approaches, it is common to primarily focus on transforming the signals into the frequency domain.

Categorizing the extracted features into univariate or multivariate, linear or nonlinear contributes significantly to a more structured and comprehensible feature extraction process. Appendix A presents an extensive overview of these features.

3.1.4 Feature Selection

The process of feature selection holds a significant position within prediction algorithms, particularly due to the intricate nature of brain dynamics and the necessity to comprehend the transitions between interictal and preictal states. The combination of multiple resources often leads to high-dimensional spaces, which demands careful selection of the most informative features. This decision-making process is significant to prevent redundancy or ambiguity that might negatively affect the classifier's performance. The aim is to identify features with strong discriminating power and avoid overfitting [15].

To achieve this objective, several techniques have been put into action, including ReliefF [140], minimum Redundancy Maximum Relevance (mRMR) [15, 138, 139, 157], maximum Difference Amplitude Distribution (mDAD) histograms [146], minimum normalized difference of percentiles [96], forward selection [158], and Genetic Algorithmss (GAs) [123, 126, 138, 159, 160]. The intention behind each of these approaches is to identify the most effective set of resources.

ReliefF quantifies the importance of features through random sampling and evaluating instance proximity to determine their significance. In contrast, mDAD operates by examining histograms illustrating amplitude distributions. The variables that lead to minimal histogram overlap for each class are considered the most distinct. On the other hand, mRMR, a widely employed method, ranks resources by enhancing their relevance while minimizing redundancy among them. GAs take inspiration from natural selection processes. It leverages biological principles, where the strongest members from an initial population survive and recombine to adapt to external shifts.

Another widely employed technique is Principal Component Analysis (PCA), which seeks to simplify high-dimensional data by transforming it into a lower-dimensional orthogonal space. In this process, the original features are combined to form what's called principal components, each representing a unique orthogonal projection. The sequence of principal components is decided by the eigenvalues of the covariance matrix, which enables the choice of projections showcasing the most significant variances. This technique is effective in maintaining the essential information of the data while making it less complex [15, 161].

Finally, in the case of DL approaches, the reduction is done by convolutional layers [109, 117, 120, 128, 132, 156] or autoencoders [107].

Table 3.3: Overview of the used features from seizure prediction over the past 11 years.

		Linear Univariate Features							Nonlinear Univariate Features						Linear Multivariate Features		Nonlinear Multivariate Features			
Study	**Other**	**Statistical Moments**	**Spectral Band related**	**Wavelets**	**Auto-regressive Modelling**	**Energy**	**Hjorth Parameters**	**Decorrelation Time**	**Phase-space and Chaos**	**Lyapunov Exponent**	**Dynamic Similarity Index**	**Line-length**	**Energy**	**Entropy**	**Ratio**	**Correlation**	**Dynamical Entrainment**	**Mean Phase Coherence**	**Nonlinear interdependence**	**Synchrony**
Assali et al. (2023) [116]	From raw data to STFT Stability Index		X											X						
Hu et al. (2023) [117]	Raw data and STFT data		X																	
Li et al. (2023) [118]	Raw data																			
Lopes et al. (2023) [102]	Raw data	X	X	X			X	X												
Pinto et al. (2023) [119]	Raw data	X	X	X		X	X	X												
Xu et al. (2023) [120]	Raw data																			
Pal Attia et al. (2022) [108]	Raw data, FFT data, and TOD		X																	
Pinto et al. (2022) [123]		X																		
Singh et al. (2022) [124]		X	X																	
Viana et al. (2022) [114]	Raw data and FFT data		X																	
Zhang et al. (2022) [125]	Total Power	X	X											X						
Nasseri et al. (2021) [76]	Raw data HR Time of the day																			
Proix et al. (2021) [86]	Temporal Features																			
Stirling et al. (2021a) [115]	Event-based cycles Seizure-based cycles																			
Stirling et al. (2021b) [72]	HR features Time of the day Sleep features																			
Tamanna et al. (2021) [127]		X		X		X								X						
Usman et al. (2021) [128]	From raw data to STFT		X																	
Vandecasteele et al. (2021) [129]	Time domain HR/HRV		X											X						
Gabara et al. (2020) [130]		X	X																	
Meisel et al. (2020) [74]	Raw data HR																			
Stojanović et al. (2020) [131]			X																	
Xu et al. (2020) [109]	Raw data																			
Daoud and Bayoumi (2019) [107]	Raw data																			
Nejedly et al. (2019) [78]	Raw data and STFT data																			
Truong et al. (2019) [132]	From raw data to STFT		X																	
Zhang et al. (2019) [110]	From raw data to CSP																			
Chamseddine et al. (2018) [99]			X																	
Kiral-Kornek et al. (2018) [133]	From raw data to Spectograms Time of the day		X																	
Kitano et al. (2018) [134]				X																
Kuhlmann et al. (2018) [67]		X	X	X	X	X	X	X	X				X					X		X
Truong et al. (2018) [111]	From raw data to STFT		X																	
Tsiouris et al. (2018) [112]	Raw data																			
Yang et al. (2018) [135]														X						
Aarabi et al. (2017) [136]										X									X	
Direito et al. (2017) [97]		X	X	X	X	X	X	X												
Karoly et al. (2017) [18]						X						X	X							
Assi et al. (2015) [138]			X				X	X												
Bandarabadi et al. (2015) [96]			X												X					
Rasekhi et al. (2015) [139]		X	X	X	X	X	X	X							X					
Alvarado-Rojas et al. (2014) [73]	Phase interaction with HFO																			
Moghim and Corne (2014) [140]		X	X	X		X			X	X										
Teixeira et al. (2014) [95]		X	X	X	X	X	X	X												
Cook et al. (2013) [68]						X						X	X							
Rabbi et al. (2013) [141]											X							X	X	X
Rasekhi et al. (2013) [142]		X	X	X	X	X	X	X												

STFT stands for Short-Time Fourier Transform, FFT for Fast-Fourier Transform, TOD for Time Of the Day, HR for Heart Rate, CSP for Common Spatial Patterns, and HFO for High-Frequency Oscillations.

3.1.5 Classification

The classification phase entails using a trained model to distinguish between preictal and, usually, the interictal state based on selected features. The methods employed span a broad spectrum, including traditional approaches and sophisticated DL algorithms (see Table 3.4). Within these DL, a common trend is the transition from utilizing Support Vector Machines (SVMs) [15, 96, 97, 125, 127, 129, 139, 140, 156] to CNNs [16, 67, 78, 99, 103, 109, 116, 128, 133] and LSTMs [72, 74, 76, 99, 107, 108, 112, 114, 128].

Furthermore, various other classification methods, such as Deep Residual Shrinkage Networks (DRSNs) [120], Transformer [117], Gated Recurrent Units (GRUs) [99], random forests and decision trees [67, 68, 72, 115, 129], k-Nearest Neighbors (kNNs) [68], Adaptive Neuro-Fuzzy Inference Systems (ANFIS) [138, 141], and logistic regressions [18, 72, 115, 123, 126], found application.

Nevertheless, data imbalance, wherein there are more interictal samples than preictal ones, presents a difficulty during the training process. In response, the authors have applied a range of strategies. These include reducing interictal sample numbers [95, 96, 97, 138], customizing classifiers more responsive to cost considerations [15, 155], or producing synthetic preictal samples using Generative Adversarial Networks (GANs) [132]. These tactics all aim to balance the representation of different states, ultimately enhancing the model's predictive capabilities.

Data partition strategies

Assessing the performance of a prediction algorithm involves subjecting it to tests using data independent of the training dataset, ensuring its ability to perform well in diverse scenarios. In order to prevent bias, it is critically important to avoid utilizing training and testing data related to the same seizures. Therefore, adopting data partitioning methods is vital in creating distinct training and testing sets.

Choosing a partitioning method involves making different assumptions regarding seizure prediction. In specific strategies [117, 108, 157, 161], a predetermined number of seizures are chosen from all patients for training purposes, with the rest reserved for the testing phase. Another viewpoint embraces an individualized strategy, where the model is trained and tested individually for each patient [97, 109, 114, 116, 124, 130, 131, 136, 140, 141], recognizing the substantial variability in the mechanisms driving seizure generation across patients. In particular cases, authors take this concept further by considering the sequence of seizures, utilizing initial seizures for training and subsequent ones for testing [73, 76, 95, 96, 123, 126, 139].

Recently, the Leave-One-Out technique has garnered attention [74, 107, 108, 110, 111, 118, 120, 121, 122, 129, 132]. Here, N-1 seizures (or patients) are used for training, leaving one seizure for testing. N represents the total number of seizures/patients. Additionally, for studies that consider concept drifts, as is the case with analyses conducted using ultra-long-term records (having a duration of several months for each individual), authors incorporate regular retraining of classifiers to ensure their effectiveness over an extended period [18, 68, 76, 133].

Table 3.4: Overview of the classification, regularization, performance, and statistical validation over the past 11 years.

Study	Training data (testing data)	Classification (regularization)	Performance	Statistical Validation
Assali et al. (2023) [116]	80% samples (20% samples)	CNN	SS=0.93 ACC=0.945	No
Hu et al. (2023) [117]	80% samples (20% samples)	Transformer	SS=0.92 FPR/h=0.00	No
Li et al. (2023) [118]	Leave-One-Out with seizures	MLPs	SS=0.93 FPR/h=0.11	No
Xu et al. (2023) [120]	Leave-One-Out with seizures	DRSN-GRU	SS=0.90 FPR/h=0.025	No
Pal Attia et al. (2022) [108]	k-fold cross validation with patients	LSTM (1h smooth)	SS=0.54 TiW=0.33	4 in 6 (0.67) Surrogate Analysis
Liang et al. (2022) [121]	(CHB-MIT) Leave-One-Out with seizures	CNN (K-of-N analysis)	SS=0.88 (CHB-MIT) FPR/h=0.04 (CHB-MIT) AUC=0.86 (AES)	No
Peng et al. (2022) [122]	Leave-One-Out with seizures	MMS-AAE + SVM	SS=0.73 (CHB-MIT) FPR/h=0.24 (CHB-MIT) SS=0.76 (FSP) FPR/h=0.19 (FSP)	No
Pinto et al. (2022) [123]	First 3 seizures (remaining seizures)	Logistic Regression (Firing Power)	SS=0.16 FPR/h=0.21	30 in 93 (0.32) Surrogate Analysis
Viana et al. (2022) [114]	Initial 1/3 of data (last 2/3 of data)	LSTM (1h smooth)	SS=0.73 TiW=0.34	5 in 6 (0.83) Surrogate Analysis
Singh et al. (2022) [124]	90% of data 10% of data	CNN	SS=0.98 SP=0.97	No
Zhang et al. (2022) [125]	SeizeIT1 dataset (SeizeIT2 dataset)	SVM	SS=0.88 FPR/h=1.93	4 in 6 (0.67) Surrogate Analysis
Nasseri et al. (2021) [76]	First 2/3 of data (last 1/3 of data)	LSTM (Kalman Filter)	AUC=0.80	5 in 6 (0.83) Random Predictor
Pinto et al. (2021) [126]	First 60% of seizures (last 40% of seizures)	Logistic Regression (Firing Power)	SS=0.37 FPR/h=0.79	6 in 19 (0.32) Surrogate Analysis
Proix et al. (2021) [86]	At least 60% of data	PP-GLMs	AUC=0.74 BSS=0.23	15 in 18 (0.83) Surrogate Analysis
Stirling et al. (2021a) [115]	Retraining and testing chronologically and iteratively	Random Forest+Log Reg	AUC=0.88	No
Stirling et al. (2021b) [72]	Retraining and testing chronologically and iteratively	LSTM+Random Forest +Log Reg (Kalman Filter)	AUC=0.74	11 in 11 (1.00) Random Forecast
Tamanna et al. (2021) [127]	80% of data (20% of data)	SVM (K-of-N analysis)	ACC=0.96 FPR/h=0.19	No
Usman et al. (2021) [128]	k-fold cross validation with seizures	CNN+LSTM	SS=0.93 SP=0.92	No
Vandecasteele et al. (2021) [129]	Leave-One-Out with seizures (EEG) with patients (ECG)	SVM (EEG) Random Forest (ECG)	SS=0.79 (EEG) SS=0.64 (ECG) FPR/h=1.00	No
Gabara et al. (2020) [130]	70% of data 30% of data	SVM	SS=0.96 ACC=0.96	No
Meisel et al. (2020) [74]	Leave-One-Out with patients	LSTM	SS=0.51 TiW=0.44	30 in 69 (0.43) Random Predictor
Stojanović et al. (2020) [131]	70% of data (30% of data)	SVM	SS=0.95 (EPI) SP=0.99 (EPI) SS=0.69 (ECO) SP=0.79 (ECO)	No
Xu et al. (2020) [109]	80% samples (20% samples)	CNN	SS=0.96 FPR/h=0.07	No
Daoud and Bayoumi (2019) [107]	Leave-One-Out with seizures	CNN, Bi-LSTM	SS=0.99 FPR/h=0.004	No
Nejedly et al. (2019) [78]	Increases over time (after training epochs)	CNN	SS=0.79 TiW=0.18	4 in 4 (1.00) Random Predictor
Truong et al. (2019) [132]	Leave-One-Out with seizures	GAN, CNN, NN	AUC=0.81	51 in 56 (0.91) Hanley-McNeil AUC test
Zhang et al. (2019) [110]	Leave-One-Out with seizures	CNN (Kalman Filter)	SS=0.92 FPR/h=0.12	Statistical comparison between methods
Chamseddine et al. (2018) [99]	80% samples (20% samples)	LSTM, GRU, CNN (Kalman Filter, Firing Power)	SS=0.88 SP=0.99	No
Kiral-Kornek et al. (2018) [133]	First 2 months (remaining duration)	CNN	SS=0.69 FPR/h=0.00	15 in 15 (1.00) Random Predictor
Kuhlmann et al. (2018)[67]	Training and testing clips	GLMs, SVM, CNN Ensembles, Boosting, Trees	AUC=0.75 FPR/h=0.58	No
Truong et al. (2018) [111]	Leave-One-Out with seizures	CNN (Kalman Filter)	SS=0.79 FPR/h=0.14	28 in 31 (0.90) Random Predictor
Tsiouris et al. (2018) [112]	K-fold with recordings	LSTM	SS=0.99 FPR/h=0.02	No
Aarabi et al. (2017) [136]	1 seizure (remaining seizures)	Thresholding	SS=0.89 FPR/h=0.11	8 in 10 (0.8) Random Predictor

Table 3.4 continued from previous page

Study	Training data (testing data)	Classification (regularization)	Performance	Statistical Validation
Direito et al. (2017) [97]	2 - 3 seizures / patient (remaining seizures)	SVM (Firing Power)	SS=0.38 FPR/h=0.20	24 in 216 (0.11) Random Predictor
Karoly et al. (2017) [18]	Day 100-200 (Day 200 onwards)	Logistic Regression (Bin width of 1h)	SS=0.60 TiW=0.23	9 in 9 (1.00) Time-matched predictor
Khan et al. (2017) [137]	10-fold cross validation	CNN	SS=0.87 FPR/h=0.14	Random Predictor
Assi et al. (2015) [138]	80% segments (Remaining segments)	SVM, ANFIS	SS=0.85 SP=0.80	No
Bandarabadi et al. (2015) [96]	First 3 seizures / patient (Remaining seizures)	SVM (Firing Power)	SS=0.76 FPR/h=0.10	23 in 24 (0.96) Random Predictor
Rasekhi et al. (2015) [139]	First 3 seizures / patient (Remaining seizures)	SVM (Firing Power)	SS=0.61 FPR/h=0.11	5 in 10 (0.50) Random Predictor
Alvarado-Rojas et al. (2014) [73]	First 4 seizures / patient and at least 10 hours of data (Remaining seizures)	Thresholding (Kalman Filter)	SS=0.47 FPR/h=0.94	7 in 53 (0.13) Random Predictor
Moghim and Corne (2014) [140]	10-fold cross validation with 70%/30% samples	SVM	SS=0.91 SP=1.00	Unspecific predictors
Teixeira et al. (2014) [95]	2 - 3 seizures / patient (Remaining seizures)	SVM, ANN (Firing Power)	SS=0.74 FPR/h=0.28	Statistical comparison between methods
Cook et al. (2013) [68]	First 4 months (Remaining duration)	kNN+Decision Tree (Smoothing)	SS=0.61 TiW=0.23	9 in 10 (0.90) Time-matched predictor
Rabbi et al. (2013) [141]	1 seizure / patient (5 seizures)	ANFIS	SS=0.80 FPR/h=0.46	No
Rasekhi et al. (2013) [142]	First 3 seizures / patient (Remaining seizures)	SVM (Firing Power)	SS=0.74 FPR/h=0.15	No

LSTM stands for Long Short-Term Memory, CNN for Convolutional Neural Network, DRSN for Deep Residual Shrinkage Network, GRU for Gated Recurrent Unit, MLP for Multi-Layer Perceptron, SVM for Support Vector Machine, ANFIS for Adaptive Neuro-Fuzzy Inference Systems, GLM for Generalized Linear Model, PP-GLM for Point Process Generalized Linear Model, GAN for Generative Adversarial Network, ANN for Artificial Neural Network, kNN for k-Nearest Neighbor, SS for Sensitivity, FPR/h for False Positive Rate per Hour, ACC for Accuracy, AUC for Area Under the Curve, BSS for Brier Skill Score, TiW for Time in Warning.

SVMs

SVMs find extensive application in seizure prediction [67, 95, 96, 97, 125, 127, 129, 130, 131, 138, 139]. In supervised machine learning, SVMs are notable for their generalization capacity and a small set of parameters requiring adjustment [15, 97, 139]. The fundamental aspect of SVMs is ascertaining a linear separation plane within an N-dimensional space, aiming to maximize the separation between the nearest points of different classes, the so-called support vectors. When dealing with nonlinear separation scenarios, SVMs incorporate nonlinear kernel functions like the Radial Basis Function (RBF), creating nonlinear decision boundaries [15, 42, 97, 139].

Linear SVMs offer notable interpretability, mainly due to their ability to construct separating hyperplanes based on critical cases of each class, commonly referred to as support vectors. Nevertheless, in cases with a high number of features, a trade-off exists between the volume of features and the interpretability of the model, necessitating careful consideration.

CNNs

CNNs [67, 78, 99, 107, 109, 110, 111, 116, 121, 124, 128, 132, 133] emerge as a subgroup of DL algorithms known for their proficiency in directly extracting essential features from raw data. Initially designed for processing multidimensional data, such as images, CNNs possess the skill to capture patterns and temporal information intrinsic to time series data [113, 162]. This proficiency becomes especially relevant in seizure prediction, given that the neural network integrates the EEG time series. To facilitate this, techniques like the Fast Fourier Transform (FFT) or wavelet decomposition can be employed to transform the raw data into a more suitable

format [110, 111, 128, 132]. As a result, researchers can approach seizure prediction using EEG as an improved visual time series, accounting for electrode arrangement and their interactions [109, 137].

The design of CNN architectures can exhibit diversity, although it typically involves a sequence of convolutional layers. These layers employ kernel convolutions to create feature maps. These maps undergo processing through pooling layers, prioritizing extracting significant features from the earlier generated maps. Subsequently, classification layers can be employed to make determinations based on the extracted features. Dropout layers are introduced to mitigate potential overfitting concerns due to the extensive number of network parameters. These layers randomly suppress the output of specific units during the training phase [137].

Recurrent Neural Networks (RNNs)

LSTMs [72, 74, 76, 108, 99, 112, 114, 128] represent an advancement of RNNs and assume a critical role within the realm of DL. They incorporate specialized units, known as gates, which regulate the retention and removal of information by adjusting corresponding weights. Diverging from CNNs, LSTMs aren't constrained by a fixed window, enabling the capture of temporal patterns in varied contexts, including seizure prediction. Nonetheless, both LSTMs and CNNs face the obstacle of requiring substantial data volumes and being prone to overfitting [107, 112, 113, 128]. In some cases [128], the combined approaches of CNNs and LSTMs are used, taking advantage of the features extracted by the CNNs to enhance the classification conducted by the LSTMs. This synergy between the two approaches effectively addresses the temporal nature of the data.

GRUs, a subtype of RNNs, share similarities with LSTMs but introduce the concepts of reset and update gates, improving the operation of hidden states. GRUs exhibit structural and computational superiority compared to LSTMs, with the added benefit of fewer parameters and reduced susceptibility for overfitting [120, 163, 164].

Despite their advantages, LSTMs and GRU face challenges when processing very long sequences. In response to this limitation, attention layers have emerged as a solution to handle more extensive sequences, likely to be further explored in the future. Their advantage lies in easy parallelization, leading to faster computation than LSTMs. However, these do not explicitly consider temporality like any RNN. Thus, the transformer model comes into play, characterized by its network architecture exclusively built on attention and fully connected layers.

3.1.6 Regularization

In the context of evaluating the classifier outputs in seizure prediction systems, it is essential to recognize the inherent limitations of their performance. Real-life scenarios reveal that classifiers rarely accurately categorize all samples due to data noise and the independent nature of analysis intervals [15, 95]. As a result, it becomes vital to integrate a postprocessing phase that addresses the temporal intricacies of algorithmic decisions, aiming to diminish false alarms and enhance the system's specificity.

A strategy for mitigating the occurrence of false alarms involves regularizing the classifier

output. This approach considers the temporal dynamics of the output, with two prominent techniques for achieving this: the Kalman Filter (KF) [72, 73, 110, 99, 76, 111] and Firing Power (FP) [95, 96, 97, 99, 123, 126, 139, 141].

FP employs a sliding window analysis to assess the proportion of samples classified as preictal within an interval corresponding to the preictal phase. If this evaluation surpasses a predefined threshold, an alarm is activated, allowing for a gradual smoothing of the classifier output over time. However, it is essential to acknowledge that this threshold has no universally optimal value. In contrast, KF relies on its ability to estimate a linear dynamic system's states, approximating the actual measurements' actual values. This method operates recursively and unimodally, predicting the present state based on the previous state and the current measurement. When the filter output surpasses a certain threshold, it triggers an alarm to identify a preictal state.

In a comparative context, researches such as the study led by Teixeira et al. (2014) [95] highlighted that the triggering power approach revealed that FP emerged as a more conservative method regarding alarms, having a more extended memory of classification dynamics. Conversely, despite its tendency to produce more false alarms, the KF displays a relatively improved sensitivity.

3.1.7 Performance Assessment

The assessment of a developed model holds critical importance, undertaken by applying specific metrics. In the context of seizure prediction, following the seizure prediction characteristic introduced by Winterhalder et al. (2003) [89], metrics like seizure sensitivity, False Prediction Rate per hour (FPR/h), and statistical validation incorporating surrogate analysis or general random predictors are suggested. However, not all authors follow this approach. Some alternatives employ metrics such as the Area Under the ROC Curve (AUC) [67, 72, 76, 86, 115, 121, 132], accuracy [116, 130], sample specificity, and sample sensitivity [99, 124, 128, 131, 138, 140], which offer insights into the classifier's performance but might not fully mirror its real-world applicability. Furthermore, the shift from prediction to forecasting introduces the Time in Warning (TiW) metric as a substitute for FPR/h [18, 68, 74, 78, 108, 114] and includes the Brier Skill Score (BSS) [18, 86].

Examining Table 3.4 reveals that a set of studies managed to attain an FPR/h below 0.15 [96, 107, 109, 110, 111, 112, 117, 118, 120, 136, 137, 142] - a significant threshold outlined by Winterhalder et al. (2003) [89] as a point of reference for alert systems in pre-surgical patients. However, a direct comparison between these studies becomes challenging due to the notable variations in the dataset, sample size, and the number of records considered. Furthermore, the selected values for SOP and SPH also manifest variability.

The dataset selection significantly impacts performance, with CHB-MIT presenting more homogeneous results and high-performance levels [107, 109, 110, 111, 112, 116, 117, 118, 120, 121, 122, 124, 127, 128, 130, 132, 137], while the EPILEPSIAE displays significant heterogeneity [73, 95, 96, 97, 123, 126, 129, 132, 139, 141, 142]. The number of patients considered directly influences this variability, ranging from 1 [141] to 278 individuals [95]. Authors typically make

patient selections based on factors such as signal quality (minimized presence of noise and artifacts), epilepsy type, seizure count, and specific seizure criteria. Regarding the homogeneity of strong outcomes with CHB-MIT, using these data to showcase the predictive capabilities of novel methods becomes questionable. However, it is important to note that CHB-MIT is a freely accessible open database, unlike EPILEPSIAE and NeuroVista.

Nevertheless, databases encompassing ultra-long-term data, such as NeuroVista [18, 67, 68, 78, 133], Neuropace-derived [76, 86], and others [72, 74, 115], provide more realistic performance evaluations and are recommended for incorporation in developing commercial seizure prediction devices.

3.2 Databases

Datasets of EEG recordings taken from epilepsy patients, used in developing algorithms for seizure detection and prediction, exhibit fundamental variations in their formatting and organization. For example, some databases offer seizures' start and end times but do not detail the associated dates. This absence of date information may lead to the inadvertent assignment of incorrect dates across multiple days. Additionally, the absence of standardized directives for using these databases significantly affects the potential for result generalization and reproducibility. Hence, evaluating the existing disparities, particularly in advantages and limitations, across the various accessible databases is essential for assessing distinctions in the acquired outcomes [165].

Most publicly accessible datasets lack standardization and comprehensive information on suitable application scenarios. However, the selection of data to employ can exert a considerable influence on the performance of prediction algorithms and the strategy adopted for their implementation. In this regard, all types of data, whether they pertain to demographics or clinical aspects like epilepsy categorization, seizure profiles, and the number of employed channels, have an impact [165]. Next subsections describe the most important datasets on this field.

3.2.1 American Epilepsy Society (AES) dataset

The dataset, registered through a collaboration between the AES and Kaggle for a seizure prediction challenge, encompasses 1333.7 hours of iEEG recordings. This dataset was initially composed of long-term data. However, only a fraction of this data is accessible, essentially converting it into short-term data in practice. These recordings originate from seven individuals, comprising two humans and five canines. In the case of human patients, the number of electrodes ranges from 15 to 24, with the first patient having deep electrodes and the second having subdural electrodes. The data recording occurred at a sampling rate of 5 kHz. Four canine subjects have recordings from 16 implanted electrodes, while the fifth has recordings from 15 implanted electrodes, with a sampling rate of 400 Hz.

Long-term ambulatory recordings of the five canines, all with naturally occurring epilepsy, were acquired utilizing the NeuroVista seizure advisory system. These recordings have extended durations, spanning from several months to a year. Conversely, the recordings of the two human subjects were conducted within a pre-surgical environment [67, 166, 167].

The dataset comprises 1-hour recordings, partitioned into six individual files, each spanning 10 minutes, with a seizure horizon onset of 5 minutes. In the case of canine data, a specific condition is imposed on interictal files, requiring a timeframe of at least one week before or after any seizure event. Conversely, this temporal window constraint extends to only 4 hours for human data.

The total duration of data recording comprises 267 seizures. It is separated into 78.8 hours for the human dataset, accounting for 46 of the total seizures (an average of less than 2 hours of available data for each seizure), and 1254.9 hours for the canine dataset, which includes the remaining 221 seizures [165]. Access to this database is open to the public, except for the test file labels and the held-out clips. Table 3.5 provides more extensive information about each subject.

Table 3.5: Details of the AES dataset.

Subject	Number of Channels	Sampling Rate (Hz)	Number of Train Files	Number of Test Files	Duration (hours)
Dog 1	16	400	504	502	167.7
Dog 2	16	400	542	1000	257
Dog 3	16	400	1512	907	403.2
Dog 4	16	400	901	990	315.2
Dog 5	15	400	480	191	111.8
Patient 1	15	5000	68	195	43.8
Patient 2	24	5000	60	150	35

3.2.2 Children's Hospital Boston - Massachusetts Institute of Technology (CHB-MIT) dataset

This database consists of scalp EEG recordings acquired at Children's Hospital Boston (CHB) and Massachusetts Institute of Technology (MIT) from 23 pediatric patients experiencing intractable seizures. Monitoring lasted for several days after a week of withdrawal from anticonvulsant drugs. This dataset includes data collected from 18 female subjects aged between 1.5 and 19 years and five male subjects aged between 3 and 22 years. The recordings, grouped into 24 cases, underwent conducting at a sampling rate of 256Hz. In total, there are 916 hours of recordings, including 173 seizure events.

The number of electrodes utilized ranges from 23 to 26, and all subjects share a set of 18 bipolar derivations: FP1-F7, F7-T7, T7-P7, P7-O1, FP1-F3, F3-C3, C3-P3, P3-O1, FZ-CZ, CZ-PZ, FP2-F4, F4-C4, C4-P4, P4-O2, FP2-F8, F8-T8, T8-P8, and P8-O2. Positioning of these channels followed the International 10-20 system.

In contrast to the AES dataset, this dataset does not come with preictal or interictal labels. Notwithstanding, the seizure timings within each patient's metadata files can infer these labels [165, 168]. This dataset provides open access to its data for all. Each patient's detailed information is available in the Table 3.6.

Table 3.6: Details of the CHB-MIT dataset.

Case	Sex	Age (years)	Number of Seizures	Duration of Recordings (hh:mm:ss)
chb01	f	11	7	40:33:08
chb02	m	11	3	35:15:59
chb03	f	14	7	38:00:06
chb04	m	22	4	156:03:54
chb05	f	7	5	39:00:10
chb06	f	1.5	10	66:44:06
chb07	f	14.5	3	67:03:08
chb08	m	3.5	5	20:00:23
chb09	f	10	4	67:52:18
chb10	m	3	7	50:01:24
chb11	f	12	3	34:47:37
chb12	f	2	40	20:41:40
chb13	f	3	12	33:00:00
chb14	f	9	8	26:00:00
chb15	m	16	20	40:00:36
chb16	f	7	10	19:00:00
chb17	f	12	3	21:00:24
chb18	f	18	6	35:38:05
chb19	f	19	3	29:55:46
chb20	f	6	8	27:36:06
chb21	f	13	4	32:49:49
chb22	f	9	3	31:00:11
chb23	f	6	7	26:33:30
chb24	-	-	16	21:17:47

Sex: female (f), male (m).

3.2.3 Epilepsy Ecosystem dataset

Towards the end of 2016, a portion of the dataset from the University of Melbourne became accessible to the public. Contained within this subset are long-term iEEG recordings obtained from three female patients (identified as patients 3, 9, and 11) who had been diagnosed with refractory focal epilepsy. It is essential to highlight that this subset was included in the global clinical trial for the implantable NeuroVista Seizure Advisory System and displayed the poorest performance in predicting seizures.

The dataset comprises a total recording duration of 1155 hours, with 390, 204, and 545 seizures recorded in patients aged 22, 51, and 50, respectively. On average, there is approximately 1 hour of available data per seizure. This recording time results in 5047 training and 1908 test segments [169]. The acquisition of this dataset involved strategically placing invasive strip electrodes in a 4x4 configuration within the focal hemisphere of the patients. Consequently, it comprises information from 16 channels, all sampled at 400 Hz.

The dataset's structure closely reflects the AES dataset, with each hour of recording divided into six 10-minute segments and the notation of a five-minute window before a seizure, referred

to as seizure horizon onset. Furthermore, it is a guarantee that the interictal files do not appear within the 4-hour window preceding and following a seizure event.

An essential characteristic of this dataset that adds complexity to the prediction task is the significant dissimilarity in data distribution between the test and training sets. This divergence arises from the fact that the test data were gathered six months after the training data, during which the patient was undergoing medication [165]. This data's accessibility is restricted, entailing form completion, security protocols, and adherence to the usage terms as defined. Similar to the AES database, the originally long-term data was also reduced to short-term in practice since only a tiny part of it is made available. In-depth information about each patient is available in Table 3.7.

Table 3.7: Details of the Epilepsy Ecosystem dataset.

Dataset features	Patient 1	Patient 2	Patient 3
Sex	f	f	f
Age (years)	22	51	50
Recording Period (days)	559	393	374
Total Recording (hours)	173	507	475
Number of Seizures	390	204	545
Number of interictal train files	570	1836	1908
Number of preictal train files	256	222	255
Number of interictal test files	16	18	18
Number of preictal test files	46	279	188
Number of channels	16	16	16
Sampling Rate (Hz)	400	400	400

Sex: female (f), male (m).

3.2.4 My Seizure Gauge dataset

The My Seizure Gauge dataset came about through the launch of the My Seizure Gauge challenge by the Epilepsy Innovation Institute (Ei2) research program, aiming to create a personalized seizure advisory system device [69].

This dataset consists of continuous recordings obtained from wearable devices worn by ten patients (see Table 3.8). It also provides data on seizure times and metadata related to the recordings. This metadata comprises the number of channels, types of channels/biosignals, sampling rate, total samples within each recording, and timestamps. The data for each patient extends for approximately 3-5 days.

Data is collected and provided from three distinct devices: Empatica E4, ByteFlies Sensor Dots, and Epilog. The E4 device, worn on the patient's wrist, collects data on ACC, BVP, EDA, Heart Rate (HR), and temperature for nine patients. Regarding the Dots Sensor, it can record ACC and 3-channel Photoplethysmography (PPG) or Electromyography (EMG) for five patients. Lastly, Epilog records single-channel EEG when placed on the patient's forehead [170]. The accessibility of this data is equal to the Epilepsy Ecosystem.

Table 3.8: Details of the My Seizure Gauge dataset.

Patient	Sensor	Signals	Number of Seizures	Duration of Recordings (hh:mm:ss)
MSEL_01097	ByteFlies Empatica E4	ACC, EMG, BVP, EDA, HR, TEMP	7	117:05:12
MSEL_01838	ByteFlies Empatica E4	ACC, PPG, BVP, EDA, HR, TEMP	11	113:37:48
MSEL_00172	ByteFlies Empatica E4	ACC, EMG, BVP, EDA, HR, TEMP	12	69:59:05
MSEL_00501	ByteFlies Empatica E4	ACC, EMG, BVP, EDA, HR, TEMP	17	88:09:29
MSEL_01808	Empatica E4	ACC, BVP, EDA, HR, TEMP	9	91:37:28
MSEL_01842	Empatica E4	ACC, BVP, EDA, HR, TEMP	12	84:14:44
MSEL_01844	Empatica E4	ACC, BVP, EDA, HR, TEMP	42	89:58:44
MSEL_01110-ICU	Empatica E4	ACC, BVP, EDA, HR, TEMP	12	84:18:39
MSEL_01860	ByteFlies Epilog	ACC, EMG, EEG	6	149:53:18
MSEL_01575	Empatica E4	ACC, BVP, EDA, HR, TEMP	82	143:14:20

ByteFlies stands for ByteFlies Sensor Dots, AAC for accelerometry, BVP for blood volume pulse, EDA for electrodermal activity, HR for heart rate, TEMP for temperature, PPG for photoplethysmography, EMG for electromyography, EEG for electroencephalogram.

3.2.5 European Epilepsy Database (EPILEPSIAE) dataset

The EPILEPSIAE project, funded by the European Union, got underway in 2008, with the active participation of six partners from hospitals, universities, and industries in France, Germany, Italy, and Portugal. For this project, they assembled what is now recognized as the largest epilepsy database, incorporating data from 278 patients. This extensive resource includes not only the EEG and Electrocardiogram (ECG) recordings of the patients but also detailed metadata [5].

This database includes scalp recordings from 227 patients, iEEG recordings from 42, and 9 patients were subjected to both. All patients had their ECG data recorded. The number of seizures experienced by individual patients ranges from 3 to 94, with an average of 9.72 per patient. Therefore, this database comprises a total of 2702 seizures. On average, the recording sessions lasted approximately 175 hours, with the most extended session lasting up to 500 hours. In total, the dataset comprises over 48000 hours of data [95].

Surface recordings took place with an electrode scheme aligned with the international 10–20 system, with supplemental electrode contacts added as necessary for particular patients. Grids, strips, and/or depth electrodes came into play for patients undergoing invasive recordings. Sampling rates varied from 250 Hz to 2.5 kHz, depending on the EEG acquisition system utilized at each hospital and whether the recording method involved surface or intracranial EEG. The number of recording channels displays variability, covering a spectrum from 14 to 124.

A notable feature that sets the EPILEPSIAE database apart from previous ones is its structured and extensive annotation scheme. A team of experienced professionals used video analysis and EEG assessment to meticulously detect all clinical seizures for each patient. However, only institutions that participate in the European Epilepsy Database (EPILEPSIAE) project have full access to this database, while other researchers can purchase a subset of 30 patients. Furthermore, Table 3.9 presents a broad comparison between EPILEPSIAE and the other databases [7, 1].

Table 3.9: General description of the databases.

Characteristic	EPILEPSIAE	AES	CHB-MIT	Epilepsy Ecosystem	My Seizure Gauge
Data Type	scalp EEG, iEEG	iEEG	scalp EEG	iEEG	scalp EEG, ACC, EMG, BVP, EDA, HR, TEMP, PPG
Number of Subjects	278	5D + 2H	23	3	10
Number of Seizures	2702	267 (221D + 46H)	173	1139	210
Average number of seizures / patient	9.72	38 (44D + 23H)	7.52	379	21
Total duration of recordings (hours)	> 48000	1333.7 (1254.9D + 78.8H)	916	1155	1032
Average recording time / patient (hours)	175	190 (251D + 39H)	40	385	103

D stands for Dogs, H for Humans, AAC for accelerometry, BVP for blood volume pulse, EDA for electrodermal activity, HR for heart rate, TEMP for temperature, PPG for photoplethysmography, EMG for electromyography, EEG for electroencephalogram.

Along with the annotated EEG and ECG data, extensive metadata is present in the EPILEPSIAE database. It allows for inferences about using Antiepileptic Drugs (AEDs) during the monitoring period. Data collection includes information about the type of electrodes used, and in the case of invasive recordings, it registers the date of implantation [7, 1].

3.2.6 Databases in Seizure Prediction Studies

According to the Table 3.1 in the Subsection 3.1.1, CHB-MIT [107, 109, 110, 111, 112, 116, 117, 118, 120, 121, 122, 124, 127, 128, 130, 132, 134, 137], EPILEPSIAE [73, 95, 96, 97, 102, 119, 123, 126, 129, 131, 132, 139, 141, 142], Freiburg [111, 122, 132, 135, 136, 140], and AES [99, 109, 111, 118, 121, 138] are the databases most frequently used in seizure prediction studies. The popularity of databases sourced from patients undergoing evaluation for epilepsy surgery, particularly CHB-MIT, can be traced back to the early stages of seizure prediction research. This trend is primarily due to CHB-MIT's open accessibility. Although EPILEPSIAE has data from 278 patients, only Pinto et al. (2022) [123], Direito et al. (2017) [97], and Teixeira et al. (2014) [95] incorporated more than 90 patients in their studies, while the rest of the studies concentrated their efforts on 53 or fewer patients.

Nevertheless, regarding the extent of data and accurately reflecting real-life conditions, the NeuroVista database stands out, containing up to two years of iEEG recordings per patient. Cook et al. (2013) [68] released the first study utilizing this database, laying the foundation for its application in several other studies [18, 133], including participation in a Kaggle competition

[67]. This competition saw the incorporation of the three patients with the poorest performance, forming what is now known as the Epilepsy Ecosystem database. Stojanović et al. (2020) [131] have already utilized this last dataset. However, the undeniable benefits of long-term records come with ethical and logistical challenges associated with their ongoing monitoring.

The adoption of wearable devices that record different biosignals, exemplified by the recent creation of the My Seizure Gauge database, has seen significant growth due to the discomfort experienced by patients during ultra-long-term data recording. Consequently, the utilization of bracelets [74, 76] and smartwatches [72] has witnessed remarkable growth in recent years.

Recent developments have led to establishment of novel databases featuring distinct EEG recording systems. A case in point is the clinical trial jointly conducted by King's College London (NCT04061707) and Zealand University Hospital [108, 114], where sqEEG recording has taken center stage. Furthermore, SeizeIT1 and SeizeIT2 [125, 129] have led the way in introducing the utilization of Behind-The-Ear EEG. Also, the studies by Nasseri et al. (2021) [76] and Proix et al. (2021) [86] resorted to data from the NeuroPace database obtained from an Responsive Neurostimulation (RNS) device.

Besides the examination of epilepsy in humans, researchers have recurrently investigated epilepsy in canines [99, 109, 111, 118, 121, 138], making use of the AES dataset.

3.3 Summary

Seizure prediction investigations adhere to a common framework, traversing a series of precisely delineated stages, starting with EEG signals acquisition, followed by signal preprocessing to eliminate interference and artifacts. Subsequently, feature extraction is engaged, being the more intricate facet, frequently employing a sliding window methodology. Historically, the predominant choice has been univariate linear features, although DL models have recently gained use for this task. Upon finishing feature extraction, the procedure advances with curating and categorizing these features, aiming to identify preictal segments within the EEG data. The classifier's output undergoes a regularization phase to address the challenge of false alarms and instill temporal context into the classifications. Notably, specific DL techniques, such as LSTMs, have been directly applied to address temporal aspects of the signal. The journey culminates in the performance assessment, with sensitivity and the FPR/h serving as crucial benchmarks. Of paramount importance is the rigorous statistical validation that underpins this evaluation. Regrettably, the latter's absence is a prevalent issue, often accompanied by presenting results for only an optimal point rather than a spectrum of values. This practice contributes to a lack of uniformity in evaluation methodologies, posing challenges for cross-study comparisons and the clinical application of these techniques.

Database quality assessment is a critical consideration, given that many databases are sourced from patients in pre-surgical monitoring, potentially lacking a complete representation of real seizure events scenarios. Thus, the choice of database significantly influences the algorithm's performance, considering variables such as the number of patients, the nature of collected signals, the number of channels employed, and, fundamentally, the duration and recording conditions of the data.

The progression of existing databases is evident. Initially, data collection was predominantly from pre-surgical monitoring. In recent years, there has been a shift towards creating databases with long-term data that better represent real life. Nonetheless, the predominant issue persists: most of these databases are not openly accessible. Even the "public" ones often offer only a portion of the data, constraining research flexibility. This challenge stems from ethical concerns associated with database privacy.

4

Methodology

This chapter provides insight into the methodologies adopted for developing the seizure prediction algorithm across various datasets. Section 4.1 presents an overview of the pipeline used for European Epilepsy Database (EPILEPSIAE) and provides a description of the seizure prediction model designed for it. The scope of this section is limited to the EPILEPSIAE dataset, which formed the basis for others due to its superior data quality. Lastly, Section 4.2 outlines all methodological deviations incorporated into the approaches for the remaining datasets.

4.1 Seizure Prediction

4.1.1 Pipeline Overview

The principal aim of this project centers around developing a patient-specific algorithm capable of predicting seizure occurrences in epilepsy patients based on Electroencephalogram (EEG) data. This endeavor took inspiration from the prevalent framework expounded upon in Section 3.1 of the literature review.

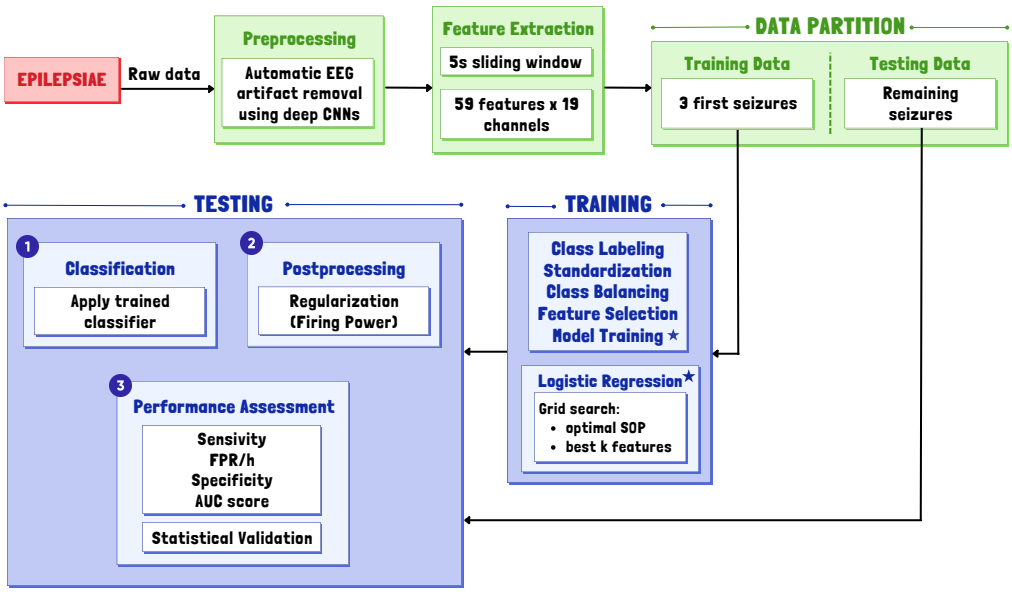

Figure 4.1: General overview of the proposed patient-specific pipeline for a real-life simulation. Asterisks indicate the inclusion of a Logistic Regression classifier in the model training phase.

Figure 4.1 presents details for each step of this algorithm's development. This pipeline is the one of choice because it offers the most accurate simulation of real-life scenarios.

4.1.2 Data

This study involved the careful selection of 40 patients afflicted by Drug Resistant Epilepsy (DRE) from the EPILEPSIAE database. The subset comprises data obtained during pre-surgical monitoring of 23 male and 17 female patients, with a mean age of 41.4 ± 15.7 years. Rigorous criteria guided the selection process of patients. Specifically, the inclusion criteria covered patients diagnosed with Temporal Lobe Epilepsy (TLE), the most common epilepsy type, and individuals with EEG data recorded at a 256 Hz sampling frequency. The 19 EEG electrodes were placed according to the International System 10-20 with the channels FP1, FP2, F3, F4, C3, C4, P3, P4, O1, O2, F7, F8, T7, T8, P7, P8, Fz, Cz and Pz.

Moreover, the selection criteria ensured the inclusion of patients who had experienced a minimum of four independent seizures, with a minimum interval of 4.5 hours between each seizure. This approach avoided the analysis of seizures belonging to the same seizure cluster. Consequently, the dataset contains 224 seizures, with 120 utilized for training and the remainder for testing, resulting in a cumulative data duration of 4656 hours (comprising 3254 hours of training data and 1402 hours of test data). The accompanying Table 4.1 provides demographic information for each patient (sex and age) and details about their seizures (number of seizures, classification, state of surveillance during seizures, and more).

Table 4.1: Detailed information of the 40 patients.

Patient ID	Age	Sex	Number of seizures (train/test)	Seizure classification	Seizure activity pattern	Vigilance at seizure onset	Recording duration (h)
402	55	f	3	FOIA, FBTC, FOIA	t, t, t	A, A, A	103.81
			2	FBTC, FOIA	t, t	A, A	29.66
8902	67	f	3	UC, FOIA, FOIA	a, b, a	A, A, A	133.91
			2	FOIA, FOIA	m, a	A, A	22.5
11002	41	m	3	UC, FOIA, FOIA	?, s, a	A, R, A	97.16
			1	FOIA	t	A	11.7
16202	46	f	3	UC, FBTC, UC	r, ?, r	A, A, A	201.32
			4	FOIA, FOIA, FOIA, FOIA	r, r, ?, r	A, A, A, A	34.45
21902	47	m	3	UC, FOIA, FOIA	t, t, t	A, A, A	67.08
			1	FOIA	b	R	9.76
23902	36	m	3	FOA, FOA, FOA	t, t, t	A, A, A	70.74
			2	FOA, FOA	d, t	A, A	33.95
26102	65	m	3	FOIA, FOIA, FOIA	m, t, t	A, A, A	60.65
			1	FOIA	t	A	22.58
30802	28	m	3	FOA, FOA, FOA	t ,t ,t	R, A, 2	87.57
			5	FOA, FOA, FOA, FOA, FOA	t, t, t, t, t	A, A, R, 2, 2	61.71
32702	62	f	3	FOIA, FOIA, FOIA	t ,t ,t	A, A, A	117.38
			2	FOIA, FOIA	r, a	A, A	20.49
45402	41	f	3	FOIA, FOIA, FOA	t, t, t	A, A, A	71.98
			1	FOIA	t	A	22.31
46702	15	f	3	FOA, FOIA, FOIA	a, a, t	A, 2, A	47.46
			2	FBTC, FOIA	b, t	2, A	12.6
50802	43	m	3	FOIA, UC, UC	t, t, t	A, 2, 2	165.93
			2	FOIA, FBTC	t, t	2, A	35.6
52302	61	f	3	UC, FOA, UC	?, ?, d	A, A, 1	76.45
			1	UC	t	A	6.85
53402	39	m	3	FOA, FOA, FOA	?, ?, ?	A, 2, A	70.31
			1	FOIA	t	A	13.73
55202	17	f	3	FOIA, FOIA, FOA	t, d, t	A, A, A	47.05
			5	UC, UC, FOA, UC, FOIA	t, t, t, r, r	A, A, A, A, A	65.37
56402	47	m	3	UC, UC, UC	t, ?, ?	A, A, A	184.22
			1	FBTC	a	A	20.25
58602	32	m	3	FOIA, FOIA, FOIA	r, t, t	A, R, A	96.94
			3	FOIA, FOIA, FOIA	r, r, t	A, A, 2	23.34

Table 4.1 continued from previous page

Patient ID	Age	Sex	Number of seizures (train/test)	Seizure classification	Seizure activity pattern	Vigilance at seizure onset	Recording duration (h)
59102	47	m	3	FOA, FOIA, FOIA	?, t, t	A, A, A	65.83
			2	FOIA, FOA	t, t	A, A	82.22
60002	55	m	3	FOIA, FOIA, FOIA	d, c, t	1, A, A	208.11
			3	UC, FOIA, FOIA	t, d, d	R, R, 1	152.4
64702	51	m	3	FOA, FBTC, FBTC	?, m, t	A, A, A	75.91
			2	FBTC, FBTC	t, t	A, 2	31.59
75202	13	m	3	FOA, FOA, UC	t, t, t	2, 2, A	100.94
			4	FOA, FOA, FOA, FOA	t, t, ?, t	A, A, A, A	52.63
80702	22	f	3	FOIA, FOIA, UC	b, b, ?	A, A, A	49.4
			3	FOIA, FBTC, FOIA	c, c, c	A, A, A	29.55
85202	54	f	3	FOIA, FOIA, UC	m, c, m	2, A, A	53.49
			2	UC, UC	m, m	A, A	20.42
93402	67	m	3	FBTC, FOIA, FOIA	t, t, t	2, 2, 2	98.0
			2	UC, UC	t, t	2, 2	54.07
93902	50	m	3	FOA, FOIA, FBTC	t, t, d	A, A, 2	370.83
			3	FOIA, FOIA, UC	d, d, d	A, 2, A	20.29
94402	37	f	3	FOA, UC, FOIA	?, d, b	A, A, A	120.23
			4	UC, FOA, UC, FOA	t, ?, b, ?	2, A ,2, A	30.37
95202	50	f	3	FBTC, FOIA, FOIA	b, b, b	2, 2, 2	57.6
			4	FOIA, UC, FOIA, UC	m, b, b, t	2, 2, 2, 2	89.53
96002	58	m	3	FOIA, FOIA, FOIA	t, t, t	A, A, A	48.4
			4	FOIA, UC ,FOIA, FOIA	d ,a ,t ,a	A, A, A, A	82.2
98102	36	m	3	FOA, UC, UC	?, ?, ?	A, A, A	108.61
			2	UC, FBTC	?, ?	A, A	45.68
98202	39	m	3	FOIA, FOIA, FOIA	t, a, t	A, A, A	111.33
			5	FBTC, FOIA, FOIA, FOIA, UC	t, t, t, t, t	A, A, A, A, A	49.88
101702	52	m	3	FOIA, FOIA, FOIA	t, t, t	A, A, A	28.41
			2	FOIA, FOIA	r, r	2, A	23.83
102202	17	m	3	FOA, UC, FOIA	b, ?, t	2, A, 2	57.45
			4	UC, FOA, FOIA, UC	?, t, t, t	A, A, 2, A	51.41
104602	17	f	3	FOIA, FBTC, FBTC	t, a, t	A, 2, 2	87.87
			2	FBTC, UC	t, d	2, 2	15.25
109502	50	m	3	FOIA, FOIA, UC	t, t, t	A, A, A	76.8
			1	UC	t	A	41.94
110602	56	m	3	FOIA, FOIA, FOIA	t, t, t	A, A, A	89.63
			2	FOIA, FOA	t, t	A, A	25.92
112802	52	m	3	UC, FOIA, UC	t, t, t	A, A, A	71.58
			3	FOIA, FOIA, UC	t, t, t	A, A, A	111.5
113902	29	f	3	UC, FOIA, FOIA	t, d, t	A, A, 2	61.98
			3	FOIA, UC, FOIA	t, t, t	A, 2, A	22.73
114702	22	f	3	FOIA, FOIA, UC	t, t, t	A, A, A	68.39
			5	FOIA, FOIA, FOIA, FOIA, FOIA	t, d, t, d, t	A, A, A, A, A	34.04
114902	16	f	3	FOA, FOIA, FOIA	s, b, s	A, A, A	26.55
			4	FBTC, UC, FOIA, FOIA	t, r, a, t	2, A, A, A	50.66
123902	25	f	3	FBTC, FBTC, FOIA	t, t, t	2, 2, R	152.11
			2	FOIA, FOA	t, t	A, A	30.15

Sex: female (f), male (m); Seizure classification: unclassified (UC), Focal Onset Aware (FOA), Focal Onset Impaired (FOIA), Focal to Bilateral Tonic-Clonic (FBTC); Seizure activity pattern: unclear (?), rhythmic sharp waves (s), alpha waves (a), rhythmic delta waves (d), rhythmic theta waves (t), rhythmic beta waves (b), repetitive spiking (r), cessation of interictal activity (c), amplitude depression (m); Vigilance state: awake (A), REM sleep stage (R), Non-REM sleep stage I (1), Non-REM sleep stage II (2).

4.1.3 Preprocessing

Within the scope of this study, EEG data underwent a preprocessing phase employing a Convolutional Neural Networks (CNNs)-based approach. This technique, developed by Lopes et al. (2021) [80], automatically and effectively eliminates artifacts like eye blinking, eye movements, muscle activity, heart activity, and electrode interference, producing results comparable to those achieved by experts. The dataset used in the Lopes et al. (2021) study comprised long-term EEG recordings of particular epilepsy patients featured in this thesis.

The CNN model underwent training using raw and manually preprocessed EEG segments, mirroring experts' steps during data preprocessing. This approach enabled the replication of expert procedures during data preprocessing. The experiments demonstrated that the model

significantly mitigated the impact of artifacts on EEG signals, all without requiring human intervention. Consequently, it is well-suited for utilization in extended, real-time monitoring contexts.

4.1.4 Feature Extraction

EEG signals were partitioned into non-overlapping 5-second windows to extract significant features. Established practices in seizure prediction guided the decision to employ this window duration, which aligns with reasonable values for stationarity, temporal, and spectral resolution.

Owing to its lower computational demands, the extraction process concentrated exclusively on univariate linear features. All available electrodes were used, given the possibility of multiple brain regions contributing to seizure generation. Consequently, a sliding window technique captured 59 features in each window's time and frequency domains for the 19 channels. The extracted features took cues from the research conducted by Lopes et al. (2023) [102] and Pinto et al. (2023) [119], who investigated patients included in this study. Within the frequency domain, these features included relative spectral power bands such as delta (0.5-4Hz), theta (4-8Hz), alpha (8-13Hz), beta (13-30Hz), and four subbands of gamma - gamma band 1 (30-47 Hz), gamma band 2 (53-75 Hz), gamma band 3 (75-97 Hz), and gamma band 4 (103-128 Hz). Furthermore, features encompassed the relationships between these bands, spectral edge frequency and power, alpha peak frequency, total power, and mean frequency. In the time domain, computed features consisted of the four statistical moments (mean, variance, asymmetry, kurtosis), Hjorth parameters (activity, mobility, complexity), decorrelation time, and energy of wavelet coefficients (from D1 to D5, employing the db4 parent wavelet). For a more in-depth description of each feature, consult Appendix A.

4.1.5 Data Splitting

This stage entailed the partitioning of resources into two distinct sets for each patient: the first set being the training set, encompassing the initial three seizures, while the remaining seizures constituted the test set. The training set was pivotal in classifier training and parameter optimization, including determining Seizure Occurrence Period (SOP) duration and number of features. The sets were split following the seizure order since time dependence and concept drifts are assumed. This chronological division aimed to replicate a practical seizure prediction scenario, where the model initially learns from a historical set of seizures before being deployed for real-time prediction on future data.

4.1.6 Training

4.1.6.1 Class Labeling

The feature set samples received categorization into preictal or interictal. The period preceding a seizure, recognized as the preictal class, corresponds to the cumulative duration of Seizure Prediction Horizon (SPH) and SOP. The project's objective led to setting the SPH duration at 10 minutes to create an algorithm designed for alert devices. These devices activate alarms, encour-

aging the patient to administer rescue medication and prevent imminent convulsions promptly. The determination of the 10-minute value considered the time it takes for rescue medications (e.g., buccal and rectal diazepam, midazolam) to take effect [171, 172, 173]. The algorithm's predictive scope extended to the SOP timeframe preceding the SPH duration. Consequently, samples linked with SPH were left out, considering them irrelevant for model training and testing.

Customizing the SOP duration for each patient involved a comprehensive grid search across values (20, 25, 30, 35, 40, 45, and 50 minutes). A deliberate selection process resulted in these values, aimed at keeping the preictal period within 60 minutes, ranging from 30 to 60 minutes.

4.1.6.2 Feature Standardization

The subsequent action involved standardizing the independent features extracted from the raw data. The selected method for this task was z-score normalization, which effectively adjusted the values of each feature to have an average of 0 and a unitary standard deviation.

4.1.6.3 Class Balancing

In the training phase, defining a class balancing strategy to manage data imbalance while preserving data representativeness becomes crucial. Given that the interictal class contains most samples, an imbalanced dataset can lead to biased results, as the classifier may overly specialize in the dominant class. Therefore, a deterministic approach to balance classes using class weights was adopted. Due to the substantial prevalence of the interictal class over the preictal class, a reduction in the weight assigned to the former occurs, leading to an inversely proportional relationship. The formula employed to compute the weights for each class corresponds to the provided Equation 4.1.

$$w_i = \frac{N_{Total\ Samples}}{2 \cdot N_{i\ Samples}}, i = 0, 1. \tag{4.1}$$

4.1.6.4 Feature Selection

Much like the process used to determine the optimal SOP value and building upon the research conducted by Pinto et al. (2023) [119], a similar methodology was applied to identify the optimal values for the k most discriminatory features. A grid search revealed the most fitting values for the k most discriminatory features, including k values from 3, 5, 7, 10, 15, 20, to 30 features. The assessment metric of choice was the ANOVA f-test (Analysis of Variance), which evaluates the degree of linear dependence between each feature and the target. Subsequently, the k most discriminative features were selected based on their classification performance, thus pinpointing the most suitable number of features.

4.1.6.5 Classifier

Logistic Regression was the classifier of choice for this study, primarily due to its computational efficiency and straightforward methodology. The shape of its curve follows a logistic function, and its built-in interpretability is a distinct advantage. This approach adjusted class weights in inverse proportion to their respective frequencies.

4.1.6.6 Grid-Search

As previously mentioned, applying a grid search methodology enabled the identification of optimal parameters, specifically the ideal SOP and the number of features (k) necessary for training the selected classifier. For this purpose, the Leave-One-Out Cross-Validation (LOOCV) strategy was employed. LOOCV partitions the training set into three subsets, with two designated for training and one for validation, ensuring that all subsets contain samples from interictal and preictal classes. Each subset contains the data before a specific training seizure, where $S1$ indicates the first seizure, $S2$ represents the second, and $S3$ corresponds to the third. This process iterates three times, repeating until each subset serves for validation. Lastly, training the classifier involves using data from $S1$, $S2$, and $S3$, aligning with the most effective parameter combination. Figure 4.2 provides a schematic representation of this process.

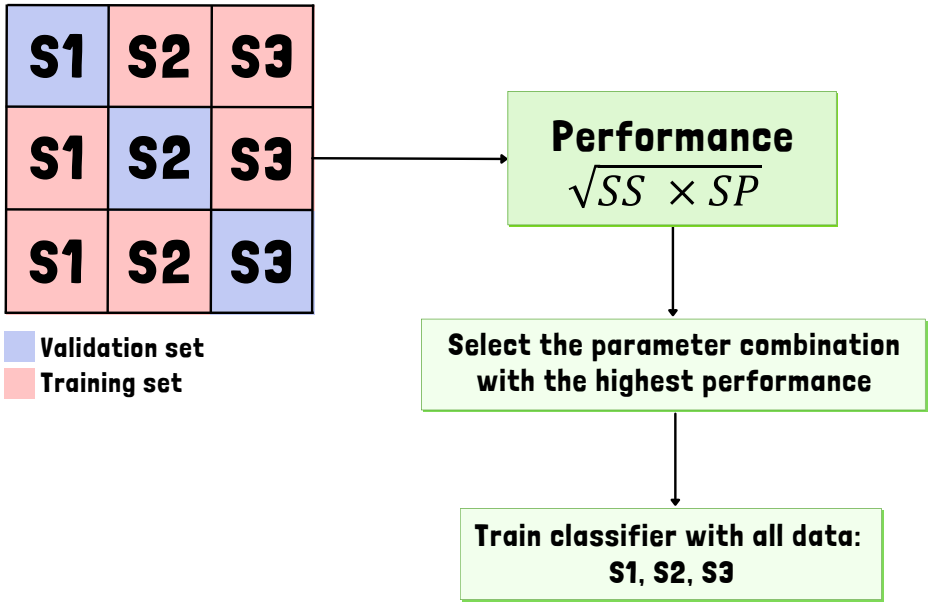

Figure 4.2: LOOCV procedure implemented to select the optimal parameters. $S1$, $S2$, and $S3$ represent the data for the first, second, and third seizures, respectively.

A performance metric, represented by Equation 4.2, was instrumental in determining the optimal parameters. This equation exposes the trade-off between SS_{sample} and SP_{sample}. Having established the optimal SOP and k values, the model underwent training using the training set.

$$\sqrt{SS_{sample} \cdot SP_{sample}} \tag{4.2}$$

4.1.7 Testing

To initiate the testing phase, conducting an out-of-sample classification analysis on the test set resulted in the formulation of predictions. As illustrated in Figure 4.3, the techniques used on the test data closely resembled those used on the training set, except for class balancing. Therefore, the test set underwent standardization using the z-score parameters obtained from the training set, and the most significant features identified during training were selected. Finally, the classifier was employed to determine the final output.

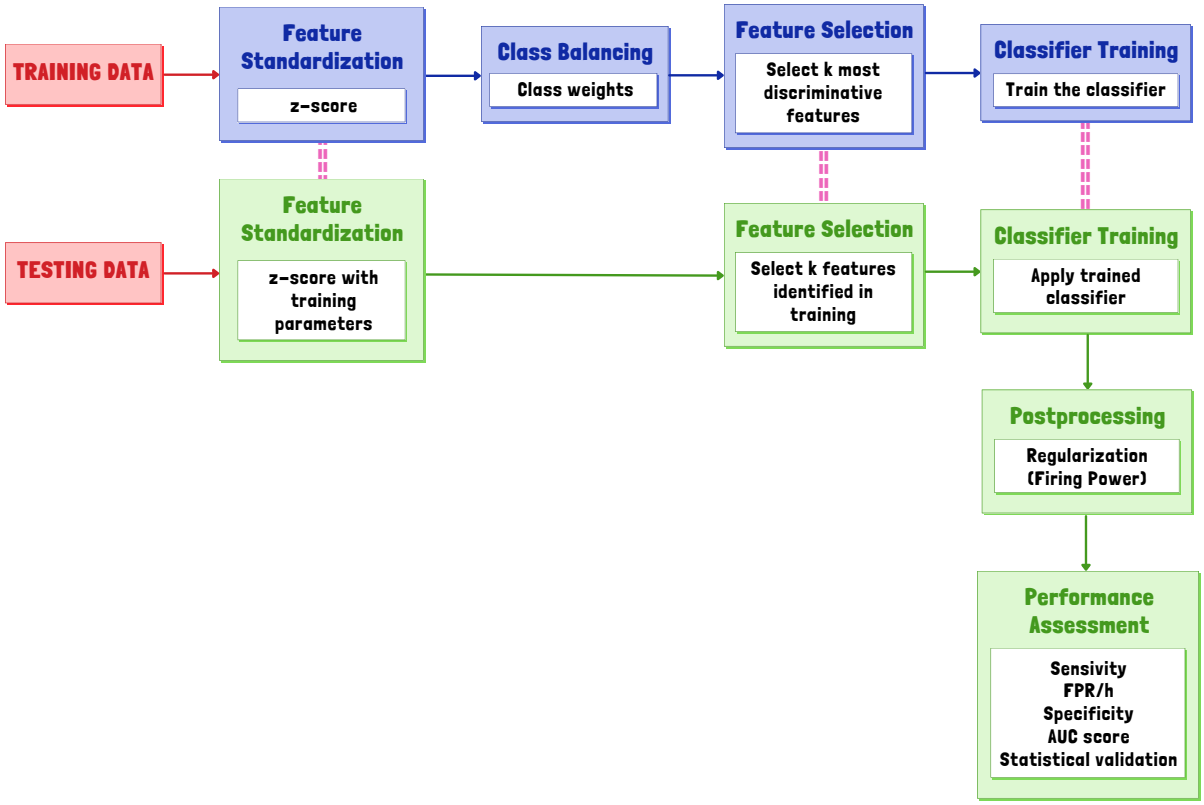

Figure 4.3: Procedure applied to train and test the seizure prediction model.

4.1.8 Postprocessing

After the classification phase, regularization became active in reducing false alarms and providing meaningful context to consecutive results while considering the temporal dynamics of the output. The selected method was Firing Power (FP) (as shown in Figure 4.7), and its calculation followed the description provided in Section 2.4.5.3. FP employs a moving average low-pass filter to smooth the signal. It triggers an alarm when the value exceeds a predefined threshold, but only if a refractory period separates it from the previous one. Setting the chosen threshold at 0.7 was influenced by studies conducted by Pinto et al. in 2023 [119], 2022 [123], and 2021 [126], which also used EPILEPSIAE. The refractory period corresponds to the entire preictal period (SOP + SPH), effectively minimizing redundant alerts during a seizure event and mitigating the patient's stress and anxiety.

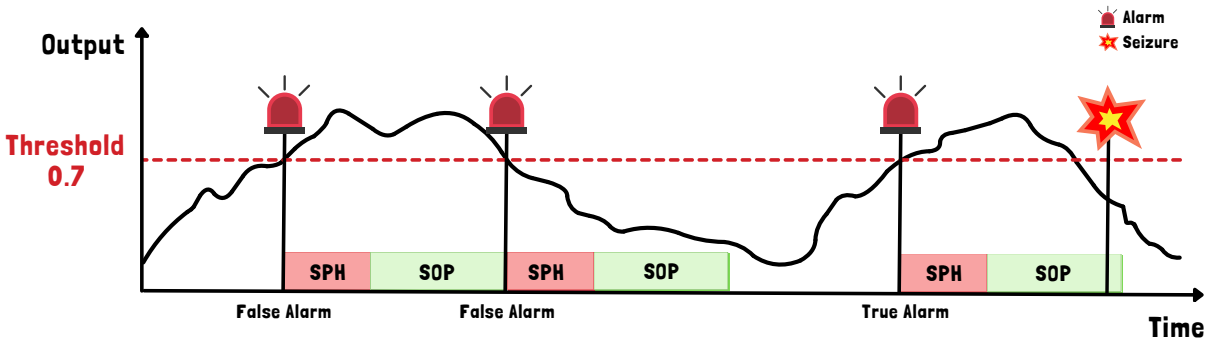

Figure 4.4: An illustration of the firing power technique used. When the firing power reaches a certain threshold (dashed line) and is at least one refractory period apart from the most recent alarm, an alert is triggered. Two false alarms and one true alarm are illustrated.

4.1.9 Performance Assessment

The assessment of the developed seizure prediction model's performance involved the use of standard metrics, such as Sensitivity (Equation 2.1) and False Prediction Rate per hour (FPR/h) (Equation 2.2), as outlined in the Section 2.4.5.1. Specificity and the Area Under the ROC Curve (AUC) score were also integrated into the evaluation to provide a comprehensive overview of the outcomes. This inclusion is essential since not all utilized databases enable the calculation of sensitivity and FPR/h. Therefore, alternative metrics are essential to facilitate comparisons.

For statistical validation, the employed method was surrogate time series analysis, which confirmed whether the developed algorithm exhibited performance exceeding that expected by chance. In this procedure, the original onset times of each seizure underwent random shifts within the interictal period. This operation was conducted individually for each seizure, ensuring that the simulated seizure times followed the original temporal distribution. The algorithm's sensitivity was then determined using the newly generated seizure times. This procedure underwent 30 repetitions to calculate an average sensitivity, subsequently comparing it to the sensitivity obtained through the proposed methodology. The algorithm's performance was evaluated as superior to chance level when its sensitivity exceeded that of the surrogate predictor and demonstrated statistical significance. With a significance level 0.05, the analysis involved a one-sample t-test to evaluate this difference and test the null hypothesis that "the sensitivity of the proposed approach is not statistically superior to the sensitivity of the surrogate predictor."

4.2 Database Pipeline Comparison

The pipeline model applied in the context of EPILEPSIAE formed the foundational framework for subsequent model implementations across other databases. However, specific alterations were imperative owing to disparities stemming from differences in the raw data available, whether related to the type of EEG data collected or the number of channels used, among other distinguishing factors. Consequently, this section will explore the modifications implemented for each analyzed dataset. The omitted steps refer to those aspects that have remained unchanged across all databases.

4.2.1 Data

AES

This research involved integrating data from all subjects in the American Epilepsy Society (AES) database, which included information from 5 dogs and two humans. Analogous to the EPILEPSIAE patient subset, human data in this database was collected within a pre-surgical environment. Nonetheless, several differentiating factors set AES human subjects apart from EPILEPSIAE patients, including Intracranial Electroencephalogram (iEEG) data, a sampling frequency of 5 kHz, and the utilization of 15 and 24 channels, among other contrasting elements.

The most notable contrast lies in the absence of temporal data, meaning there is no information about the timing of seizures; only 10-minute files categorized as preictal or interictal are available. In the case of canines, analogous disparities are apparent, coupled with the fact that the recordings in this context are of a long-term ambulatory nature. Considering the differentiating values, the canine recordings underwent collection at a sampling frequency of 400 Hz, utilizing 15 and 16 channels.

Despite comprising 267 seizures, only 51 seizures were used in this study. Of these, 34 seizures were earmarked for training, leaving 17 for testing. The decision to work with only a subset of the total seizures stemmed from the inaccessibility of labels for the available test files. Section 4.2.4 details the solution to this issue. Consequently, the study encompassed a recording duration of 627.6 hours. Refer to the Table 4.2 for a thorough presentation of details about each subject.

Table 4.2: Detailed information of the 7 subjects.

Subject	Number of channels	Sampling rate (Hz)	Number of train files	Number of test files	Duration (hours)
Dog 1	16	400	468	12	80
Dog 2	16	400	476	24	83.3
Dog 3	16	400	1392	48	240
Dog 4	16	400	742	62	134
Dog 5	15	400	426	24	75
Patient 1	15	5000	38	12	8.3
Patient 2	24	5000	30	12	7

CHB-MIT

Not all patient data within the Children's Hospital Boston from the Massachusetts Institute of Technology (CHB-MIT) dataset was part of the study. Instead, a meticulous selection process was undertaken among the 24 available cases, resulting in the identification of only 6 cases (chb01, chb06, chb10, chb14, chb15, chb24) that met all the necessary criteria. These individuals were the exclusive ones who experienced a minimum of 4 independent seizures, with a requisite minimum interval of 4.5 hours between each seizure. Determining the criterion value for delineating seizures entailed comprehensively evaluating different possible intervals (1, 2, 3, 4, 4.5, and 5 hours). This evaluation involved assessing parameters like the number of patients with a minimum of 4 independent seizures, the total count of independent seizures, and the mean count per patient (see Figure 4.5). Given the close alignment between values obtained for 4, 4.5, and 5 hours, the optimal choice appeared to be 4.5 hours, thereby maintaining consistency with the approach taken in the EPILEPSIAE context.

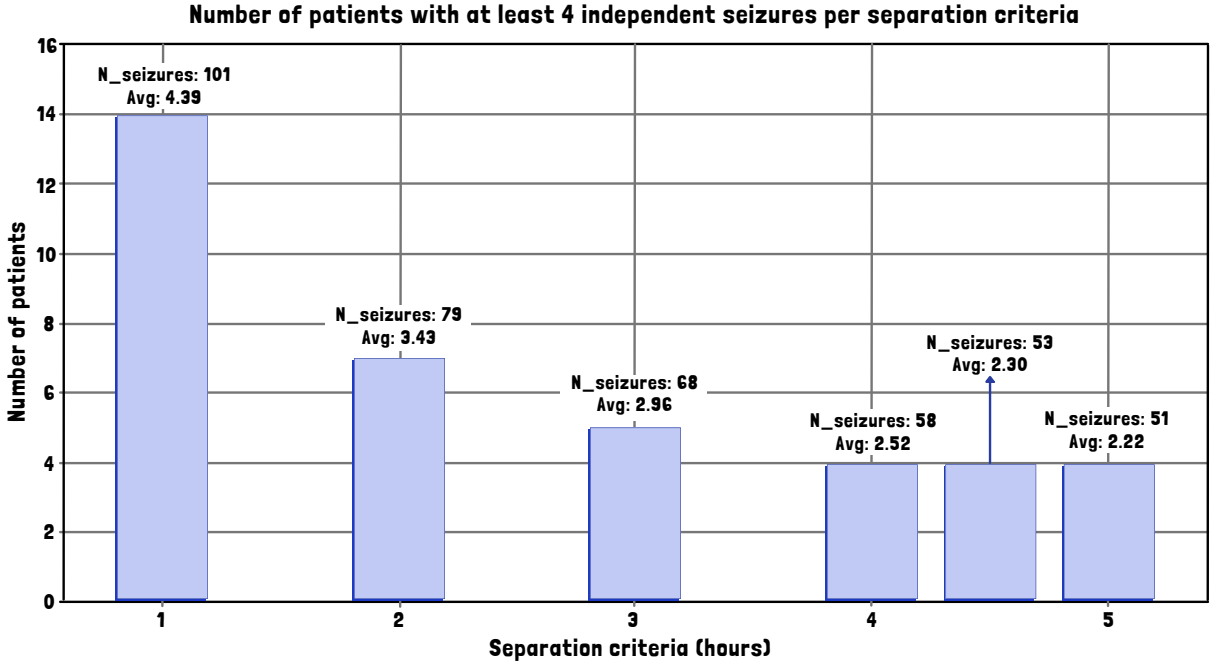

Figure 4.5: Influence of separation criterion values on patients with at least four independent seizures, total seizure count, and average seizures per patient.

Figure 4.6 exhibits a plot illustrating the count of independent seizures for each patient, utilizing a separation criterion of 4.5 hours. The plot reveals that cases chb12, chb13, and chb18 exhibit sufficient independent seizures to qualify for selection. Nevertheless, additional considerations led to the exclusion of these cases. Both chb12 and chb13 experienced multiple electrode alterations during their recordings, leading to their exclusion from the study. In the case of chb18, the available temporal window for a single test seizure was excessively short, rendering its inclusion unviable. Thus, the resultant subset encompasses 32 seizures, with 18 designated for training and 14 reserved for testing. Consequently, the overall duration of target data for the study is 244 hours, with roughly 47 hours allocated to training data and a substantial

197 hours dedicated to test data.

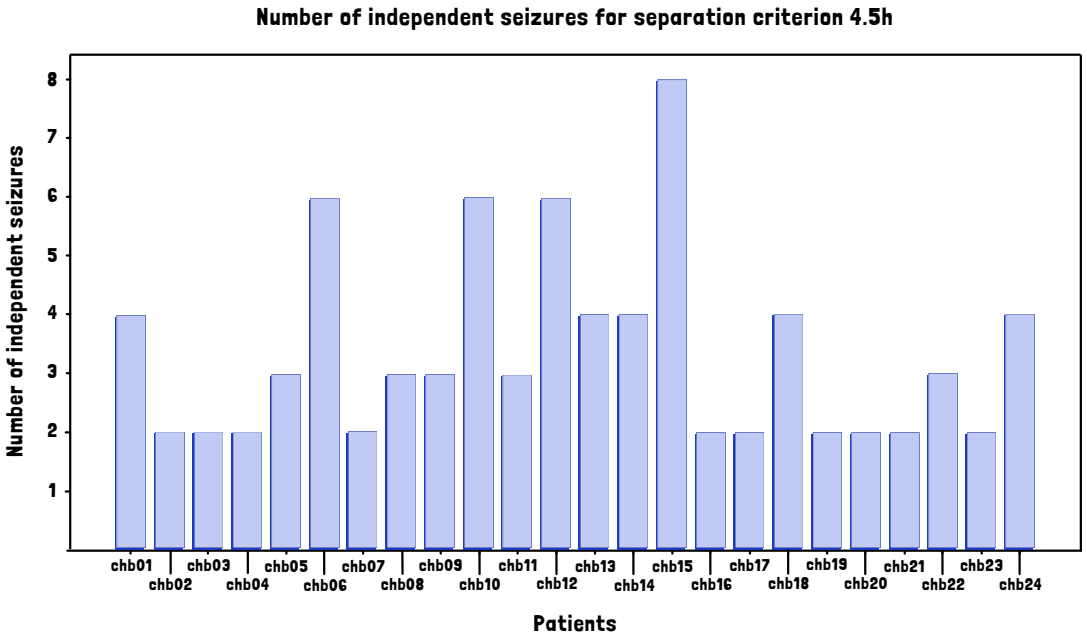

Figure 4.6: Independent seizure occurrences per patient at a separation criterion of 4.5 hours.

The average age of the three women and two men included in the selection is 8.1 ± 5.4 years. However, it is worth noting that the age and gender of case chb24 remain unknown. Data from all these patients were collected at a sampling rate of 256 Hz using 23 channels arranged under the International System 10-20, except for case chb15, which utilized 32 channels. Remarkably, this dataset closely mirrors the EPILEPSIAE database, featuring the same signal type, sampling frequency, and availability of temporal data. Nonetheless, a notable difference is the absence of metadata. The Table 4.3 presents a comprehensive overview of the most relevant information for each of the cases that were subjects of study.

Table 4.3: Detailed information of the 6 cases.

Patient	Age	Sex	Number of channels	Number of seizures (train/test)	Recording duration (h)
chb01	11	f	23	3	10.59
				1	4.83
chb06	1.5	f	23	3	8.19
				3	31.95
chb10	3	m	23	3	4.18
				3	111.24
chb14	9	f	23	3	8.3
				1	9.32
chb15	16	m	32	3	9.75
				5	36.56
chb24	-	-	23	3	7.83
				1	5.41

Sex: female (f), male (m).

Epilepsy Ecosystem

Epilepsy Ecosystem is the exclusive database where data from every accessible patient is studied. Originating from the NeuroVista database, the dataset under consideration focuses on the three patients who demonstrated the poorest results. The real-life data, collected at a sampling rate of 400 Hz, is from three female patients. The average age of these three women is 41±13.5 years. The dataset comprises long-term iEEG recordings acquired from 16 channels. Notably, the data accessibility structure closely aligns with the AES database. However, in this case, the use of the test files was enabled by the public availability of their labels.

Consequently, in the execution of this study, data totaling only 935.3 hours was incorporated from the 1155 hours that the dataset contains. Training received an allocation of 841.2 hours from this duration, with the remaining hours designated for testing. This database exhibits a comparable blend of distinctions and similarities with AES, analogous to the relationship between AES and EPILEPSIAE. Key distinctions include the absence of temporal information, variations in the type of EEG data collected, differences in sampling rate, and the absence of metadata. The Table 4.4 contains detailed data characteristics.

Table 4.4: Detailed information of the 3 patients.

Patient	Age	Sex	Number of channels	Sampling rate (Hz)	Number of train files	Number of test files	Recording duration (h)
1	21	f	16	400	826	62	148.0
2	51	f	16	400	2058	297	392.5
3	50	f	16	400	2163	206	394.8

Gender: female (f), male (m).

My Seizure Gauge

My Seizure Gauge collects an assortment of data from various wearable devices. However, it is crucial to note that only one of these devices, namely Epilog, played a role in this study due to its capacity to collect EEG signals. Given these circumstances, the decision was to select data from a single individual (MSEL_01860) out of the ten available patients. In order to ensure eligibility, the requirement was to guarantee a minimum of 4 independent seizures, each separated by a minimum of 3.5 hours. Since this patient's data did not meet the criteria to fulfill this requirement, the exclusion of the patient became necessary, resulting in the impossibility of analyzing data from this database in this study.

4.2.2 Preprocessing

The preprocessing procedure diverged from the approach used in EPILEPSIAE for all the databases. Instead of implementing the technique introduced by Lopes et al. (2021) [102], filtering was selectively performed within specific frequency bands to simplify the process. When the EEG signal was intracranial, such as AES and Epilepsy Ecosystem, a high-pass filter was employed with a cutoff frequency of 0.5 Hz. In contrast, for database CHB-MIT, the preprocessing procedure entailed using both a high-pass filter with a 0.5 Hz cutoff and a low-pass filter with a 60 Hz cutoff. Additionally, it became necessary to downsample datasets that initially had different sampling rates from 256 Hz. Therefore, this additional step was necessary for all seven AES subjects and the three patients from the Epilepsy Ecosystem dataset.

4.2.3 Feature Extraction

The feature extraction process remained essentially unaltered, with the sole variance being the adjustment of the number of channels to align with each patient's specific value.

4.2.4 Data Splitting

Unlike feature extraction, data splitting experienced more extensive adaptations. EEG segments referring to each seizure or preictal and interictal segments can compose the two distinct datasets. For the only dataset containing temporal data (CHB-MIT), the segments utilized correspond to each seizure, mirroring the approach adopted in EPILEPSIAE. Also, the training dataset comprises the initial three seizures, with the remaining seizures allocated to the test dataset.

Concerning AES, where information regarding seizure timing is unavailable, both the training and testing datasets are constructed using interictal and preictal files. Additionally, since the labels of the original test files from this database are inaccessible, the training files had to be partitioned for training and testing. Initially, this division considered a 70/30 ratio for training/testing preictal files. However, due to the sequential arrangement of files, this approach meant, for instance, that the first six files belonged to the same 1-hour preictal period. Consequently, to ensure that data from the same preictal period did not appear in the training and test sets, the split was adjusted to the closest 70/30 ratio, guaranteeing a split where the sets of 6 files were not separated. In order to maintain balance within the training data, the number of interictal files added to the training set equaled the number of preictal files, with the remaining interictal files assigned to the testing set.

The Epilepsy Ecosystem dataset also includes preictal and interictal files. The data's configuration remained consistent with its publicly available structure, with the data already divided into two sets: one for training and the other for testing purposes. The singular adaptation mirrored the procedure applied in AES, ensuring that the quantity of interictal training files equaled the number of preictal training files. Table 4.5 provides a concise summary of the information elucidated in this subsection.

Table 4.5: Comparison of data splitting approaches for the analyzed databases.

Dataset	Main approach		Interval between seizures (hours)	Data division	
	Alarm	Sample		Train	Test
EPILEPSIAE	X	-	4.5	3 first seizures	Remaining seizures
CHB-MIT	X	-	4.5	3 first seizures	Remaining seizures
AES	-	X	N.A.	$\approx$ 70% of preictal original train files (x) + x interictal train files	Remaining train files
Epilepsy Ecosystem	-	X	N.A.	All preictal original train files (x) + x interictal train files	All test files

x refers to the number of preictal train files.

4.2.5 Training

4.2.5.1 Class Labeling

This step remained unchanged for CHB-MIT. Conversely, it was bypassed for AES and Epilepsy Ecosystem, as the data had already been classified and separated into preictal and interictal segments.

4.2.5.2 Class Balancing

Data balance was maintained by incorporating class weights for CHB-MIT. However, for AES and Epilepsy Ecosystem, this procedure was simplified, entailing the selection of an equal number of interictal and preictal files for the training set during data splitting.

4.2.5.3 Grid-Search

Determining optimal parameters followed a uniform approach for CHB-MIT. In contrast, for AES and Epilepsy Ecosystem, the focus was solely on identifying the ideal number of features (k), as the data had already undergone classification and the SOP period was predetermined. The LOOCV strategy was not employed, and the data was divided into the closest 70/30 proportion for training and validation, preserving the integrity of sets comprising six consecutive files belonging to the same data group. Thus, finding the best k value was not repeated three times.

4.2.6 Testing

4.2.6.1 Postprocessing

The application of data regularization through the FP method extended to the CHB-MIT dataset. However, for AES and Epilepsy Ecosystem data, this step was excluded due to the inability to set alarms without seizure timing information. Therefore, as the approach for these datasets centered on the individuality of each sample, regularization was not part of the applied methodology.

4.2.6.2 Performance Assessment

The procedure for evaluating the algorithm's performance and conducting statistical validation remained consistent for CHB-MIT data, using the same metrics. In contrast, for AES and Epilepsy Ecosystem data, calculating Alarm Sensitivity or FPR/h was impossible. The calculation covered only Sample Sensitivity, Sample Specificity, and AUC score. The approach to statistical validation had to be slightly different. EPILEPSIAE and CHB-MIT adopted the surrogate analysis of time series, altering the temporal positioning of seizure onset while maintaining consecutive order within preictal periods. However, this method did not apply to AES and Epilepsy Ecosystem data. For these datasets, performing 30 random shuffles of all samples allowed the determination of an average sensitivity, which was then compared to the sensitivity obtained through the proposed methodology.

4.2.7 Pipeline Overview

In order to provide a summary of the modifications implemented in each dataset relative to the model utilized for EPILEPSIAE, Table 4.6 delineates the key distinctions presented in this section. Furthermore, in the Appendix B, visual representations are available illustrating the models utilized for the CHB-MIT, AES, and Epilepsy Ecosystem databases, following the structure of Figure 4.1.

Table 4.6: Differences in methodology across databases.

Dataset	EPILEPSIAE	CHB-MIT	AES	Epilepsy Ecosystem
Number of patients	40	6	7	3
Signal	scalp EEG	scalp EEG	iEEG	iEEG
Sampling rate (Hz)	256	256	400 D + 5000 H	400
Total hours	4656	248	627	935
Hours/seizure	20.8	7.8	12.31	4.4
Temporal seizure data	Yes	Yes	No	No
Preprocessing	CNNs-based approach	0.5Hz high-pass, 60Hz low-pass filters	0.5Hz high-pass filter	0.5Hz high-pass filter
Downsampling	No	No	Yes	Yes
Data splitting approach	Seizures	Seizures	Preictal and interictal files	Preictal and interictal files
Calculated metrics	SS_{alarm}, FPR/h, SS_{sample}, SP_{sample}, AUC	SS_{alarm}, FPR/h, SS_{sample}, SP_{sample}, AUC	SS_{sample}, SP_{sample}, AUC	SS_{sample}, SP_{sample}, AUC

D stands for dogs, H for humans.

5

Results and Discussion

This chapter takes a comprehensive look at the outcomes obtained by the proposed methodology. Section 5.1 embarks on a detailed analysis of the results achieved during the training phase. Section 5.2 covers the presentation, analysis, and discussion of the results acquired in the testing phase. Section 5.3 involves a comparative assessment of the outcomes yielded by the proposed methodology and those reported in studies by other authors utilizing the same databases. Lastly, Section 5.4 elucidates the limitations inherent to this study.

5.1 Training Results

As expounded in the Chapter 4, the training phase involved conducting a grid search to ascertain the optimal parameters for each patient within each database. Classifier training involved using either the initial three seizures of each patient (for European Epilepsy Database (EPILEPSIAE) and Children's Hospital Boston from the Massachusetts Institute of Technology (CHB-MIT)) or data categorized as preictal or interictal (in the case of American Epilepsy Society (AES) and Epilepsy Ecosystem). Tables 5.1, 5.2, 5.3, and 5.4 compile the optimal parameters identified for each patient, along with the corresponding sample Sensitivity (SS_{Sample}) and sample Specificity (SP_{Sample}).

A comprehensive review of the tables reveals significant fluctuations in the Seizure Occurrence Period (SOP) values, with no clear-cut ideal SOP period standing out. Concerning the number of features, data from AES and CHB-MIT primarily tend to converge around 3. However, for the Epilepsy Ecosystem database, limited patient data makes it challenging to identify a clear trend. Conversely, EPILEPSIAE exhibits a diverse range of values for the number of features, spanning from 3 to 30, with no apparent inclination toward a particular value.

The results obtained for SS_{Sample} and SP_{Sample} facilitate the division of the databases into two distinct groups: EPILEPSIAE, and CHB-MIT forming one group, while AES and Epilepsy Ecosystem comprise the other. Metric values are notably higher in patients from AES and Epilepsy Ecosystem. These high values can be attributed to the intracranial data nature, which reduces susceptibility to noise and artifacts or the absence of temporal distribution reflecting real-world scenarios, simplifying the classification process.

The closely aligned values observed for EPILEPSIAE and CHB-MIT align with expectations, given the similarity in data type and organizational structure. Notably, the specificity values for EPILEPSIAE and CHB-MIT data slightly exceeded the sensitivity, indicating a more remarkable classifier ability to identify interictal samples than preictal ones.

Table 5.1: Training results for the EPILEPSIAE database. SOP stands for Seizure Occurrence Period, SS_{Sample} for Sample Sensitivity, and SP_{Sample} for Sample Specificity.

Patient	SOP (mins)	k-features	SS_{Sample}	SP_{Sample}
402	50	20	0.35	0.52
8902	25	7	0.87	0.81
11002	20	7	0.45	0.73
16202	20	30	0.64	0.82
21902	40	10	0.65	0.76
23902	45	15	0.71	0.55
26102	50	30	0.29	0.66
30802	50	5	0.74	0.83
32702	20	7	0.72	0.72
45402	25	20	0.69	0.53
46702	30	20	0.19	0.72
50802	20	10	0.74	0.84
52302	45	30	0.55	0.69
53402	40	20	0.37	0.70
55202	45	3	0.50	0.75
56402	20	10	0.51	0.76
58602	20	3	0.09	0.77
59102	35	30	0.40	0.55
60002	35	7	0.57	0.59
64702	40	3	0.36	0.69
75202	25	30	0.73	0.83
80702	40	30	0.30	0.82
85202	20	20	0.31	0.70
93402	20	3	0.39	0.66
93902	45	5	0.60	0.63
94402	45	30	0.51	0.53
95202	25	15	0.48	0.71
96002	25	3	0.70	0.74
98102	25	20	0.36	0.62
98202	25	30	0.17	0.73
101702	50	30	0.65	0.37
102202	50	3	0.31	0.73
104602	35	30	0.24	0.79
109502	30	20	0.35	0.66
110602	40	10	0.51	0.67
112802	20	3	0.33	0.66
113902	45	30	0.32	0.61
114702	35	30	0.13	0.76
114902	25	10	0.55	0.63
123902	25	3	0.66	0.88
Overall	33.13±10.96	16.05±10.82	0.47±0.19	0.69±0.11

The less-than-ideal results achieved for EPILEPSIAE and CHB-MIT underscore the complexity of the seizure prediction problem when confronted with a scenario replicating the realistic temporal dynamics of seizure occurrences. Nonetheless, assessing the classifier's real predictive prowess is possible only during testing phase.

Table 5.2: Training results for the CHB-MIT database. SOP stands for Seizure Occurrence Period, SS_{Sample} for Sample Sensitivity, and SP_{Sample} for Sample Specificity.

Patient	SOP (mins)	k-features	SS_{Sample}	SP_{Sample}
chb01	40	3	0.53	0.64
chb06	50	3	0.68	0.82
chb10	20	30	0.51	0.81
chb14	45	3	0.57	0.47
chb15	25	3	0.25	0.58
chb24	25	15	0.36	0.71
Overall	30.00±13.23	9.50±11.13	0.48±0.15	0.67±0.14

Table 5.3: Training results for the AES database. SS_{Sample} stands for Sample Sensitivity, and SP_{Sample} for Sample Specificity.

Patient	k-features	SS_{Sample}	SP_{Sample}
Dog 1	3	1.00	0.50
Dog 2	3	1.00	1.00
Dog 3	3	1.00	1.00
Dog 4	5	1.00	1.00
Dog 5	3	1.00	1.00
Patient 1	3	1.00	1.00
Patient 2	3	1.00	1.00
Overall	3.29±0.76	1.00±0.00	0.93±0.19

Table 5.4: Training results for the Epilepsy Ecosystem database. SS_{Sample} stands for Sample Sensitivity, and SP_{Sample} for Sample Specificity.

Patient	k-features	SS_{Sample}	SP_{Sample}
Patient 1	30	0.95	0.96
Patient 2	5	0.96	0.79
Patient 3	30	1.00	1.00
Overall	21.67±14.43	0.97±0.03	0.92±0.11

5.2 Testing Results

During the testing phase, the evaluation of patient-specific models occurred, taking into consideration the remaining seizures (for EPILEPSIAE and CHB-MIT) or preictal/interictal data (for AES and Epilepsy Ecosystem). This comprehensive evaluation involved the examination of multiple metrics, including SS_{Alarm} and False Prediction Rate per hour (FPR/h), for databases containing temporal information on seizures. Additionally, for all databases SS_{Sample}, SP_{Sample}, and Area Under the ROC Curve (AUC) were computed. Tables 5.5, 5.6, 5.7, and 5.8 showcase the predictive outcomes for each patient from EPILEPSIAE, CHB-MIT, AES, and Epilepsy Ecosystem, respectively. Furthermore, statistical validation took place in conjunction with the performance evaluation. For EPILEPSIAE and CHB-MIT, this validation utilized the surrogate time series analysis for comparison with SS_{Alarm} and SS_{Sample}. Meanwhile, the remaining databases underwent SS_{Sample} comparison via a file shuffle approach.

As indicated by Tables 5.5 and 5.6, the number of seizures evaluated varies from 1 to 5, posing challenges when comparing patient SS_{Alarm} values. The challenge arises because, when assessing patients with only one tested seizure, sensitivity is constrained to either 0 (indicating an unforeseen seizure) or 1 (indicating a correctly predicted seizure). However, sensitivity can yield a range of values when evaluating five seizures. Therefore, a sensitivity value of 1 does not hold the same significance for patients with different numbers of evaluated seizures. From the tables, it is evident that only patients 8902, 93402, and chb01 achieved an alarm sensitivity value of 1, and these patients had only 2 and 1 seizures evaluated in the cases of EPILEPSIAE and CHB-MIT patients, respectively. Furthermore, 57.5% of EPILEPSIAE patients had only 1 or 2 seizures evaluated in the test phase and 50% of CHB-MIT patients had only one seizure evaluated. This implies that, in most cases, only 1 or 2 seizures are set aside for testing, significantly constraining the range of values achieved for SS_{Alarm}. Hence, this aspect represents a limitation of the study, stemming from the need for a more extensive dataset involving a larger patient population.

Table 5.5: Testing results for the CHB-MIT database. SS_{Alarm} stands for Alarm Sensitivity, SS_{Sample} for Sample Sensitivity, SP_{Sample} for Sample Specificity, and AUC for Area Under the Curve.

Patient	Tested Seizures	FPR/h	SS_{Alarm}	SS_{Sample}	SP_{Sample}	AUC
chb01	1	0.31	1.00	0.77	0.46	0.62
chb06	3	0.89	0.33	0.91	0.46	0.68
chb10	3	0.38	0.33	0.49	0.57	0.53
chb14	1	0.52	0.00	0.19	0.51	0.35
chb15	5	0.10	0.00	0.00	0.91	0.46
chb24	1	0.95	0.00	0.35	0.56	0.46
Overall	2.33±1.63	0.53±0.34	0.28±0.39	0.45±0.34	0.58±0.17	0.52±0.12

Table 5.6: Testing results for the EPILEPSIAE database. SS_{Alarm} stands for Alarm Sensitivity, SS_{Sample} for Sample Sensitivity, SP_{Sample} for Sample Specificity, and AUC for Area Under the Curve.

Patient	Tested Seizures	FPR/h	SS_{Alarm}	SS_{Sample}	SP_{Sample}	AUC
402	2	0.00	0.00	0.34	0.64	0.49
8902	2	0.10	1.00	0.96	0.92	0.94
11002	1	0.71	0.00	0.50	0.51	0.50
16202	4	0.03	0.00	0.07	0.91	0.49
21902	1	0.00	0.00	0.01	0.88	0.45
23902	2	1.09	0.50	0.68	0.45	0.56
26102	1	0.00	0.00	0.26	0.68	0.47
30802	5	0.37	0.20	0.68	0.75	0.71
32702	2	0.05	0.50	0.50	0.86	0.68
45402	1	0.55	0.00	0.51	0.61	0.56
46702	2	0.00	0.00	0.41	0.58	0.49
50802	2	0.26	0.00	0.23	0.87	0.55
52302	1	0.94	0.00	0.53	0.30	0.41
53402	1	0.27	0.00	0.74	0.65	0.70
55202	5	0.52	0.20	0.66	0.64	0.65
56402	1	0.51	0.00	0.42	0.64	0.53
58602	3	0.52	0.00	0.49	0.58	0.53
59102	2	0.99	0.50	0.76	0.52	0.64
60002	3	0.05	0.00	0.19	0.68	0.43
64702	2	0.52	0.00	0.48	0.65	0.57
75202	4	0.04	0.00	0.18	0.87	0.52
80702	3	0.27	0.33	0.58	0.52	0.55
85202	2	0.11	0.00	0.11	0.87	0.49
93402	2	0.46	1.00	0.85	0.69	0.78
93902	3	0.12	0.00	0.32	0.79	0.56
94402	4	0.71	0.00	0.40	0.49	0.45
95202	4	0.34	0.00	0.40	0.78	0.59
96002	4	0.52	0.25	0.25	0.64	0.45
98102	2	0.12	0.00	0.50	0.83	0.66
98202	5	0.02	0.00	0.33	0.67	0.50
101702	2	0.66	0.00	0.46	0.58	0.52
102202	4	0.04	0.00	0.21	0.85	0.53
104602	2	0.37	0.00	0.51	0.62	0.57
109502	1	1.95	0.00	0.36	0.36	0.36
110602	2	0.31	0.50	0.61	0.71	0.66
112802	3	0.68	0.33	0.53	0.64	0.59
113902	3	0.05	0.00	0.36	0.68	0.52
114702	5	0.00	0.00	0.20	0.80	0.50
114902	4	0.00	0.00	0.28	0.92	0.60
123902	2	0.00	0.00	0.00	0.99	0.50
Overall	1.00±2.06	0.36±0.40	0.13±0.26	0.42±0.22	0.69±0.16	0.56±0.11

In the scenarios of AES and Epilepsy Ecosystem, examining the number of seizures proves to be unviable due to the absence of seizure-timing data. Instead, only the quantity of preictal and interictal files is accessible. The proportion of preictal files within the test dataset varies, ranging from 1.28 to 4.03% for AES dogs, 13.64 to 16.67% for AES humans, and 5.90 to 31.94% for Epilepsy Ecosystem patients. Moreover, given that this data analysis does not incorporate temporal aspects, the computation of SS_{Alarm} and FPR/h remains beyond reach.

Nonetheless, these two metrics are available within the remaining databases, enabling a direct comparison. The average SS_{Alarm} values achieved by the 40 patients in the EPILEPSIAE group and the six patients in the CHB-MIT group are 0.13±0.26 and 0.28±0.39, respectively. Patients who had one correctly predicted seizure were 23902 (in 2 seizures), 30802 (in 5), 32702 (in 2), 55202 (in 5), 59102 (in 2), 80702 (in 3), 96002 (in 4), 112802 (in 3), chb01 (in 1), chb06 (in 3), chb10 (in 3). The most successful in terms of sensitivity were patients 8902, 93402, and chb01, all of whom had all their seizures correctly predicted. The remaining patients did not have any predicted seizures. These low alarm sensitivity values emphasize the classifier's limited capability to predict seizures accurately.

The average FPR/h values amounted to 0.36±0.40 for EPILEPSIAE and 0.53±0.34 for CHB-MIT. In the context of real-life application, an ideal FPR/h value is 0.15. Nevertheless, the elevated values raised doubts about the system's suitability for real-life scenarios, given that a high rate of false alarms per hour can negatively impact the patient's health. Nonetheless, patient 8902 achieved the best performance, accurately predicting all seizures and maintaining an FPR/h value of 0.10, falling within the desired range. Despite only predicting half of the seizures, for patient 32702 it achieved a commendable FPR/h value of 0.05. Unfortunately, for the remaining patients who experienced at least one predicted seizure, the FPR/h values were unsatisfactory, consistently exceeding the ideal threshold by at least twice the value.

Divergent results are evident when assessing the SS_{Alarm} and FPR/h values between CHB-MIT and EPILEPSIAE data. CHB-MIT data exhibits a higher SS_{Alarm} value, while its FPR/h value suggests a higher rate of false alarms per hour than EPILEPSIAE. A closer look at the data reveals that in the EPILEPSIAE dataset, 29 out of 40 patients demonstrate zero sensitivity, and among them, 16 record FPR/h values below the ideal value. This revelation implies that 40% of patients with favorable FPR/h values had no predicted seizures. As a result, these less favorable data influence the substantial reduction in the global value of FPR/h for EPILEPSIAE data.

Nevertheless, both datasets exhibit improved sensitivity when restricting the analysis to patients with at least one predicted seizure. EPILEPSIAE achieves an average sensitivity of 0.50, while CHB-MIT reaches 0.56. Regarding the FPR/h value, it only changes for EPILEPSIAE to 0.49, underscoring the impact of the abovementioned cases on the results.

The remaining three metrics (SS_{Sample}, SP_{Sample}, and AUC) were computed for all data from all databases, allowing for comparisons. The average SS_{Sample} values demonstrate remarkable consistency across the EPILEPSIAE, CHB-MIT, and AES datasets, with values of 0.42, 0.45, and 0.48, respectively. Conversely, the Epilepsy Ecosystem dataset exhibits a significantly higher average value, reaching 0.75. This remarkable result signifies that 75% of the preictal samples were accurately classified, underscoring its highly favorable performance.

Table 5.7: Testing results for the AES database. SS_{Sample} stands for Sample Sensitivity, SP_{Sample} for Sample Specificity, and AUC for Area Under the Curve.

Patient	Tested files (preictal\interictal)	SS_{Sample}	SP_{Sample}	AUC
Dog 1	468 (6\462)	0.50	0.54	0.52
Dog 2	482 (12\470)	0.75	0.79	0.77
Dog 3	1416 (24\1392)	0.35	0.76	0.56
Dog 4	769 (31\738)	0.41	0.67	0.54
Dog 5	444 (12\432)	0.76	0.54	0.65
Patient 1	44 (6\38)	0.40	0.50	0.45
Patient 2	36 (6\30)	0.16	0.69	0.42
Overall	-	0.48±0.22	0.64±0.12	0.56±0.12

Table 5.8: Testing results for the Epilepsy Ecosystem database. SS_{Sample} stands for Sample Sensitivity, SP_{Sample} for Sample Specificity, and AUC for Area Under the Curve.

Patient	Tested files (preictal\interictal)	SS_{Sample}	SP_{Sample}	AUC
Patient 1	72 (23\49)	0.80	0.43	0.61
Patient 2	305 (18\287)	0.71	0.45	0.58
Patient 3	207 (18\189)	0.73	0.24	0.42
Overall	-	0.75±0.05	0.37±0.12	0.54±0.10

However, this increase in SS_{Sample} was coupled with a reduction in SP_{Sample} compared to the other databases. The highest SP_{Sample} value was observed in EPILEPSIAE (0.69), followed by AES (0.64), CHB-MIT (0.58), and lastly, Epilepsy Ecosystem (0.37). This pattern might be associated with the average number of hours available per seizure, where datasets containing more interictal data contributed to more accurate interictal sample classification. The time-per-seizure ratios for these datasets were 20.8, 12.31, 7.8, and 4.4 hours for EPILEPSIAE, AES, CHB-MIT, and Epilepsy Ecosystem, respectively. Consequently, higher SP_{Sample} values appear to correspond to datasets where this ratio is higher, and vice versa. Notably, among the results, patient 8902 stands out with the most favorable combination of SS_{Sample} (0.96) and SP_{Sample} (0.92) values.

Lastly, the AUC was computed, with values ranging from 0 to 1, where 1 represents perfectly accurate predictions. Consequently, a higher AUC value indicates superior classifier performance. The average AUC scores remain relatively consistent across all databases, typically averaging around 0.55. In line with the optimal combination of SS_{Sample} and SP_{Sample} values,

patient 8902 achieved the highest AUC score (0.94). In the context of the other databases, the top AUC value was secured by patient chb06 for CHB-MIT, registering a score of 0.68. In the case of AES, Dog 2 emerged with the highest AUC at 0.77. Lastly, in the Epilepsy Ecosystem database, patient 1 obtained the leading AUC score of 0.61.

The study also included a phase of statistical validation to ascertain whether the model's performance arises from its ability to identify random phenomena within Electroencephalogram (EEG) signals rather than patterns associated with seizures. This aspect is relevant, considering seizure prediction is a rare event problem, with a considerable imbalance between interictal and preictal intervals. Table 5.9 exhibits the results obtained during this phase. The disparity in results between the alarm approach and the sample approach is evident. Among the 46 patients investigated, only 6 achieved performance exceeding the chance level in the alarm-based method. These six patients include five from the EPILEPSIAE dataset (8902, 32702, 80702, 93402, and 110602), along with one from CHB-MIT (chb01).

Table 5.9: Statistical validation results for all databases (EPILEPSIAE, CHB-MIT, AES e Epilepsy Ecosystem). SS_{Sample} stands for Sample Sensitivity, and SP_{Sample} for Sample Specificity.

Patient	SS_{Alarm}	SS_{Alarm} Surrogate	p-value Alarm	SS_{Sample}	SS_{Sample} Surrogate	p-value Sample	Above chance (Alarm)	Above chance (Sample)
EPILEPSIAE								
402	0.00	0.00	1.00	0.34	0.00	0.00		•
8902	1.00	0.13	2.97×10^{-15}	0.96	0.00	1.18×10^{-86}	•	•
11002	0.00	0.17	1.00	0.50	0.00	1.77×10^{-73}		•
16202	0.00	0.03	1.00	0.07	0.00	0.00		•
21902	0.00	0.00	1.00	0.01	0.00	0.00		•
23902	0.50	0.42	0.86	0.68	0.00	1.96×10^{-84}		•
26102	0.00	0.00	1.00	0.26	0.00	0.00		•
30802	0.20	0.39	1.00	0.68	0.00	2.31×10^{-86}		•
32702	0.50	0.03	2.01×10^{-10}	0.50	0.00	2.64×10^{-81}	•	•
45402	0.00	0.27	1.00	0.51	0.00	2.82×10^{-73}		•
46702	0.00	0.00	1.00	0.41	0.00	0.00		•
50802	0.00	0.07	1.00	0.23	0.00	2.95×10^{-68}		•
52302	0.00	0.27	1.00	0.53	0.00	6.06×10^{-82}		•
53402	0.00	0.10	1.00	0.74	0.00	1.10×10^{-95}		•
55202	0.20	0.32	1.00	0.66	0.00	1.61×10^{-84}		•
56402	0.00	0.20	1.00	0.42	0.00	2.03×10^{-69}		•
58602	0.00	0.12	1.00	0.49	0.00	2.61×10^{-73}		•
59102	0.50	0.42	0.36	0.76	0.00	9.01×10^{-83}		•
60002	0.00	0.04	1.00	0.19	0.00	3.43×10^{-74}		•
64702	0.00	0.23	1.00	0.48	0.00	1.45×10^{-81}		•
75202	0.00	0.01	1.00	0.18	0.00	1.63×10^{-78}		•
80702	0.33	0.18	1.82×10^{-8}	0.58	0.00	9.02×10^{-86}	•	•
85202	0.00	0.05	1.00	0.11	0.00	2.95×10^{-64}		•
93402	1.00	0.23	1.37×10^{-9}	0.86	0.00	6.25×10^{-79}	•	•
93902	0.00	0.03	1.00	0.32	0.00	4.67×10^{-85}		•
94402	0.00	0.24	1.00	0.40	0.00	1.76×10^{-77}		•
95202	0.00	0.12	1.00	0.40	0.00	4.28×10^{-77}		•

Table 5.9 continued from previous page

Patient	SS_{Alarm}	SS_{Alarm} Surrogate	p-value Alarm	SS_{Sample}	SS_{Sample} Surrogate	p-value Sample	Above chance (Alarm)	Above chance (Sample)
96002	0.25	0.18	0.14	0.25	0.00	6.16×10^{-68}		•
98102	0.00	0.07	1.00	0.50	0.00	2.55×10^{-82}		•
98202	0.00	0.03	1.00	0.33	0.00	1.15×10^{-78}		•
101702	0.00	0.28	1.00	0.46	0.00	3.94×10^{-81}		•
102202	0.00	0.01	1.00	0.21	0.00	2.13×10^{-87}		•
104602	0.00	0.08	1.00	0.51	0.00	1.96×10^{-82}		•
109502	0.00	0.43	1.00	0.36	0.00	8.57×10^{-71}		•
110602	0.50	0.15	3.66×10^{-7}	0.61	0.00	3.56×10^{-84}	•	•
112802	0.33	0.26	0.08	0.53	0.00	7.79×10^{-69}		•
113902	0.00	0.06	1.00	0.36	0.00	0.00		•
114702	0.00	0.00	1.00	0.20	0.00	0.00		•
114902	0.00	0.00	1.00	0.29	0.00	0.00		•
123902	0.00	0.00	1.00	0.00	0.00	1.00		
CHB-MIT								
chb01	1.00	0.07	5.58×10^{-10}	0.77	0.00	1.69×10^{-86}	•	•
chb06	0.33	0.40	1.00	0.91	0.00	1.63×10^{-90}		•
chb10	0.33	0.44	1.00	0.49	0.00	8.79×10^{-48}		•
chb14	0.00	0.13	1.00	0.19	0.00	1.01×10^{-69}		•
chb15	0.00	0.01	1.00	0.004	0.000	1.54×10^{-25}		•
chb24	0.00	0.20	1.00	0.35	0.00	6.31×10^{-73}		•
AES								
Dog 1	-	-	-	0.5012	0.5503	1.00	-	
Dog 2	-	-	-	0.7481	0.4811	8.02×10^{-41}	-	•
Dog 3	-	-	-	0.3493	0.5140	1.00	-	
Dog 4	-	-	-	0.4091	0.5194	1.00	-	
Dog 5	-	-	-	0.7596	0.3390	3.34×10^{-45}	-	•
Patient 1	-	-	-	0.4036	0.5994	1.00	-	
Patient 2	-	-	-	0.1619	0.2675	1.00	-	
Epilepsy Ecosystem								
Patient 1	-	-	-	0.7985	0.4301	2.94×10^{-47}	-	•
Patient 2	-	-	-	0.7144	0.3465	2.16×10^{-49}	-	•
Patient 3	-	-	-	0.7315	0.4216	1.67×10^{-45}	-	•

Conversely, in the sample-based approach, most patients demonstrated performance above the chance level. Out of the 56 patients studied, 50 outperformed the surrogate predictor. Notably, AES is the dataset with the lowest percentage (29%) of statistically validated patients. The notable differences in the number of validated patients between the two approaches raise the question of whether the less favorable results of the alarm approach stem from the conservative choice of a 0.7 threshold for Firing Power (FP) during postprocessing. However, this conservative threshold also ensures that FPR/h values remain within an acceptable range.

The potential for comparisons between these databases does have its limits, mainly due to the numerous variables in play. Even with a method that upholds a high degree of rigor, the distinct data organization and the presence of diverse information introduce complexities to standardizing the process.

5.3 Comparative Analysis with Other Studies

The results achieved through the developed seizure prediction pipeline are open to comparison with previous studies mentioned in Chapter 3. To achieve this goal, a selection of eight studies includes four that rely on the EPILEPSIAE database, three that use CHB-MIT data, two that utilize AES, and only one that counts on Epilepsy Ecosystem data. Worth noting is that all studies using EPILEPSIAE data have undergone statistical validation, whereas studies involving other databases are relatively scarce in this regard. Table 5.10 encapsulates the methodology details applied to all patients and presents them exclusively for statistically validated patients.

Commencing the comparison with studies utilizing the EPILEPSIAE database, it becomes apparent that the sensitivity value achieved by the developed methodology occupies the worst position in the table. The only study that demonstrates a similar sensitivity value is the one conducted by Pinto et al. (2022) [123]. Nonetheless, it is crucial to note that the Pinto et al. study examined a significantly larger patient population, over twice the number of patients compared to this research. Additionally, this study employs a simplistic classifier, in contrast to the approach taken by Lopes et al. (2023) [102], which incorporates Deep Learning (DL) methods. Therefore, the expectation in the present study was for a lower sensitivity value. However, the achieved FPR/h value is quite well situated, being outperformed only by the value obtained by Pinto et al. (2022) [123]. Nevertheless, it is essential to note that this better FPR/h value is somewhat "masked" because a careful examination of the data reveals that this lower value predominantly originates from patients who registered an FPR/h equal to zero concurrently with zero sensitivity. It signifies that although it did not trigger false alarms, it did not predict seizures.

When examining the percentage of statistically validated patients, it becomes evident that Lopes et al. (2023) [102], Pinto et al. (2022) [123], and Pinto et al. (2021) [126] hold an advantage, boasting a higher percentage of validated patients. Alvarado-Rojas et al. (2014) [73] achieved a lower percentage of validated patients. Despite the lower value, it is worth noting that the approach employed for statistical validation differed, with Alvarado-Rojas et al. using the random predictor. The comparison of specificity and AUC values proves challenging, given the limited number of studies calculating these metrics for EPILEPSIAE data.

About the CHB-MIT dataset, it is evident that all the studies demonstrated superior performance in both sensitivity and FPR/h compared to the developed methodology. Furthermore, the AUC values obtained by Li et al. (2023) [118] and Xu et al. (2023) [120] were significantly higher. Concerning statistical validation, only Truong et al. (2018) [111] conducted this step, achieving an impressive validation percentage of 92%, which surpasses the results obtained in this study. It is essential to recognize that the approach employed by Truong et al. differed, involving using the random predictor.

In the context of AES, it is evident that the metrics achieved by Li et al. (2023) [118] and Truong et al. (2018) [111] significantly outperformed those obtained by the developed methodology. Remarkably, Truong et al. achieved a statistical validation rate of 86%, nearly three times higher than the rate obtained in this study (29%).

Comparing studies utilizing data from the Epilepsy Ecosystem proves challenging due to

the limited number of studies using this data. In contrast to the prevailing trend observed with previous databases, the developed algorithm showcased an enhanced sensitivity value (0.75) compared to Stojanović et al. (2020) [131] (0.69). However, the specificity is considerably lower (0.37 compared to 0.79). Stojanović et al. did not conduct statistical validation, a crucial aspect for comparison, as all patients in this study demonstrated performance above the chance level.

Table 5.10: Seizure prediction performance for studies under comparison.

Study	Database	No. of Patients	SS	FPR/h	SP	AUC	Validated Patients
Li et al. (2023) [118]	CHB-MIT	18	0.97	0.06	0.87	0.94	-
	AES	4	0.93	0.03	0.92	0.97	
Lopes et al. (2023) [102]	EPILEPSIAE	41	0.34	0.90	-	-	51%
Xu et al. (2023) [120]	CHB-MIT	4	0.91	0.11	-	0.89	-
Pinto et al. (2022) [123]	EPILEPSIAE	93	0.16	0.21	-	-	32%
Pinto et al. (2021) [126]	EPILEPSIAE	19	0.37	0.79	-	-	32%
Stojanović et al. (2020) [131]	Epilesy Ecosystem	3	0.69	-	0.79	-	-
Truong et al. (2018) [111]	CHB-MIT	13	0.81	0.16	-	-	92%
	AES	7	0.75	0.21			86%
Alvarado-Rojas et al. (2014) [73]	EPILEPSIAE	53	0.47	0.94	-	-	13%
Developed methodology	EPILEPSIAE	40	0.13	0.36	0.69	0.56	12.5%
	CHB-MIT	6	0.28	0.53	0.58	0.52	17%
	AES	7	0.48	-	0.64	0.56	29%
	Epilepsy Ecosystem	3	0.75	-	0.37	0.54	100%
Developed methodology (validated patients)	EPILEPSIAE	5	0.67	0.24	0.74	0.72	-
	CHB-MIT	1	1	0.31	0.46	0.62	
	AES	2	0.75	-	0.66	0.71	
	Epilepsy Ecosystem	3	0.75	-	0.37	0.54	

Directly comparing the work presented in this document with selected studies poses notable challenges, primarily due to the substantial variability in patient selection and the choice of parameters employed in the methodologies. Most studies' lack of statistical validation is a significant obstacle to this comparison. Additionally, several authors highlight their best results exclusively, making it challenging to gain a comprehensive and realistic understanding of the problem. For example, the Table 5.10 presents metrics values obtained by the developed methodology for all patients and those who passed statistical validation. Values are substantially better for validated patients. However, these values do not represent the overall situation and may obscure the real problem. Therefore, when authors only report their best outcomes and fail to acknowledge setbacks as opportunities for improvement, their studies tend to overestimate performance.

Furthermore, using assumptions to simulate real-life leads to disastrous results. This assertion finds support in the observation that similarly unsatisfactory results occur when applying these assumptions to databases already recognized for their very high performance, such as CHB-MIT. Consequently, studies reporting extremely high results rely on unrealistic assumptions that do not align with real-life scenarios, representing illusions in solving the problem.

5.4 Limitations

A limitation inherent in this study pertains to including pre-surgical monitoring data from databases characterized by short durations spanning just a few hours or days. In these settings, patients undergo medication withdrawal and sleep deprivation, intending to provoke a higher frequency of seizures in a shorter timeframe. However, these conditions do not represent an everyday living environment. Therefore, obtaining more extensive ultra-long recordings encompassing extended daily life duration is crucial to render the assessment more comprehensive and reflective of real-world scenarios.

Furthermore, the limited temporal coverage of the data also has a detrimental effect on another aspect: the scarcity of independent seizures. Consequently, the study was constrained to utilize only three seizures for training and a minimum of 1 seizure for testing. Any increase in the minimum number of seizures reserved for testing would inevitably lead to the exclusion of a substantial number of patients who did not satisfy the required minimum seizure criteria. This aspect holds significant importance in this study because it was impractical to incorporate data from the My Seizure Gauge database due to the insufficient number of seizures that satisfied the 4.5-hour separation criterion.

Considering the computational speed, the analysis considered only the preceding 4 hours of each training seizure. As it is strongly advisable to use all available data from training seizures, this becomes a limitation. Utilizing all available data would improve the representativeness of interictal data.

Although the primary objective of this study is to assess the predictive "quality" of the data, it is important to acknowledge that using a relatively basic machine learning pipeline represents a limitation. Therefore, employing more complex classifiers like Multi-Layer Perceptron, Support Vector Machine (SVM), and random forest, among others, could have allowed for a more fair comparison with other studies.

Furthermore, the organization and characteristics of data within different databases differ significantly. Several databases lack essential metadata, which is pivotal in addressing this issue. Metadata, encompassing information such as the patient's epilepsy type, gender, age, and precise seizure timings, holds substantial significance for meticulous data analysis. These database differences introduce significant complexity, making employing a uniform set of rules and assumptions challenging and complicating result comparisons.

Accessibility poses an additional complication, as only pre-surgical monitoring data is openly accessible in its entirety. In contrast, numerous currently existing datasets remain partially accessible or entirely restricted, occasionally lacking label information or a portion of the dataset.

6

Conclusion

This thesis aimed to develop a methodology capable of predicting epileptic seizures and establishing comparisons between the performance obtained when applied to 4 different databases. For this purpose, a patient-specific seizure prediction algorithm was created, following the most common pipeline in the literature. For European Epilepsy Database (EPILEPSIAE) and Children's Hospital Boston from the Massachusetts Institute of Technology (CHB-MIT) datasets, the chosen approach involved triggering alarms due to the availability of temporal seizure data. Conversely, American Epilepsy Society (AES) and Epilepsy Ecosystem relied on a sample-by-sample approach due to the lack of temporal data.

A clear conclusion emerges when assessing the training phase results across different databases. Handling the problem less rigorously, without considering the temporal aspect of seizure occurrence and disregarding long-term interictal data, leads to better results. Nonetheless, this improved performance does not necessarily translate into a more accurate representation of real-life scenarios; it can even have the opposite effect. In fact, the assumptions made to simulate real-life alarm situations result in unfavorable outcomes, as demonstrated by the results obtained from the EPILEPSIAE and CHB-MIT datasets. Nevertheless, these assumptions are indispensable for addressing the problem and its practical applicability. Therefore, obtaining impressive results holds little value if they lack realism.

The conclusions stemming from comparing the test results and results obtained by other studies utilizing identical databases align closely are analogous. The anticipation was for somewhat weaker results due to utilizing a relatively straightforward pipeline, but not to this extent. Once again, the prevailing belief is that the meticulous care and assumptions made to enhance the representation of real-life scenarios have led to these low-performance results. Many authors do not have this level of rigor in realistically approaching the problem.

Additionally, the alarm approach yields inferior outcomes compared to the sample approach. There are instances where no alarms are triggered, but the classifier effectively identifies many samples as preictal. These cases prompt a consideration of the chosen Firing Power (FP) threshold value is overly conservative.

A comparison of the values obtained across datasets for each approach reveals that, in the sample approach, the results demonstrate substantial consistency. However, in the case of the alarm approach, disparities in the metrics that reflect a real-life context (such as SS_{Alarm} and False Prediction Rate per hour (FPR/h)) emerge between the EPILEPSIAE and CHB-MIT datasets. Factors like data duration and inherent nature play a role in causing these discrepancies, affecting the fidelity of replicating realistic scenarios.

Extracting definitive insights from the obtained results is challenging despite these evident conclusions. The many variables at play make it difficult to ascertain the specific factors contributing to the observed value differences. Even with a rigorous methodology, the varying data types, organizational structures, and accessibility across different databases introduce significant complexity to the standardization process.

In order to overcome the limitations elucidated above, future work should involve replicating this study using more extensive, systematically structured, and thoroughly annotated long-term datasets. Achieving this entails the acquisition and dissemination of additional data into public databases. Ensuring this novel data is collected in environments mirroring a patient's everyday life is of utmost significance. Subsequently, it is crucial to make this data readily accessible to the public, accompanied by essential information to enable a realistic problem-solving approach. Furthermore, the developed methodology should undergo testing with parameter variations, including exploring alternative classifiers and the standardization of the preprocessing step, to assess the resulting disparities in outcomes.

Bibliography

[1] "The European Epilepsy Database." `http://www.epilepsiae.eu/`. Accessed on 2022-10-10.

[2] "CHB-MIT Scalp EEG Database." `https://physionet.org/content/chbmit/1.0.0/`. Accessed on 2022-10-15.

[3] "American Epilepsy Society Seizure Prediction Challenge." `https://www.kaggle.com/c/seizure-prediction`. Accessed on 2022-10-22.

[4] "Epilepsy Ecosystem. Seizure Prediction Data." `https://www.epilepsyecosystem.org/`. Accessed on 2022-10-22.

[5] M. Ihle, H. Feldwisch-Drentrup, C. A. Teixeira, A. Witon, B. Schelter, J. Timmer, and A. Schulze-Bonhage, "Epilepsiae–a european epilepsy database," *Computer methods and programs in biomedicine*, vol. 106, no. 3, pp. 127–138, 2012.

[6] N. Jette and J. Engel, "Refractory epilepsy is a life-threatening disease: Lest we forget," 2016.

[7] J. Klatt, H. Feldwisch-Drentrup, M. Ihle, V. Navarro, M. Neufang, C. Teixeira, C. Adam, M. Valderrama, C. Alvarado-Rojas, A. Witon, *et al.*, "The epilepsiae database: An extensive electroencephalography database of epilepsy patients," 2012.

[8] M. Sazgar and B. F. Bourgeois, "Aggravation of epilepsy by antiepileptic drugs," *Pediatric neurology*, vol. 33, no. 4, pp. 227–234, 2005.

[9] K. M. Fiest, K. M. Sauro, S. Wiebe, S. B. Patten, C.-S. Kwon, J. Dykeman, T. Pringsheim, D. L. Lorenzetti, and N. Jetté, "Prevalence and incidence of epilepsy: a systematic review and meta-analysis of international studies," *Neurology*, vol. 88, no. 3, pp. 296–303, 2017.

[10] L. A. Jones and R. H. Thomas, "Sudden death in epilepsy: Insights from the last 25 years," *Seizure*, vol. 44, pp. 232–236, 2017.

[11] M. R. Sperling, "The consequences of uncontrolled epilepsy," *CNS spectrums*, vol. 9, no. 2, pp. 98–109, 2004.

[12] C. Rathore and K. Radhakrishnan, "Concept of epilepsy surgery and presurgical evaluation," *Epileptic disorders*, vol. 17, no. 1, pp. 19–31, 2015.

[13] C. Baumgartner, J. P. Koren, and M. Rothmayer, "Automatic computer-based detection of epileptic seizures," *Frontiers in neurology*, vol. 9, p. 639, 2018.

[14] L. Kuhlmann, K. Lehnertz, M. P. Richardson, B. Schelter, and H. P. Zaveri, "Seizure prediction—ready for a new era," *Nature Reviews Neurology*, vol. 14, no. 10, pp. 618–630, 2018.

[15] E. B. Assi, D. K. Nguyen, S. Rihana, and M. Sawan, "Towards accurate prediction of

epileptic seizures: A review," *Biomedical Signal Processing and Control*, vol. 34, pp. 144–157, 2017.

[16] D. R. Freestone, P. J. Karoly, and M. J. Cook, "A forward-looking review of seizure prediction," *Current opinion in neurology*, vol. 30, no. 2, pp. 167–173, 2017.

[17] F. Mormann, R. G. Andrzejak, C. E. Elger, and K. Lehnertz, "Seizure prediction: the long and winding road," *Brain*, vol. 130, no. 2, pp. 314–333, 2007.

[18] P. J. Karoly, H. Ung, D. B. Grayden, L. Kuhlmann, K. Leyde, M. J. Cook, and D. R. Freestone, "The circadian profile of epilepsy improves seizure forecasting," *Brain*, vol. 140, no. 8, pp. 2169–2182, 2017.

[19] A. Tsymbal, M. Pechenizkiy, P. Cunningham, and S. Puuronen, "Dynamic integration of classifiers for handling concept drift," *Information fusion*, vol. 9, no. 1, pp. 56–68, 2008.

[20] L. D. Iasemidis, "Epileptic seizure prediction and control," *IEEE Transactions on Biomedical Engineering*, vol. 50, no. 5, pp. 549–558, 2003.

[21] R. S. Fisher, W. V. E. Boas, W. Blume, C. Elger, P. Genton, P. Lee, and J. Engel Jr, "Epileptic seizures and epilepsy: definitions proposed by the international league against epilepsy (ilae) and the international bureau for epilepsy (ibe)," *Epilepsia*, vol. 46, no. 4, pp. 470–472, 2005.

[22] R. S. Fisher, C. Acevedo, A. Arzimanoglou, A. Bogacz, J. H. Cross, C. E. Elger, J. Engel Jr, L. Forsgren, J. A. French, M. Glynn, *et al.*, "Ilae official report: a practical clinical definition of epilepsy," *Epilepsia*, vol. 55, no. 4, pp. 475–482, 2014.

[23] I. E. Scheffer, S. Berkovic, G. Capovilla, M. B. Connolly, J. French, L. Guilhoto, E. Hirsch, S. Jain, G. W. Mathern, S. L. Moshé, *et al.*, "Ilae classification of the epilepsies: Position paper of the ilae commission for classification and terminology," *Epilepsia*, vol. 58, no. 4, pp. 512–521, 2017.

[24] R. S. Fisher, J. H. Cross, J. A. French, N. Higurashi, E. Hirsch, F. E. Jansen, L. Lagae, S. L. Moshé, J. Peltola, E. Roulet Perez, *et al.*, "Operational classification of seizure types by the international league against epilepsy: Position paper of the ilae commission for classification and terminology," *Epilepsia*, vol. 58, no. 4, pp. 522–530, 2017.

[25] R. S. Fisher, J. H. Cross, C. D'souza, J. A. French, S. R. Haut, N. Higurashi, E. Hirsch, F. E. Jansen, L. Lagae, S. L. Moshé, *et al.*, "Instruction manual for the ilae 2017 operational classification of seizure types," *Epilepsia*, vol. 58, no. 4, pp. 531–542, 2017.

[26] H. Hasson, "Generalized onset tonic-clonic seizures. . . ,"

[27] J. J. Falco-Walter, I. E. Scheffer, and R. S. Fisher, "The new definition and classification of seizures and epilepsy," *Epilepsy research*, vol. 139, pp. 73–79, 2018.

[28] A. M. Pack, "Epilepsy overview and revised classification of seizures and epilepsies," *CONTINUUM: Lifelong Learning in Neurology*, vol. 25, no. 2, pp. 306–321, 2019.

[29] N. Gayatri and J. Livingston, "Aggravation of epilepsy by anti-epileptic drugs," *Developmental Medicine & Child Neurology*, vol. 48, no. 5, pp. 394–398, 2006.

[30] K. H. Noe and J. F. Drazkowski, "Safety of long-term video-electroencephalographic monitoring for evaluation of epilepsy," in *Mayo Clinic Proceedings*, vol. 84, pp. 495–500, Elsevier, 2009.

[31] A. Rose, P. McCabe, F. Gilliam, B. Smith, J. Boggs, D. Ficker, J. Moore, E. Passaro,

C. Bazil, *et al.*, "Occurrence of seizure clusters and status epilepticus during inpatient video-eeg monitoring," *Neurology*, vol. 60, no. 6, pp. 975–978, 2003.

[32] S. R. Haut, C. Swick, K. Freeman, and S. Spencer, "Seizure clustering during epilepsy monitoring," *Epilepsia*, vol. 43, no. 7, pp. 711–715, 2002.

[33] R. Caraballo, R. Cersosimo, G. Capovilla, and N. Fejerman, "Benign focal seizures of adolescence," *Fejerman N, Caraballo R. Benign focal epilepsies in infancy, childhood and adolescence. Montrouge: John Libbey, 2007a*, pp. 243–51, 2007.

[34] S. J. Smith, "Eeg in the diagnosis, classification, and management of patients with epilepsy," *Journal of Neurology, Neurosurgery & Psychiatry*, vol. 76, no. suppl 2, pp. ii2–ii7, 2005.

[35] J. W. C. Medithe and U. R. Nelakuditi, "Study of normal and abnormal eeg," in *2016 3rd International conference on advanced computing and communication systems (ICACCS)*, vol. 1, pp. 1–4, IEEE, 2016.

[36] N. Jmail, M. Gavaret, F. Wendling, A. Kachouri, G. Hamadi, J.-M. Badier, and C.-G. Bénar, "A comparison of methods for separation of transient and oscillatory signals in eeg," *Journal of neuroscience methods*, vol. 199, no. 2, pp. 273–289, 2011.

[37] R. Sankar and J. Natour, "Automatic computer analysis of transients in eeg," *Computers in biology and medicine*, vol. 22, no. 6, pp. 407–422, 1992.

[38] I. Osorio, H. P. Zaveri, M. G. Frei, and S. Arthurs, *Epilepsy: the intersection of neurosciences, biology, mathematics, engineering, and physics*. CRC press, 2016.

[39] T. P. Exarchos, A. T. Tzallas, D. I. Fotiadis, S. Konitsiotis, and S. Giannopoulos, "A data mining based approach for the eeg transient event detection and classification," in *18th IEEE Symposium on Computer-Based Medical Systems (CBMS'05)*, pp. 35–40, IEEE, 2005.

[40] T. P. Exarchos, A. T. Tzallas, D. I. Fotiadis, S. Konitsiotis, and S. Giannopoulos, "Eeg transient event detection and classification using association rules," *IEEE Transactions on Information Technology in Biomedicine*, vol. 10, no. 3, pp. 451–457, 2006.

[41] S. Sanei and J. A. Chambers, *EEG signal processing*. John Wiley & Sons, 2013.

[42] A. Varsavsky, I. Mareels, and M. Cook, *Epileptic seizures and the EEG: measurement, models, detection and prediction*. Taylor & Francis, 2011.

[43] V. Jurcak, D. Tsuzuki, and I. Dan, "10/20, 10/10, and 10/5 systems revisited: their validity as relative head-surface-based positioning systems," *Neuroimage*, vol. 34, no. 4, pp. 1600–1611, 2007.

[44] M. H. Libenson, *Practical approach to electroencephalography*. Elsevier Health Sciences, 2009.

[45] S. Beniczky and D. L. Schomer, "Electroencephalography: basic biophysical and technological aspects important for clinical applications," *Epileptic Disorders*, vol. 22, no. 6, pp. 697–715, 2020.

[46] A. Biondi, V. Santoro, P. F. Viana, P. Laiou, D. K. Pal, E. Bruno, and M. P. Richardson, "Noninvasive mobile eeg as a tool for seizure monitoring and management: A systematic review," *Epilepsia*, vol. 63, no. 5, pp. 1041–1063, 2022.

[47] S. Debener, R. Emkes, M. De Vos, and M. Bleichner, "Unobtrusive ambulatory eeg using

a smartphone and flexible printed electrodes around the ear," *Scientific reports*, vol. 5, no. 1, pp. 1–11, 2015.

[48] S. Kovac, V. N. Vakharia, C. Scott, and B. Diehl, "Invasive epilepsy surgery evaluation," *Seizure*, vol. 44, pp. 125–136, 2017.

[49] S. Shorvon, R. Guerrini, M. Cook, and S. Lhatoo, *Oxford textbook of epilepsy and epileptic seizures*. OUP Oxford, 2012.

[50] AboutKidsHealth, "Invasive electroencephalography (eeg) monitoring before epilepsy surgery," 2023.

[51] R. P. Lesser, N. E. Crone, and W. Webber, "Subdural electrodes," *Clinical neurophysiology*, vol. 121, no. 9, pp. 1376–1392, 2010.

[52] J. Engel, "What can we do for people with drug-resistant epilepsy?: the 2016 wartenberg lecture," *Neurology*, vol. 87, no. 23, pp. 2483–2489, 2016.

[53] P. Perucca, I. E. Scheffer, and M. Kiley, "The management of epilepsy in children and adults," *Medical Journal of Australia*, vol. 208, no. 5, pp. 226–233, 2018.

[54] S. L. Moshé, E. Perucca, P. Ryvlin, and T. Tomson, "Epilepsy: new advances," *The Lancet*, vol. 385, no. 9971, pp. 884–898, 2015.

[55] A. Mehdizadeh, M. Barzegar, S. Negargar, A. Yahyavi, and S. Raeisi, "The current and emerging therapeutic approaches in drug-resistant epilepsy management," *Acta Neurologica Belgica*, vol. 119, no. 2, pp. 155–162, 2019.

[56] M. J. Brodie and P. Kwan, "Staged approach to epilepsy management," *Neurology*, vol. 58, no. 8 suppl 5, pp. S2–S8, 2002.

[57] R. van Griethuysen, W. A. Hofstra, S. M. van der Salm, M. D. Bourez-Swart, and A. W. de Weerd, "Safety and efficiency of medication withdrawal at home prior to long-term eeg video-monitoring," *Seizure*, vol. 56, pp. 9–13, 2018.

[58] J. Engel Jr, "Why is there still doubt to cut it out? why is there still doubt to cut it out?," *Epilepsy currents*, vol. 13, no. 5, pp. 198–204, 2013.

[59] L. Touma, B. Dansereau, A. Y. Chan, N. Jetté, C.-S. Kwon, K. P. Braun, D. Friedman, L. Jehi, J. D. Rolston, S. Vadera, *et al.*, "Neurostimulation in people with drug-resistant epilepsy: Systematic review and meta-analysis from the ilae surgical therapies commission," *Epilepsia*, 2022.

[60] P. Ryvlin, S. Rheims, L. J. Hirsch, A. Sokolov, and L. Jehi, "Neuromodulation in epilepsy: state-of-the-art approved therapies," *The Lancet Neurology*, vol. 20, no. 12, pp. 1038–1047, 2021.

[61] T. Xue, S. Chen, Y. Bai, C. Han, A. Yang, and J. Zhang, "Neuromodulation in drug-resistant epilepsy: A review of current knowledge," *Acta Neurologica Scandinavica*, vol. 146, no. 6, pp. 786–797, 2022.

[62] S. A Alomar and R. J Saeedi, "Different modalities of invasive neurostimulation for epilepsy," *Neurological Sciences*, vol. 41, no. 12, pp. 3527–3536, 2020.

[63] H. D. Simpson, A. Schulze-Bonhage, G. D. Cascino, R. S. Fisher, B. C. Jobst, M. R. Sperling, and B. N. Lundstrom, "Practical considerations in epilepsy neurostimulation," *Epilepsia*, vol. 63, no. 10, pp. 2445–2460, 2022.

[64] S. R. Haut, S. Seinfeld, and J. Pellock, "Benzodiazepine use in seizure emergencies: a

systematic review," *Epilepsy & Behavior*, vol. 63, pp. 109–117, 2016.

[65] M. Gaínza-Lein, R. Benjamin, C. Stredny, M. McGurl, K. Kapur, and T. Loddenkemper, "Rescue medications in epilepsy patients: a family perspective," *Seizure*, vol. 52, pp. 188–194, 2017.

[66] M. O. Baud, T. Proix, N. M. Gregg, B. H. Brinkmann, E. S. Nurse, M. J. Cook, and P. J. Karoly, "Seizure forecasting: bifurcations in the long and winding road," *Epilepsia*, 2022.

[67] L. Kuhlmann, P. Karoly, D. R. Freestone, B. H. Brinkmann, A. Temko, A. Barachant, F. Li, G. Titericz Jr, B. W. Lang, D. Lavery, *et al.*, "Epilepsyecosystem. org: crowd-sourcing reproducible seizure prediction with long-term human intracranial eeg," *Brain*, vol. 141, no. 9, pp. 2619–2630, 2018.

[68] M. J. Cook, T. J. O'Brien, S. F. Berkovic, M. Murphy, A. Morokoff, G. Fabinyi, W. D'Souza, R. Yerra, J. Archer, L. Litewka, *et al.*, "Prediction of seizure likelihood with a long-term, implanted seizure advisory system in patients with drug-resistant epilepsy: a first-in-man study," *The Lancet Neurology*, vol. 12, no. 6, pp. 563–571, 2013.

[69] S. B. Dumanis, J. A. French, C. Bernard, G. A. Worrell, and B. E. Fureman, "Seizure forecasting from idea to reality. outcomes of the my seizure gauge epilepsy innovation institute workshop," *Eneuro*, vol. 4, no. 6, 2017.

[70] M. Nasseri, E. Nurse, M. Glasstetter, S. Böttcher, N. M. Gregg, A. Laks Nandakumar, B. Joseph, T. Pal Attia, P. F. Viana, E. Bruno, *et al.*, "Signal quality and patient experience with wearable devices for epilepsy management," *Epilepsia*, vol. 61, pp. S25–S35, 2020.

[71] S. Cui, L. Duan, Y. Qiao, and Y. Xiao, "Learning eeg synchronization patterns for epileptic seizure prediction using bag-of-wave features," *Journal of Ambient Intelligence and Humanized Computing*, pp. 1–16, 2018.

[72] R. E. Stirling, D. B. Grayden, W. D'Souza, M. J. Cook, E. Nurse, D. R. Freestone, D. E. Payne, B. H. Brinkmann, T. Pal Attia, P. F. Viana, *et al.*, "Forecasting seizure likelihood with wearable technology," *Frontiers in neurology*, vol. 12, p. 704060, 2021.

[73] C. Alvarado-Rojas, M. Valderrama, A. Fouad-Ahmed, H. Feldwisch-Drentrup, M. Ihle, C. Teixeira, F. Sales, A. Schulze-Bonhage, C. Adam, A. Dourado, *et al.*, "Slow modulations of high-frequency activity (40–140 hz) discriminate preictal changes in human focal epilepsy," *Scientific reports*, vol. 4, no. 1, p. 4545, 2014.

[74] C. Meisel, R. El Atrache, M. Jackson, S. Schubach, C. Ufongene, and T. Loddenkemper, "Machine learning from wristband sensor data for wearable, noninvasive seizure forecasting," *Epilepsia*, vol. 61, no. 12, pp. 2653–2666, 2020.

[75] C. Meisel and K. A. Bailey, "Identifying signal-dependent information about the preictal state: A comparison across ecog, eeg and ekg using deep learning," *EBioMedicine*, vol. 45, pp. 422–431, 2019.

[76] M. Nasseri, T. Pal Attia, B. Joseph, N. M. Gregg, E. S. Nurse, P. F. Viana, G. Worrell, M. Dümpelmann, M. P. Richardson, D. R. Freestone, *et al.*, "Ambulatory seizure forecasting with a wrist-worn device using long-short term memory deep learning," *Scientific reports*, vol. 11, no. 1, p. 21935, 2021.

[77] B. H. Brinkmann, E. E. Patterson, C. Vite, V. M. Vasoli, D. Crepeau, M. Stead, J. J.

Howbert, V. Cherkassky, J. B. Wagenaar, B. Litt, *et al.*, "Forecasting seizures using intracranial eeg measures and svm in naturally occurring canine epilepsy," *PloS one*, vol. 10, no. 8, p. e0133900, 2015.

[78] P. Nejedly, V. Kremen, V. Sladky, M. Nasseri, H. Guragain, P. Klimes, J. Cimbalnik, Y. Varatharajah, B. H. Brinkmann, and G. A. Worrell, "Deep-learning for seizure forecasting in canines with epilepsy," *Journal of neural engineering*, vol. 16, no. 3, p. 036031, 2019.

[79] Y. Varatharajah, R. K. Iyer, B. M. Berry, G. A. Worrell, and B. H. Brinkmann, "Seizure forecasting and the preictal state in canine epilepsy," *International journal of neural systems*, vol. 27, no. 01, p. 1650046, 2017.

[80] F. Lopes, A. Leal, J. Medeiros, M. F. Pinto, A. Dourado, M. Dümpelmann, and C. Teixeira, "Automatic electroencephalogram artifact removal using deep convolutional neural networks," *IEEE Access*, vol. 9, pp. 149955–149970, 2021.

[81] F. Lopes, A. Leal, J. Medeiros, M. F. Pinto, A. Dourado, M. Dümpelmann, and C. Teixeira, "Epic: Annotated epileptic eeg independent components for artifact reduction," *Scientific Data*, vol. 9, no. 1, p. 512, 2022.

[82] R. Cherian and E. G. Kanaga, "Theoretical and methodological analysis of eeg based seizure detection and prediction: An exhaustive review," *Journal of Neuroscience Methods*, p. 109483, 2022.

[83] C. C. Jouny, P. J. Franaszczuk, and G. K. Bergey, "Improving early seizure detection," *Epilepsy & Behavior*, vol. 22, pp. S44–S48, 2011.

[84] M. Bialer, S. I. Johannessen, M. J. Koepp, R. H. Levy, E. Perucca, T. Tomson, and H. S. White, "A summary of data presented at the xiv conference on new antiepileptic drug and devices (eilat xiv)," 2019.

[85] M. O. Baud, T. Proix, V. R. Rao, and K. Schindler, "Chance and risk in epilepsy," *Current opinion in neurology*, vol. 33, no. 2, pp. 163–172, 2020.

[86] T. Proix, W. Truccolo, M. G. Leguia, T. K. Tcheng, D. King-Stephens, V. R. Rao, and M. O. Baud, "Forecasting seizure risk in adults with focal epilepsy: a development and validation study," *The Lancet Neurology*, vol. 20, no. 2, pp. 127–135, 2021.

[87] P. J. Karoly, V. R. Rao, N. M. Gregg, G. A. Worrell, C. Bernard, M. J. Cook, and M. O. Baud, "Cycles in epilepsy," *Nature Reviews Neurology*, vol. 17, no. 5, pp. 267–284, 2021.

[88] M. O. Baud and V. R. Rao, "Gauging seizure risk," *Neurology*, vol. 91, no. 21, pp. 967–973, 2018.

[89] M. Winterhalder, T. Maiwald, H. Voss, R. Aschenbrenner-Scheibe, J. Timmer, and A. Schulze-Bonhage, "The seizure prediction characteristic: a general framework to assess and compare seizure prediction methods," *Epilepsy & Behavior*, vol. 4, no. 3, pp. 318–325, 2003.

[90] B. Schelter, M. Winterhalder, T. Maiwald, A. Brandt, A. Schad, A. Schulze-Bonhage, and J. Timmer, "Testing statistical significance of multivariate time series analysis techniques for epileptic seizure prediction," *Chaos: An Interdisciplinary Journal of Nonlinear Science*, vol. 16, no. 1, p. 013108, 2006.

[91] B. Schelter, M. Winterhalder, T. Maiwald, A. Brandt, A. Schad, J. Timmer, and

A. Schulze-Bonhage, "Do false predictions of seizures depend on the state of vigilance? a report from two seizure-prediction methods and proposed remedies," *Epilepsia*, vol. 47, no. 12, pp. 2058–2070, 2006.

[92] B. Schelter, R. G. Andrzejak, and F. Mormann, "Can your prediction algorithm beat a random predictor?," *Seizure prediction in epilepsy: from basic mechanisms to clinical applications*, pp. 237–248, 2008.

[93] R. G. Andrzejak, D. Chicharro, C. E. Elger, and F. Mormann, "Seizure prediction: any better than chance?," *Clinical Neurophysiology*, vol. 120, no. 8, pp. 1465–1478, 2009.

[94] R. G. Andrzejak, F. Mormann, T. Kreuz, C. Rieke, A. Kraskov, C. E. Elger, and K. Lehnertz, "Testing the null hypothesis of the nonexistence of a preseizure state," *Physical Review E*, vol. 67, no. 1, p. 010901, 2003.

[95] C. A. Teixeira, B. Direito, M. Bandarabadi, M. Le Van Quyen, M. Valderrama, B. Schelter, A. Schulze-Bonhage, V. Navarro, F. Sales, and A. Dourado, "Epileptic seizure predictors based on computational intelligence techniques: A comparative study with 278 patients," *Computer methods and programs in biomedicine*, vol. 114, no. 3, pp. 324–336, 2014.

[96] M. Bandarabadi, C. A. Teixeira, J. Rasekhi, and A. Dourado, "Epileptic seizure prediction using relative spectral power features," *Clinical Neurophysiology*, vol. 126, no. 2, pp. 237–248, 2015.

[97] B. Direito, C. A. Teixeira, F. Sales, M. Castelo-Branco, and A. Dourado, "A realistic seizure prediction study based on multiclass svm," *International journal of neural systems*, vol. 27, no. 03, p. 1750006, 2017.

[98] C. Teixeira, B. Direito, M. Bandarabadi, and A. Dourado, "Output regularization of svm seizure predictors: Kalman filter versus the "firing power" method," in *2012 Annual International Conference of the IEEE Engineering in Medicine and Biology Society*, pp. 6530–6533, 2012.

[99] A. Chamseddine and M. Sawan, "Deep learning based method for output regularization of the seizure prediction classifier," in *2018 IEEE Life Sciences Conference (LSC)*, pp. 118–121, IEEE, 2018.

[100] J. Lu, A. Liu, F. Dong, F. Gu, J. Gama, and G. Zhang, "Learning under concept drift: A review," *IEEE transactions on knowledge and data engineering*, vol. 31, no. 12, pp. 2346–2363, 2018.

[101] J. Gama, I. Žliobaitė, A. Bifet, M. Pechenizkiy, and A. Bouchachia, "A survey on concept drift adaptation," *ACM computing surveys (CSUR)*, vol. 46, no. 4, pp. 1–37, 2014.

[102] F. Lopes, A. Leal, M. F. Pinto, A. Dourado, A. Schulze-Bonhage, M. Dümpelmann, and C. Teixeira, "Removing artefacts and periodically retraining improve performance of neural network-based seizure prediction models," *Scientific Reports*, vol. 13, no. 1, p. 5918, 2023.

[103] S. Khan, L. Nobili, R. Khatami, T. Loddenkemper, C. Cajochen, D.-J. Dijk, and S. H. Eriksson, "Circadian rhythm and epilepsy," *The Lancet Neurology*, vol. 17, no. 12, pp. 1098–1108, 2018.

[104] C. Blume, R. Del Giudice, M. Wislowska, J. Lechinger, and M. Schabus, "Across the consciousness continuum—from unresponsive wakefulness to sleep," *Frontiers in human neuroscience*, vol. 9, p. 105, 2015.

[105] R. K. Tripathy, S. K. Ghosh, P. Gajbhiye, and U. R. Acharya, "Development of automated sleep stage classification system using multivariate projection-based fixed boundary empirical wavelet transform and entropy features extracted from multichannel eeg signals," *Entropy*, vol. 22, no. 10, p. 1141, 2020.

[106] S. Chokroverty, "Overview of normal sleep," *Sleep disorders medicine: Basic science, technical considerations and clinical aspects*, pp. 5–27, 2017.

[107] H. Daoud and M. A. Bayoumi, "Efficient epileptic seizure prediction based on deep learning," *IEEE transactions on biomedical circuits and systems*, vol. 13, no. 5, pp. 804–813, 2019.

[108] T. Pal Attia, P. F. Viana, M. Nasseri, J. Duun-Henriksen, A. Biondi, J. S. Winston, I. P. Martins, E. S. Nurse, M. Dümpelmann, G. A. Worrell, *et al.*, "Seizure forecasting using minimally invasive, ultra-long-term subcutaneous eeg: Generalizable cross-patient models," *Epilepsia*, 2022.

[109] Y. Xu, J. Yang, S. Zhao, H. Wu, and M. Sawan, "An end-to-end deep learning approach for epileptic seizure prediction," in *2020 2nd IEEE International Conference on Artificial Intelligence Circuits and Systems (AICAS)*, pp. 266–270, IEEE, 2020.

[110] Y. Zhang, Y. Guo, P. Yang, W. Chen, and B. Lo, "Epilepsy seizure prediction on eeg using common spatial pattern and convolutional neural network," *IEEE Journal of Biomedical and Health Informatics*, vol. 24, no. 2, pp. 465–474, 2019.

[111] N. D. Truong, A. D. Nguyen, L. Kuhlmann, M. R. Bonyadi, J. Yang, S. Ippolito, and O. Kavehei, "Convolutional neural networks for seizure prediction using intracranial and scalp electroencephalogram," *Neural Networks*, vol. 105, pp. 104–111, 2018.

[112] K. M. Tsiouris, V. C. Pezoulas, M. Zervakis, S. Konitsiotis, D. D. Koutsouris, and D. I. Fotiadis, "A long short-term memory deep learning network for the prediction of epileptic seizures using eeg signals," *Computers in biology and medicine*, vol. 99, pp. 24–37, 2018.

[113] Y. LeCun, Y. Bengio, G. Hinton, *et al.*, "Deep learning. nature, 521 (7553), 436-444," *Google Scholar Google Scholar Cross Ref Cross Ref*, p. 25, 2015.

[114] P. F. Viana, T. Pal Attia, M. Nasseri, J. Duun-Henriksen, A. Biondi, J. S. Winston, I. Pavão Martins, E. S. Nurse, M. Dümpelmann, A. Schulze-Bonhage, *et al.*, "Seizure forecasting using minimally invasive, ultra-long-term subcutaneous electroencephalography: Individualized intrapatient models," *Epilepsia*, 2022.

[115] R. E. Stirling, M. J. Cook, D. B. Grayden, and P. J. Karoly, "Seizure forecasting and cyclic control of seizures," *Epilepsia*, vol. 62, pp. S2–S14, 2021.

[116] I. Assali, A. G. Blaiech, A. B. Abdallah, K. B. Khalifa, M. Carrère, and M. H. Bedoui, "Cnn-based classification of epileptic states for seizure prediction using combined temporal and spectral features," *Biomedical Signal Processing and Control*, vol. 82, p. 104519, 2023.

[117] S. Hu, J. Liu, R. Yang, Y. Wang, A. Wang, K. Li, W. Liu, and C. Yang, "Exploring the applicability of transfer learning and feature engineering in epilepsy prediction using hybrid transformer model," *IEEE Transactions on Neural Systems and Rehabilitation Engineering*, vol. 31, pp. 1321–1332, 2023.

[118] C. Li, C. Shao, R. Song, G. Xu, X. Liu, R. Qian, and X. Chen, "Spatio-temporal mlp network for seizure prediction using eeg signals," *Measurement*, vol. 206, p. 112278, 2023.

[119] M. F. Pinto, J. Batista, A. Leal, F. Lopes, A. Oliveira, A. Dourado, S. I. Abuhaiba, F. Sales, P. Martins, and C. A. Teixeira, "The goal of explaining black boxes in eeg seizure prediction is not to explain models' decisions," *Epilepsia Open*, 2023.

[120] X. Xu, Y. Zhang, R. Zhang, and T. Xu, "Patient-specific method for predicting epileptic seizures based on drsn-gru," *Biomedical Signal Processing and Control*, vol. 81, p. 104449, 2023.

[121] D. Liang, A. Liu, C. Li, J. Liu, and X. Chen, "A novel consistency-based training strategy for seizure prediction," *Journal of Neuroscience Methods*, vol. 372, p. 109557, 2022.

[122] P. Peng, Y. Song, L. Yang, and H. Wei, "Seizure prediction in eeg signals using stft and domain adaptation," *Frontiers in Neuroscience*, vol. 15, p. 825434, 2022.

[123] M. Pinto, T. Coelho, A. Leal, F. Lopes, A. Dourado, P. Martins, and C. Teixeira, "Interpretable eeg seizure prediction using a multiobjective evolutionary algorithm," *Scientific Reports*, vol. 12, no. 1, p. 4420, 2022.

[124] K. Singh and J. Malhotra, "Predicting epileptic seizures from eeg spectral band features using convolutional neural network," *Wireless Personal Communications*, vol. 125, no. 3, pp. 2667–2684, 2022.

[125] J. Zhang, C. Chatzichristos, K. Vandecasteele, L. Swinnen, V. Broux, E. Cleeren, W. Van Paesschen, and M. De Vos, "Automatic annotation correction for wearable eeg based epileptic seizure detection," *Journal of Neural Engineering*, vol. 19, no. 1, p. 016038, 2022.

[126] M. F. Pinto, A. Leal, F. Lopes, A. Dourado, P. Martins, and C. A. Teixeira, "A personalized and evolutionary algorithm for interpretable eeg epilepsy seizure prediction," *Scientific reports*, vol. 11, no. 1, p. 3415, 2021.

[127] T. Tamanna, M. A. Rahman, S. Sultana, M. H. Haque, and M. Z. Parvez, "Predicting seizure onset based on time-frequency analysis of eeg signals," *Chaos, Solitons & Fractals*, vol. 145, p. 110796, 2021.

[128] S. M. Usman, S. Khalid, and Z. Bashir, "Epileptic seizure prediction using scalp electroencephalogram signals," *Biocybernetics and Biomedical Engineering*, vol. 41, no. 1, pp. 211–220, 2021.

[129] K. Vandecasteele, T. De Cooman, C. Chatzichristos, E. Cleeren, L. Swinnen, J. Macea Ortiz, S. Van Huffel, M. Dümpelmann, A. Schulze-Bonhage, M. De Vos, *et al.*, "The power of ecg in multimodal patient-specific seizure monitoring: added value to an eeg-based detector using limited channels," *Epilepsia*, vol. 62, no. 10, pp. 2333–2343, 2021.

[130] A. Gabara, R. Yousri, D. Hamdy, M. H. Zakhari, and H. Mostafa, "Patient specific epileptic seizures prediction based on support vector machine," in *2020 32nd International Conference on Microelectronics (ICM)*, pp. 1–4, IEEE, 2020.

[131] O. Stojanović, L. Kuhlmann, and G. Pipa, "Predicting epileptic seizures using nonnegative matrix factorization," *PloS one*, vol. 15, no. 2, p. e0228025, 2020.

[132] N. D. Truong, L. Kuhlmann, M. R. Bonyadi, D. Querlioz, L. Zhou, and O. Kavehei, "Epileptic seizure forecasting with generative adversarial networks," *IEEE Access*, vol. 7, pp. 143999–144009, 2019.

[133] I. Kiral-Kornek, S. Roy, E. Nurse, B. Mashford, P. Karoly, T. Carroll, D. Payne, S. Saha,

S. Baldassano, T. O'Brien, *et al.*, "Epileptic seizure prediction using big data and deep learning: toward a mobile system," *EBioMedicine*, vol. 27, pp. 103–111, 2018.

[134] L. A. S. Kitano, M. A. A. Sousa, S. D. Santos, R. Pires, S. Thome-Souza, and A. B. Campo, "Epileptic seizure prediction from eeg signals using unsupervised learning and a polling-based decision process," in *Artificial Neural Networks and Machine Learning–ICANN 2018: 27th International Conference on Artificial Neural Networks, Rhodes, Greece, October 4-7, 2018, Proceedings, Part II 27*, pp. 117–126, Springer, 2018.

[135] Y. Yang, M. Zhou, Y. Niu, C. Li, R. Cao, B. Wang, P. Yan, Y. Ma, and J. Xiang, "Epileptic seizure prediction based on permutation entropy," *Frontiers in computational neuroscience*, vol. 12, p. 55, 2018.

[136] A. Aarabi and B. He, "Seizure prediction in patients with focal hippocampal epilepsy," *Clinical Neurophysiology*, vol. 128, no. 7, pp. 1299–1307, 2017.

[137] H. Khan, L. Marcuse, M. Fields, K. Swann, and B. Yener, "Focal onset seizure prediction using convolutional networks," *IEEE Transactions on Biomedical Engineering*, vol. 65, no. 9, pp. 2109–2118, 2017.

[138] E. B. Assi, M. Sawan, D. K. Nguyen, and S. Rihana, "A hybrid mrmr-genetic based selection method for the prediction of epileptic seizures," in *2015 IEEE Biomedical Circuits and Systems Conference (BioCAS)*, pp. 1–4, IEEE, 2015.

[139] J. Rasekhi, M. R. K. Mollaei, M. Bandarabadi, C. A. Teixeira, and A. Dourado, "Epileptic seizure prediction based on ratio and differential linear univariate features," *Journal of medical signals and sensors*, vol. 5, no. 1, p. 1, 2015.

[140] N. Moghim and D. W. Corne, "Predicting epileptic seizures in advance," *PloS one*, vol. 9, no. 6, p. e99334, 2014.

[141] A. F. Rabbi, L. Azinfar, and R. Fazel-Rezai, "Seizure prediction using adaptive neuro-fuzzy inference system," in *2013 35th Annual International Conference of the IEEE Engineering in Medicine and Biology Society (EMBC)*, pp. 2100–2103, IEEE, 2013.

[142] "Preprocessing effects of 22 linear univariate features on the performance of seizure prediction methods," *Journal of neuroscience methods*, vol. 217, no. 1-2, pp. 9–16, 2013.

[143] Z. Zhang, Z. Chen, Y. Zhou, S. Du, Y. Zhang, T. Mei, and X. Tian, "Construction of rules for seizure prediction based on approximate entropy," *Clinical neurophysiology*, vol. 125, no. 10, pp. 1959–1966, 2014.

[144] K. Rasheed, A. Qayyum, J. Qadir, S. Sivathamboo, P. Kwan, L. Kuhlmann, T. O'Brien, and A. Razi, "Machine learning for predicting epileptic seizures using eeg signals: A review," *IEEE Reviews in Biomedical Engineering*, vol. 14, pp. 139–155, 2020.

[145] S. Selim, E. Elhinamy, H. Othman, W. Abouelsaadat, and M. A.-M. Salem, "A review of machine learning approaches for epileptic seizure prediction," in *2019 14th International Conference on Computer Engineering and Systems (ICCES)*, pp. 239–244, IEEE, 2019.

[146] M. Bandarabadi, J. Rasekhi, C. A. Teixeira, M. R. Karami, and A. Dourado, "On the proper selection of preictal period for seizure prediction," *Epilepsy & Behavior*, vol. 46, pp. 158–166, 2015.

[147] J. Müller, H. Yang, M. Eberlein, G. Leonhardt, O. Uckermann, L. Kuhlmann, and R. Tetzlaff, "Coherent false seizure prediction in epilepsy, coincidence or providence?," *Clinical*

Neurophysiology, vol. 133, pp. 157–164, 2022.

[148] A. Leal, M. F. Pinto, F. Lopes, A. M. Bianchi, J. Henriques, M. G. Ruano, P. de Carvalho, A. Dourado, and C. A. Teixeira, "Heart rate variability analysis for the identification of the preictal interval in patients with drug-resistant epilepsy," *Scientific reports*, vol. 11, no. 1, p. 5987, 2021.

[149] J. Yang and M. Sawan, "From seizure detection to smart and fully embedded seizure prediction engine: A review," *IEEE Transactions on Biomedical Circuits and Systems*, vol. 14, no. 5, pp. 1008–1023, 2020.

[150] M. Shahbazi and H. Aghajan, "A generalizable model for seizure prediction based on deep learning using cnn-lstm architecture," in *2018 IEEE Global Conference on Signal and Information Processing (GlobalSIP)*, pp. 469–473, IEEE, 2018.

[151] K. Gadhoumi, J.-M. Lina, F. Mormann, and J. Gotman, "Seizure prediction for therapeutic devices: A review," *Journal of neuroscience methods*, vol. 260, pp. 270–282, 2016.

[152] F. Mormann, T. Kreuz, C. Rieke, R. G. Andrzejak, A. Kraskov, P. David, C. E. Elger, and K. Lehnertz, "On the predictability of epileptic seizures," *Clinical neurophysiology*, vol. 116, no. 3, pp. 569–587, 2005.

[153] M. A. F. Harrison, I. Osorio, M. G. Frei, S. Asuri, and Y.-C. Lai, "Correlation dimension and integral do not predict epileptic seizures," *Chaos: An Interdisciplinary Journal of Nonlinear Science*, vol. 15, no. 3, 2005.

[154] P. E. McSharry, L. A. Smith, and L. Tarassenko, "Prediction of epileptic seizures: are nonlinear methods relevant?," *Nature medicine*, vol. 9, no. 3, pp. 241–242, 2003.

[155] Y. Park, L. Luo, K. K. Parhi, and T. Netoff, "Seizure prediction with spectral power of eeg using cost-sensitive support vector machines," *Epilepsia*, vol. 52, no. 10, pp. 1761–1770, 2011.

[156] P. Agarwal, H.-C. Wang, and K. Srinivasan, "Epileptic seizure prediction over eeg data using hybrid cnn-svm model with edge computing services," in *MATEC web of conferences*, vol. 210, p. 03016, EDP Sciences, 2018.

[157] M. Bandarabadi, C. A. Teixeira, B. Direito, and A. Dourado, "Epileptic seizure prediction based on a bivariate spectral power methodology," in *2012 Annual International Conference of the IEEE Engineering in Medicine and Biology Society*, pp. 5943–5946, IEEE, 2012.

[158] J. J. Howbert, E. E. Patterson, S. M. Stead, B. Brinkmann, V. Vasoli, D. Crepeau, C. H. Vite, B. Sturges, V. Ruedebusch, J. Mavoori, *et al.*, "Forecasting seizures in dogs with naturally occurring epilepsy," *PloS one*, vol. 9, no. 1, p. e81920, 2014.

[159] B. Direito, F. Ventura, C. Teixeira, and A. Dourado, "Optimized feature subsets for epileptic seizure prediction studies," in *2011 Annual International Conference of the IEEE Engineering in Medicine and Biology Society*, pp. 1636–1639, IEEE, 2011.

[160] M. D'Alessandro, R. Esteller, G. Vachtsevanos, A. Hinson, J. Echauz, and B. Litt, "Epileptic seizure prediction using hybrid feature selection over multiple intracranial eeg electrode contacts: a report of four patients," *IEEE transactions on biomedical engineering*, vol. 50, no. 5, pp. 603–615, 2003.

[161] U. R. Acharya, S. V. Sree, G. Swapna, R. J. Martis, and J. S. Suri, "Automated eeg

analysis of epilepsy: a review," *Knowledge-Based Systems*, vol. 45, pp. 147–165, 2013.

[162] P. Mirowski, D. Madhavan, Y. LeCun, and R. Kuzniecky, "Classification of patterns of eeg synchronization for seizure prediction," *Clinical neurophysiology*, vol. 120, no. 11, pp. 1927–1940, 2009.

[163] A. Shoeibi, M. Khodatars, N. Ghassemi, M. Jafari, P. Moridian, R. Alizadehsani, M. Panahiazar, F. Khozeimeh, A. Zare, H. Hosseini-Nejad, *et al.*, "Epileptic seizures detection using deep learning techniques: A review," *International Journal of Environmental Research and Public Health*, vol. 18, no. 11, p. 5780, 2021.

[164] Y. Zhang, S. Yao, R. Yang, X. Liu, W. Qiu, L. Han, W. Zhou, and W. Shang, "Epileptic seizure detection based on bidirectional gated recurrent unit network," *IEEE Transactions on Neural Systems and Rehabilitation Engineering*, vol. 30, pp. 135–145, 2022.

[165] R. Rahman, S. M. Varnosfaderani, O. Makke, N. J. Sarhan, E. Asano, A. Luat, and M. Alhawari, "Comprehensive analysis of eeg datasets for epileptic seizure prediction," in *2021 IEEE International Symposium on Circuits and Systems (ISCAS)*, pp. 1–5, IEEE, 2021.

[166] B. H. Brinkmann, J. Wagenaar, D. Abbot, P. Adkins, S. C. Bosshard, M. Chen, Q. M. Tieng, J. He, F. Muñoz-Almaraz, P. Botella-Rocamora, *et al.*, "Crowdsourcing reproducible seizure forecasting in human and canine epilepsy," *Brain*, vol. 139, no. 6, pp. 1713–1722, 2016.

[167] "Kaggle - seizure prediction." `https://www.kaggle.com/c/seizure-prediction`. Accessed on 2023-04-23.

[168] J. Prasanna, M. Subathra, M. A. Mohammed, R. Damaševičius, N. J. Sairamya, and S. T. George, "Automated epileptic seizure detection in pediatric subjects of chb-mit eeg database—a survey," *Journal of Personalized Medicine*, vol. 11, no. 10, p. 1028, 2021.

[169] S. Wong and L. Kuhlmann, "Computationally efficient epileptic seizure prediction based on extremely randomised trees," in *Proceedings of the Australasian Computer Science Week Multiconference*, pp. 1–3, 2020.

[170] "Epilepsy ecosystem - my seizure gauge." `https://www.epilepsyecosystem.org/my-seizure-gauge-1`. Accessed on 2023-03-23.

[171] J. Cloyd, S. Haut, E. Carrazana, and A. L. Rabinowicz, "Overcoming the challenges of developing an intranasal diazepam rescue therapy for the treatment of seizure clusters," *Epilepsia*, vol. 62, no. 4, pp. 846–856, 2021.

[172] M. R. Bouw, S. S. Chung, B. Gidal, A. King, J. Tomasovic, J. W. Wheless, and P. J. Van Ess, "Clinical pharmacokinetic and pharmacodynamic profile of midazolam nasal spray," *Epilepsy Research*, vol. 171, p. 106567, 2021.

[173] S. H. Boddu and S. Kumari, "A short review on the intranasal delivery of diazepam for treating acute repetitive seizures," *Pharmaceutics*, vol. 12, no. 12, p. 1167, 2020.

[174] A. Aarabi, R. Fazel-Rezai, and Y. Aghakhani, "Eeg seizure prediction: measures and challenges," in *2009 Annual International Conference of the IEEE Engineering in Medicine and Biology Society*, pp. 1864–1867, IEEE, 2009.

[175] P. R. Carney, S. Myers, and J. D. Geyer, "Seizure prediction: methods," *Epilepsy & behavior*, vol. 22, pp. S94–S101, 2011.

[176] B. Hjorth, "Eeg analysis based on time domain properties," *Electroencephalography and clinical neurophysiology*, vol. 29, no. 3, pp. 306–310, 1970.

[177] L. Chisci, A. Mavino, G. Perferi, M. Sciandrone, C. Anile, G. Colicchio, and F. Fuggetta, "Real-time epileptic seizure prediction using ar models and support vector machines," *IEEE Transactions on Biomedical Engineering*, vol. 57, no. 5, pp. 1124–1132, 2010.

[178] Z. Zhang and K. K. Parhi, "Seizure prediction using polynomial svm classification," in *2015 37th Annual International Conference of the IEEE Engineering in Medicine and Biology Society (EMBC)*, pp. 5748–5751, IEEE, 2015.

[179] K. Gadhoumi, J.-M. Lina, and J. Gotman, "Seizure prediction in patients with mesial temporal lobe epilepsy using eeg measures of state similarity," *Clinical Neurophysiology*, vol. 124, no. 9, pp. 1745–1754, 2013.

[180] H. Ocak, "Automatic detection of epileptic seizures in eeg using discrete wavelet transform and approximate entropy," *Expert Systems with Applications*, vol. 36, no. 2, pp. 2027–2036, 2009.

[181] L. Wang, C. Wang, F. Fu, X. Yu, H. Guo, C. Xu, X. Jing, H. Zhang, and X. Dong, "Temporal lobe seizure prediction based on a complex gaussian wavelet," *Clinical Neurophysiology*, vol. 122, no. 4, pp. 656–663, 2011.

[182] P. Grassberger and I. Procaccia, "Characterization of strange attractors," *Physical review letters*, vol. 50, no. 5, p. 346, 1983.

[183] L. D. Iasemidis, D.-S. Shiau, J. C. Sackellares, P. M. Pardalos, and A. Prasad, "Dynamical resetting of the human brain at epileptic seizures: application of nonlinear dynamics and global optimization techniques," *IEEE transactions on biomedical engineering*, vol. 51, no. 3, pp. 493–506, 2004.

[184] M. Le Van Quyen, J. Martinerie, M. Baulac, and F. Varela, "Anticipating epileptic seizures in real time by a non-linear analysis of similarity between eeg recordings," *Neuroreport*, vol. 10, no. 10, pp. 2149–2155, 1999.

[185] F. Mormann, T. Kreuz, R. G. Andrzejak, P. David, K. Lehnertz, and C. E. Elger, "Epileptic seizures are preceded by a decrease in synchronization," *Epilepsy research*, vol. 53, no. 3, pp. 173–185, 2003.

[186] E. Oja and A. Hyvarinen, "Independent component analysis: algorithms and applications," *Neural networks*, vol. 13, no. 4-5, pp. 411–430, 2000.

[187] F. Mormann, R. G. Andrzejak, T. Kreuz, C. Rieke, P. David, C. E. Elger, and K. Lehnertz, "Automated detection of a preseizure state based on a decrease in synchronization in intracranial electroencephalogram recordings from epilepsy patients," *Physical Review E*, vol. 67, no. 2, p. 021912, 2003.

Appendices

A

Features Description

The focus of this chapter lies in a comprehensive exploration, revealing the most extracted features from the state-of-the-art, along with the univariate linear features utilized during the development of this thesis.

Univariate Linear Features

Extracting univariate linear characteristics from the Electroencephalogram (EEG) signal involves characterizing each channel's signal's phase/frequency and amplitude information. This extraction assumes that the EEG is approximately stationary within each time window.

Statistical Moments

Within the EEG time series context, statistical moments are pivotal in elucidating the amplitude and distribution characteristics. Typically computed concerning the mean, these moments encompass various measures. The first moment, which corresponds to the mean, sheds light on the central tendency of the distribution. The second moment, known as the variance, quantifies the dispersion around the mean. These initial moments collectively offer valuable details regarding the location and variability of the amplitude distribution within the time series. Furthermore, the third moment indicates the slope and thus reveals the degree of skewness in the distribution. Finally, the kurtosis moment illustrates the distribution's peak degree.

A comprehensive summary of this information is available in the provided Table A.1. N signifies the total number of samples encompassed by the sliding window, and x denotes a vector containing the input values.

Table A.1: Statistical moments

Order	Formula	Definition
1^{st} (Mean)	$\mu = \frac{1}{N}\sum_{i=1}^{N} x_i$	Measures the central tendency of the amplitude of the samples
2^{nd} (Variance)	$\sigma^2 = \frac{1}{N-1}\sum_{i=1}^{N}(x_i - \mu)^2$	Measures the dispersion of the amplitude of the samples around its mean
3^{rd} (Skewness)	$\chi = \frac{\frac{1}{N-1}\sum_{i=1}^{N}(x_i-\mu)^3}{\sigma^3}$	Measures the degree of asymmetries of the amplitude distribution
4^{th} (Kurtosis)	$\kappa = \frac{\frac{1}{N-1}\sum_{i=1}^{N}(x_i-\mu)^4}{(N-1)\sigma^4} - 3$	Measures the relative flatness or peakedness of the amplitude distribution

These methodologies distinguish between interictal and ictal states, thereby providing significant value in detecting seizures characterized by substantial amplitude. Noteworthy findings from several studies [95, 174] demonstrate a decrease in variance alongside an increase in kurtosis during the preictal period, contrasting with the interictal period [174, 175].

Hjorth Parameters

Hjorth [176] established three normalized slope descriptor parameters — activity, mobility, and complexity — in the time domain. Activity represents the signal's variability and assesses its average power. Mobility, in contrast, involves computing the ratio of the Root Mean Square (RMS) of the slopes of the EEG signal to the RMS of the amplitudes within a moving time window, providing an estimation of the mean frequency. On the other hand, complexity employs the RMS measure of the rate of slope changes relative to an idealized curve, offering an estimate of the signal's bandwidth.

According to the research conducted by Mormann et al. (2005) [152], there was a substantial increase in mobility and complexity of the Hjorth descriptors observed during the preictal phase compared to the interictal phase [174].

Auto-regressive Models

The linear method described herein predicts the values of a linear time series at a specific time point by employing a weighted sum of preceding values along with noise. Auto-regressive models are applied to model the EEG signal under the assumption of stationarity, enabling the examination of neuronal synchronization. To handle the non-stationarity inherent in such signals, the signal is segmented into shorter intervals using a sliding window approach.

Utilizing auto-regressive modeling, a series of measures were computed and integrated into the set of characteristics in several studies, allowing for the identification of preictal alterations [67, 97, 95, 139, 142]. The authors, in their investigations, utilized either the modeling error resulting from a seizure generation process [142] or the values of the modeling coefficients as characteristic indicators [177].

Decorrelation Time

Similar to auto-regressive models, decorrelation time finds application in exploring neuronal synchronization. Autocorrelation, which pertains to the correlation between signal values at different temporal instances, assumes significance in this context. The correlation time, in turn, corresponds to the moment when the autocorrelation sequence of a specific EEG signal first crosses zero.

A decrease in the decorrelation time implies a decrease in the correlation exhibited by the signal samples. For example, in the case of a white noise sequence, the correlation time is theoretically zero, indicating a complete absence of correlation among its samples.

The correlation among EEG signal samples decreases in the lead-up to a seizure. The evidence supporting this finding was established by Mormann et al. (2005) [152], who reported decreased decorrelation time before seizures [95, 174].

Relative Spectral Power

Authors typically describe the EEG signal in its major frequency bands: delta, theta, alpha, beta, and gamma. They often employ frequency domain features to capture the frequency variations from low to high frequencies and calculate their relative power. The relative power within a particular frequency band is determined by calculating the area under the power spectrum curve within the corresponding bandwidth and normalizing it by the total power encompassing all frequency bands.

These are the characteristics prevalent in the literature [67, 95, 96, 97, 99, 102, 108, 111, 114, 116, 117, 119, 124, 125, 128, 129, 130, 131, 132, 133, 138, 139, 140, 142] and are obtained by computing the Power Spectral Density (PSD) through the application of the Fast Fourier Transform (FFT) to the EEG time series. Afterward, the computation involves finding the average of the squared coefficients within the frequency range of interest. Accurate PSD estimation relies on assuming statistical stationarity in the EEG signal, which requires segmenting the signal into windows of sufficient length to capture low-frequency brain activity while still being short enough to satisfy the stationarity assumption.

The literature has documented a shift in power from lower to higher frequencies [95, 96, 142, 152]. In particular, Mormann et al. (2005) [152] observed a relative decrease in power within the delta band, accompanied by a relative increase in the remaining frequency bands. Furthermore, Bandarabadi et al. (2015) [96] conducted an in-depth analysis of spectral powers across different subbands and electrodes, highlighting their potential for detecting gradual changes that precede seizures [96, 155, 174, 178].

Wavelet Transform

The inherent limitation of Fourier transforms in effectively handling instantaneous signal changes underscores the need to investigate methods within the time-frequency domain. The Wavelet Transform (WT) is a more appropriate choice, characterized by its ability to decompose the continuous signal into subbands known as wavelets derived from a mother wavelet.

Moreover, EEG signals manifest considerable complexity, characterized by their nonlinear and non-stationary behavior. The wavelet transformation offers a suitable approach for investigating the elements constituting chaotic and time-variant signals, such as EEG signals, as it exhibits favorable localization properties in both time and frequency domains. By providing concurrent insights into time and frequency characteristics, this approach identifies transient characteristics within the data, including epileptic spikes.

The quantification of energy across diverse frequency bands represents a notable characteristic achievable through utilizing the WT, as evidenced in prior studies [95, 142, 179]. A key advantage of WT is its capacity to employ variable window sizes, which empowers the method to yield precise frequency information at lower frequencies and accurate time-related insights at higher frequencies [180, 181].

Spectral Edge Frequency

EEG signals distribute spectral power across the entire frequency spectrum, with a significant portion concentrating within 0 to 40 Hz. Spectral Edge Frequency (SEF) and Spectral Edge Power (SEP) metrics provide a means to quantify power distribution within this frequency range.

SEF is a crucial measure, providing insight into the distribution of signal energy in the frequency spectrum and highlighting the concentration of signal power. Quantifying it involves determining the frequency below which a specific percentage (x) of the total signal energy resides, with x varying from 0 to 100. In the context of seizure prediction, the widely adopted value for x is 50%, facilitating the determination of the minimum frequency within the 0-40 Hz band that contains 50% of the power. The area under the SEF curve corresponds to SEP, as supported by pertinent studies [17, 95, 140].

Univariate Nonlinear Features

Linear measures are a direct computation from the time series or power spectrum. In contrast, nonlinear features, including the correlation dimension, greatest Lyapunov exponent, entropy, and the dynamic similarity index, are derived from the principles of dynamical systems theory [140, 152]. Given the noisy and non-stationary nature of EEG time series, a reduction in its chaotic behavior may indicate an impending seizure, as brain dynamics become more predictable before seizure events. Consequently, chaotic measures can aid in describing brain dynamics by detecting increased brain synchrony preceding seizures. However, a disadvantage of employing such features is their computational complexity, posing challenges when implementing them within online systems [15].

Correlation Sum and Dimension

Proposed by Grassberger and Procaccia (1983) [182], the correlation dimension is a prominent method for evaluating the fractal dimension of a signal. The dimension arises from examining the spatial distribution occupied by the signal samples. Additionally, considering a given distance, the correlation sum considers the likelihood of two vectors in the state space trajectory being close to each other. The correlation dimension and correlation sum jointly contribute essential knowledge concerning attractor spatial structure and complexity, offering a mathematically grounded approach to signal analysis.

Lyapunov Exponent

Chaos theory's fundamental concept emphasizes that a system's predictability depends on its initial conditions. Chaotic behavior exhibits itself through the exponential divergence of neighboring trajectories in state space, which can be quantified using Lyapunov exponents. These exponents are critical in measuring the separation rate between neighboring trajectories, offering invaluable insights into the dynamics and predictability of intricate events observed in diverse systems.

Lyapunov exponents find widespread applications in various research domains, including studying events such as seizures. However, the outcomes can be divergent, with some studies indicating a decrease in the highest Lyapunov exponent shortly before the event [183], while others suggest an increase approximately 30 minutes before [152]. Nonetheless, the analysis of Lyapunov exponents remains essential for comprehending the intricate dynamics of complex systems and their responsiveness to initial conditions.

Entropy

Entropy is a crucial metric for evaluating the regularity and unpredictability of fluctuations within EEG data. Various forms of entropy, including approximation entropy, sample entropy, permutation entropy, and spectral entropy, can be utilized to assess the complexity of the EEG signals. Entropy has proven valuable in detecting transitions from an interictal to a preictal state, considering seizures often exhibit synchronized brain activity. Several studies have explored this metric, presenting relevant results [116, 125, 127, 129, 135].

Dynamic Similarity Index

The Dynamic Similarity Index (DSI), a metric introduced by Le Van Quyen et al. (1999) [184], plays a pivotal role in quantitatively measuring the level of dynamic similarity between two specific segments within an EEG signal. This method selects one element as a reference, representing a brief interictal segment, while another component functions as a mobile test window. The DSI effectively compares the dynamics of these two windows, and upon surpassing a predetermined threshold, it identifies the preictal period.

A noteworthy aspect of this measurement is its incorporation of time delay, enabling the extraction of nonlinear features and enhancing the precision of EEG segment dynamics evaluation. DSI has emerged as a valuable tool for detecting the preictal period, as evidenced by several studies exploring its potential in this domain [15, 17, 184].

Bivariate and Multivariate Linear Features

The comprehensive evaluation of interactions among different brain regions is made possible through bivariate or multivariate linear features, which concurrently assess two or multiple electrodes. The preictal stage, marked by complexity in both spatial and temporal aspects, involves seizures arising from brain synchronization. This state can be effectively captured and quantified by carefully selecting appropriate features [15, 141].

Maximum Linear Cross-correlation

The maximum linear cross-correlation is a widely employed characteristic for analyzing the synchronization between two electrode channels, constituting a bivariate measure. This assessment effectively quantifies the degree of delay synchronization between the channels and precisely determines the time delay τ by which two identical signals shift. As a result, it stands as an indispensable indicator for measuring the similarity inherent in the two time series. With values

ranging between 0 and 1, results close to 1 indicate high signal similarity, featuring a possible time delay τ. In contrast, asynchronous signals yield values nearing 0 [15, 17, 162, 185].

Ration and Differences

The assessment of brain activities requires a holistic perspective on the interrelationships between multiple regions, achieved through the comparison of the same feature obtained from different channels. This approach offers a generalized outlook on the interconnected brain dynamics. This approach quantifies these interrelationships using relative and differential features. Relative features involve dividing the resources of one channel by those of another, whereas differential features involve subtracting the resources of one channel from those of another.

ICA

Independent Component Analysis (ICA) [186] is a powerful approach that assumes that each measured signal comprises a linear combination of independent signals. This technique effectively decomposes multidimensional data vectors into statistically independent components, which are valuable for feature extraction. However, ICA demonstrates remarkable success in eliminating artifacts from EEG signals and decomposing the EEG into different component signals originating from various sources.

Bivariate and Multivariate Nonlinear Features

Bivariate and multivariate nonlinear features are extensively employed as they excel at capturing changes in synchrony within EEG signals. These measures simultaneously examine information from two or multiple electrodes, using concepts of similarity and mutual information.

Mean Phase Coherence

Mean Phase Coherence (MPC) is a widely adopted measure for quantifying the phase synchronization between two time series. The metric produces values between 0 and 1, with outcomes close to 1 denoting a high degree of synchronization [67, 141, 152]. Some studies consistently report a reduction in MPC values preceding the onset of seizures [141, 187], indicating MPC's relevance as an informative indicator for detecting phase synchronization changes associated with seizure events.

Dynamic Entrainment

Dynamic entrainment, a feature introduced by Iasemidis et al. (2004) [183], draws inspiration from chaos theory and focuses on quantifying the nonlinear interaction between two time series. As a multivariate version of the Lyapunov exponent, dynamic entrainment demands the computation of the greatest Lyapunov exponent for each analyzed channel.

Nonlinear Interdependence

The evaluation of nonlinear connectivity between two EEG signals derived from different channels indicates generalized synchronization. This state arises when one coupled system's behavior dynamically affects the other's behavior [136, 141].

B

Databases Pipeline Overview

To provide a concise overview of the content discussed within section 4.2, Figures B.1, B.2, and B.3 illustrate the models employed for the Children's Hospital Boston from the Massachusetts Institute of Technology (CHB-MIT), American Epilepsy Society (AES), and Epilepsy Ecosystem databases. These figures facilitate straightforward comparisons with Figure 4.1, depicting the model utilized for European Epilepsy Database (EPILEPSIAE).

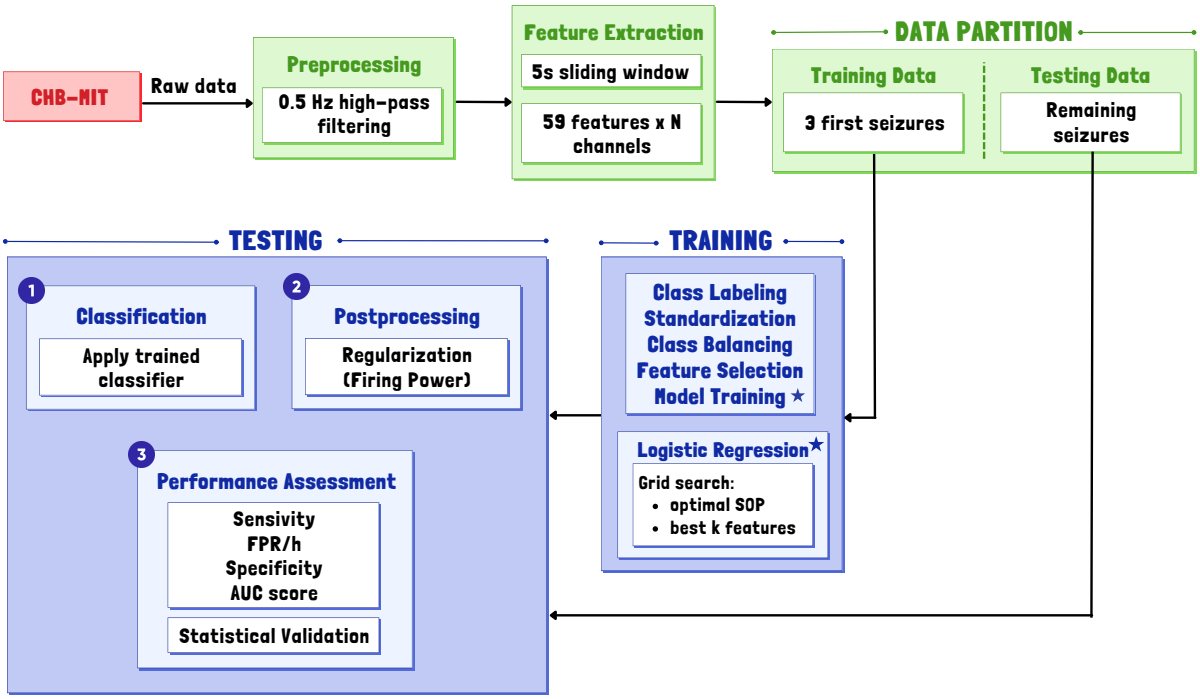

Figure B.1: General overview of the proposed patient-specific pipeline for CHB-MIT database. N can assume any of the following values: 23 or 32. Asterisks indicate the inclusion of a Logistic Regression classifier in the model training phase.

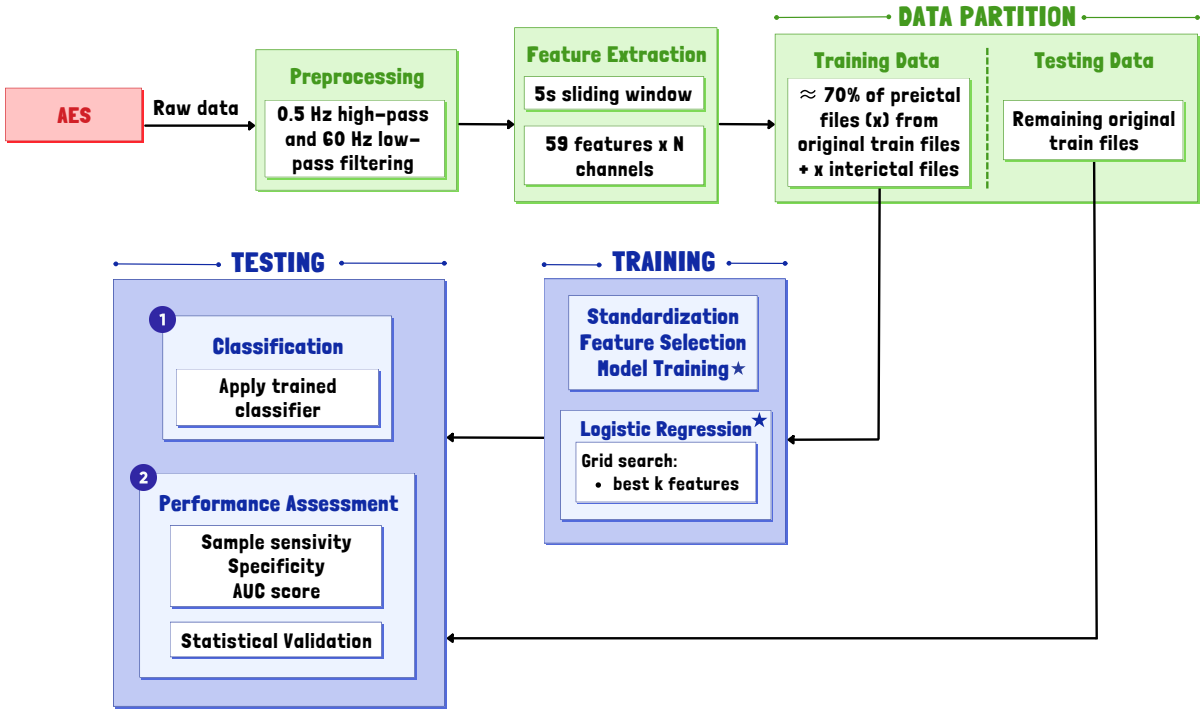

Figure B.2: General overview of the proposed patient-specific pipeline for AES database. N can assume any of the following values: 15, 16, or 24. x refers to the number of preictal train files. Asterisks indicate the inclusion of a Logistic Regression classifier in the model training phase.

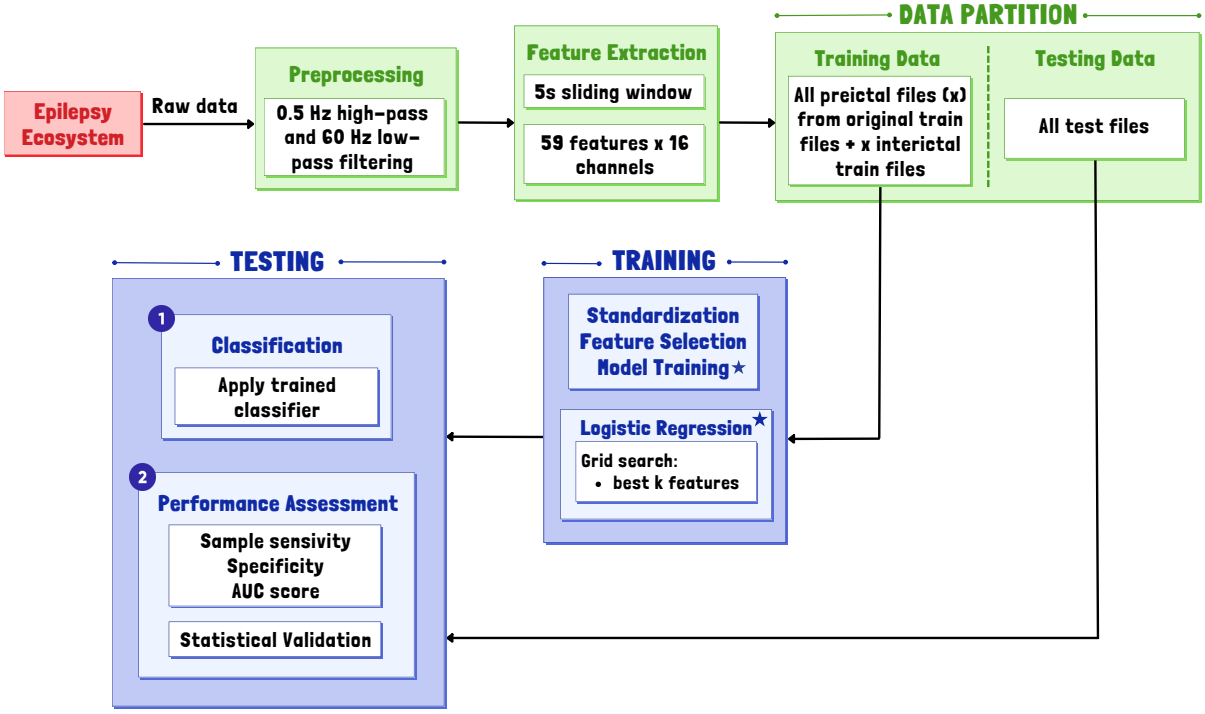

Figure B.3: General overview of the proposed patient-specific pipeline for Epilepsy Ecosystem database. x refers to the number of preictal train files. Asterisks indicate the inclusion of a Logistic Regression classifier in the model training phase.